HEATS OF MIXING OF GASES

BY

FLOW CALORIMETRY

A thesis presented for the degree of

Doctor of Philosophy in Chemical Engineering

at the

University of Canterbury,

Christchurch, New Zealand

by

C. J. MAYHEW

1978

ACKNOWLEDGEMENTS

I wish to record my grateful thanks and appreciation to Professor A. G. Williamson for his interest, advice and forebearance during this project. Thanks, also, are due to Dr. P. J. McElroy for his able guidance and assistance while Professor Williamson was on leave.

Many thanks are due to the technical staff of the Chemical Engineering Department for their valuable assistance in the construction of the apparatus. The assistance of Mr. F. Downing of the Chemistry Department with the glass blowing and construction of the calorimeter was greatly appreciated.

Special thanks are due to Professor A. M. Kennedy who made sure that the problem of finance never arose. Financial assistance for a part of this project was in the form of a Postgraduate Scholarship from Fletcher Industrial Holdings (N.Z.) Ltd.

Finally I wish to thank Miss B. Nottingham for her help in reducing my scrawl to a typed script.

CONTENTS

SUMMARY

A flow calorimeter to measure the heats of mixing of gases, at pressures below 100 kPa, has been constructed and tested.

The heat of mixing of benzene and cyclohexane has been determined over a range of temperatures and the results have been compared with previous measurements. The results have also been compared with the directly measured excess second virial coefficients via a function of the form

$$\varepsilon = a + b \exp(c/T)$$

with a, b and c chosen to best fit both the p-v-T data and the heats of mixing.

The heat of mixing of acetone and chloroform has been measured over a range of temperature and pressure. The analysis of these results in conjunction with p-v-T data supports the idea of complex formation due to hydrogen bonding. The results were used to calculate a value for the standard heat of formation of the complex, $\Delta H^{\dagger} = -20 \pm 3$ kJ mol^{-1}.

Finally, suggestions for further work on improvements to the apparatus, and further studies of complex forming gas mixtures are presented.

1. INTRODUCTION

The p-v-T-x properties of gases, vapours and their mixtures are of interest to chemical engineers in the design of chemical engineering unit operations. For example, in the distillation column a knowledge of the vapour phase chemical potential aids the calculation of liquid-vapour equilibria, allowing for more accurate design of the equipment.

The understanding of intermolecular forces is also helped by knowledge of p-v-T-x properties through the application of statistical thermodynamics (Hill (1960)).

1.1 THE VIRIAL EQUATION OF STATE

The p-v-T-x properties of a gas at low pressures and moderate temperatures are often described by the virial equation of state expressed as either a density series,

$$pv/RT = 1 + B(T)/v + C(T)/v^2 + \ldots \qquad (1.1)$$

or a pressure series,

$$pv = RT + B'(T)p + C'(T)p^2 + \ldots \qquad (1.2)$$

where p is the absolute pressure, v the molar volume, T the absolute temperature, and R the gas constant. The coefficients B(T), C(T),... of the density series are called the second, third, ... virial coefficients and are uniquely related to the coefficients in the pressure series by relations of the type,

$$B'(T) = B(T) \qquad (1.3)$$

$$C'(T) = (C(T) - B(T)^2)/RT \qquad (1.4)$$

It should be noted that Equations (1.3) and (1.4) hold only for the infinite series.

Statistical thermodynamics (Hill (1960)) provides a theoretical basis for the virial equation of state in which B(T) is seen to represent a measure of two-molecule interactions, C(T), three molecule interactions, etc. The second virial coefficient B(T) is also of interest because it is related through statistical thermodynamics (Hill (1960)) to the intermolecular potential $U_{ij}(r)$. For the simple case where the interactions between molecules have no angular dependence (i.e. the molecules are spherically symmetrical),

$$B_{ij}(T) = -2\pi N_A \int_0^\infty (e^{-U_{ij}(r)/kT} - 1) r^2 dr \tag{1.5}$$

where i, j indicate the molecule types, N_A is Avogadro's number, k is Boltzmans constant, and r is the intermolecular distance. Similarly the third virial coefficient C(T), for spherically symmetrical molecules, is given by,

$$C_{ijk}(T) = -\frac{N_A^2}{3V} \iiint_V (e^{-U(r_{12})/kT} - 1)(e^{-U(r_{13})/kT} - 1)(e^{-U(r_{23})/kT} - 1) \, dr_1 dr_2 dr_3 \tag{1.6}$$

For non spherically-symmetrical molecules the relationships become more complex and must take into account the relative orientations of the molecules (Mason and Spurling (1969), Hirschfelder Curtiss and Bird (1954)).

For a gas mixture the virial coefficients depend on the composition of the mixture and one may represent the virial coefficients B_m, C_m, as averages of all possible interactions between groups of molecules and hence write (Mason and Spurling (1969)),

$$B_m = \sum_i \sum_j x_i x_j B_{ij} \tag{1.7}$$

$$C_m = \sum_i \sum_j \sum_k x_i x_j x_k C_{ijk} \tag{1.8}$$

Consequently for a binary mixture, three virial coefficients are needed to describe the binary interactions, while the third virial coefficient, representing ternary interactions has four terms,

$$B_m = x_1^2 B_{11} + 2x_1x_2 B_{12} + x_2^2 B_{22} \tag{1.9}$$

and $$C_m = x_1^3 C_{111} + 3x_1^2x_2C_{112} + 3x_1x_2^2C_{122} + x_2^3C_{222} \tag{1.10}$$

where x_1, x_2 are the mole fractions of components 1 and 2, B_{11}, B_{22} are the second virial coefficients of the pure components, and B_{12} is the second virial coefficient of the unlike molecule interactions. Similarly C_{111}, C_{222} are the third virial coefficients for the pure components, and C_{112}, C_{122} are the third virial coefficients of the unlike molecule interactions.

For mixtures it is convenient to define the excess quantities,

$$\varepsilon = B_{12} - \frac{1}{2}(B_{11} + B_{22}) \tag{1.11}$$

$$F_1 = C_{112} - \frac{1}{3}(2C_{111} + C_{222}) \tag{1.12}$$

and $$F_2 = C_{122} - \frac{1}{3}(C_{111} + 2C_{222}) \tag{1.13}$$

In terms of these excess quantities Equations (1.9) and (1.10) become,

$$B_m = x_1B_{11} + x_2B_{22} + 2x_1x_2\varepsilon \tag{1.14}$$

and $$C_m = x_1C_{111} + x_2C_{222} + 3x_1x_2(x_1F_1 + x_2F_2) \tag{1.15}$$

The problem of relating the properties of a mixture to those of its components then becomes one of relating B_{ij} to B_{ii} and B_{jj}. One common way of doing this is via the Principle of Corresponding States, (Guggenheim (1950)) which provides a method of correlating the behaviour and properties of molecules which all have the same functional form for their intermolecular potential. This method uses the critical properties of the components as scaling factors, so that for the second virial coefficients,

$$B_{ij}/V_{ij}^c = f(T/T_{ij}^c) \tag{1.16}$$

By postulating combining rules pseudocritical properties may be calculated to fit the same framework. One of the commonest sets of combining rules (Prausnitz (1969)) is,

$$T_{12}^c = (T_{11}^c \, T_{22}^c)^{\frac{1}{2}} \tag{1.17}$$

$$V_{12}^c = (V_{11}^{c1/3} + V_{22}^{c1/3})^3/8 \tag{1.18}$$

For the purpose of testing the various sets of combining rules, using second virial coefficient data, it is desirable to have values of B_{ij} at least as accurate as those of B_{ii} and B_{jj}.

The determination of B_{12} from measurements of the second virial coefficient of mixtures is described by Equation (1.9) in the form,

$$B_{12} = (B_m - (x_1^2 B_{11} + x_2^2 B_{22}))/2x_1x_2 \tag{1.19}$$

For $x_1 = x_2 = 0.5$ this becomes

$$B_{12} = 2B_m - (B_{11} + B_{22})/2 \tag{1.20}$$

and if the observable quantities B_m, B_{11}, and B_{22} each have an associated error ∂B, it can be seen that the maximum corresponding error in B_{12} is $\partial B_{12} \simeq 3\partial B$.

To overcome this problem of accumulating error it has become more common recently to measure either the pressure change on mixing at constant volume (Knobler et al (1959)) or the volume change on mixing at constant pressure (Edwards and Roseveare (1942)). These quantities are related to the excess second virial coefficient

$$\varepsilon = B_{12} - (B_{11} + B_{22})/2 \tag{1.11}$$

by the expressions

$$\varepsilon = RTp^E/2x_1x_2p^2(1+p^E/p) \tag{1.21}$$

and

$$\varepsilon = V^E/2x_1x_2 . \tag{1.22}$$

As long as V^E or p^E can be measured sufficiently precisely, values of B_{12} thus obtained are only slightly less accurate than B_{11} and B_{22} used in Equation (1.11).

However a series of measurements of B_{11}, B_{22}, and $\varepsilon(B_{12})$ over a range of temperatures does not necessarily lead to the most precise value of the temperature coefficient dB_{12}/dT. For a pure substance the temperature coefficient dB_{ii}/dT can be determined from the Joule-Thomson coefficient using the relation (Mason and Spurling (1969))

$$\lim_{p\to 0}(dH/dp)_T = B_{ii} - T(dB_{ii}/dT) \tag{1.23}$$

For gas mixtures the Joule-Thomson coefficient is less useful because it leads only to the temperature coefficient of the second virial coefficient of the mixture, dB_m/dT. A more useful quantity is the excess enthalpy of mixing of the gases H_m^E, which is related to ε by the equation

$$\lim_{p\to 0} H_m^E/p = 2x_1x_2(\varepsilon - Td\varepsilon/dT) \tag{1.24}$$

Thus it can be seen that measurements of H_m^E complement those of ε in providing a more accurate description of the behaviour of ε and therefore B_{12} over a wide range of temperature.

In addition to their usefulness in testing intermolecular pair potentials and combining rules B_{11}, B_{22} and ε are often required in more mundane thermodynamic calculations. For example in the study of liquid-vapour equilibria it is ε rather than B_{12} or B_m that is required for the conversion of accurate vapour pressure measurements into excess chemical potentials using the relation (Williamson (1967))

$$\mu_i^E = RT\ln(py_i/p_i^o x_i) + (B_{ii} - v_i^o)(p - p_i^o) + 2py_j^2\varepsilon \tag{1.25}$$

1-1.1 Correlation of Second Virial Coefficients

Many differing types of relations have been used to correlate second virial coefficients. These range from those based on statistical thermodynamics using Equation (1.5)

$$B_{ij} = -2\pi N_A \int_o^\infty (e^{-U_{ij}(r)/kT} - 1) r^2 dr \qquad (1.5)$$

and an appropriate form for the intermolecular pair potential $U_{ij}(r)$ to semi-empirical relations devised to fit the properties of simple fluids and based on the Principle of Corresponding States. Guggenheim (1953) and Knobler (1978) have reviewed these methods of correlating second virial coefficients and compared them with respect to their performance in fitting the known data.

Francis et al (1969) assumed a functional form for B(T) where

$$B(T) = A + B\exp(C/T) \qquad (1.26)$$

to enable them to use the isothermal Joule-Thomson coefficient data for benzene vapour in conjunction with measurements of B and $T^2 d^2B/dT^2$ in an investigation of the temperature dependence of the second virial coefficient of benzene.

1-1.2 Vapour Phase Complexes

An early approach to the problem of explaining gas imperfections was to treat the departure from expected behaviour as a result of gas association. Lambert et al (1949) measured the second virial coefficients of pure vapours and concluded that, for some highly polar substances dimerization, represented by the relation

$$2A \rightleftharpoons A_2 \qquad (1.27)$$

accounted for the large values of the experimental second virial coefficient. These workers postulated that

$$B(\text{expt}) = B(\text{phys}) + B(\text{chem}) \qquad (1.28)$$

where B(phys) is the second virial coefficient calculated from critical data using a corresponding states procedure and accounts for the 'physical' interactions. B(chem.), due to the chemical association described in Equation (1.27), is related to the equilibrium constant

$$K_p = P_{A_2}/P_A^2 \tag{1.29}$$

by the relation (Lambert et al (1949))

$$B(\text{chem}) = -RT\,K_p \tag{1.30}$$

The extension of this treatment to binary mixtures of A + B involves consideration of three possible equilibria,

$$2A \rightleftharpoons A_2 \tag{1.27}$$

$$2B \rightleftharpoons B_2 \tag{1.31}$$

$$A+B \rightleftharpoons AB \tag{1.32}$$

When dealing with the formation of a complex AB, it can be shown (Lambert et al (1959)) that the experimental interaction second virial coefficient can again be written as the sum of two contributions

$$B_{12}(\text{expt}) = B_{12}(\text{phys}) + B_{12}(\text{chem.}) \tag{1.33}$$

where B_{12}(phys) is related to the departures from ideality due to Van der Waals forces and B_{12}(chem) takes into account the effect of chemical association. It will be shown in section 1-3 that

$$B_{12}(\text{chem}) = -RT\,K_p/2 \tag{1.34}$$

where K_p is the formation constant for the complex. If B_{12}(expt), for an associating mixture, is measured and B_{12}(phys) calculated from some set of combining rules B_{12}(chem) and K_p can be obtained.

The standard heat of formation of the complex $\Delta H^{\dagger}$, can be obtained in two ways,

(1) From the relation

$$\underset{p\to 0}{\text{Lt}}\ d(\ln K_p)/d(1/T) = -\Delta H^{\dagger}/R \tag{1.35}$$

by plotting $\ln K_p$ against $1/T$ or

(2) From measurements of the volume of mixing leading to B_{12}(chem) and calorimetric measurements of the heat of mixing.

Because of the simple relationship of the heat of mixing of gases, at low pressures, to the excess second virial coefficient and therefore the interaction second virial coefficient, it was considered worthwhile to develop a method for studying the heats of mixing of gases at low pressures.

1-2 BASIC RELATIONSHIPS

As a starting point in developing expressions for the heat of mixing H_m^E, and the standard heat of reaction $\Delta H^{\dagger}$, we use the thermodynamic relation,

$$(\partial G/\partial p)_T = V \tag{1.36}$$

For a real gas mixture the Gibbs free energy is given by

$$G_m^{rg}(T,p,n_1,n_2\ldots) = G_m^{rg\dagger}(T,n_1,n_2\ldots) + \int_{p^{\dagger}}^{p} V_m dp \tag{1.37}$$

where $G_m^{rg\dagger}(T,n_1,n_2\ldots)$ is the Gibbs free energy of the real gas mixture at some standard pressure $p^{\dagger}$, and can be expressed as

$$G_m^{rg\dagger}(T,n_1,n_2\ldots) = G_m^{rg}(T,p=0,n_1,n_2\ldots) + \int_0^{p^{\dagger}} V_m dp \tag{1.38}$$

Similarly for a perfect gas mixture,

$$G_m^{pg\dagger}(T,n_1,n_2,\ldots) = G_m^{pg}(T,p=0,n_1,n_2,\ldots) + \int_0^{p^{\dagger}} (\Sigma n_i RT/p)\,dp \tag{1.39}$$

$$\text{As } p\to 0 \quad G_m^{rg}(T,p=0,n_1,n_2\ldots) = G_m^{pg}(T,p=0,n_1,n_2,\ldots) \tag{1.40}$$

Consequently Equation (1.38) becomes

$$G_m^{rg\dagger}(T,n_1,n_2\ldots) = G_m^{pg\dagger}(T,n_1,n_2,\ldots)+\int_0^{p^\dagger}(V_m-\Sigma n_i RT/p)\,dp \tag{1.41}$$

If we now use Equation (1.41) Equation (1.37) becomes

$$\begin{aligned} G_m^{rg}(T,p,n_1,n_2,\ldots) &= G_m^{pg\dagger}(T,n_1,n_2,\ldots) + \int_0^{p^\dagger}(V_m-\Sigma n_i RT/p)\,dp \\ &\quad + \int_{p^\dagger}^{p} V_m\,dp \\ &= G_m^{pg\dagger}(T,n_1,n_2,\ldots) + \int_0^{p}(V_m-\Sigma n_i RT/p)\,dp \\ &\quad + \int_{p^\dagger}^{p}(\Sigma n_i RT/p)\,dp \end{aligned} \tag{1.42}$$

The standard Gibbs free energy of a perfect gas mixture is given by the relation,

$$\begin{aligned} G_m^{pg\dagger}(T,n_1,n_2,\ldots) &= \Sigma n_i \mu_i^{pg\dagger}(T,x_i) \\ &= \Sigma n_i \mu_i^{opg\dagger}(T) + \Sigma n_i RT\ln x_i \end{aligned} \tag{1.43}$$

where $\mu_i^{pg\dagger}(T,n_i)$ is the standard chemical potential of component i in the mixture and $\mu_i^{opg\dagger}(T)$, the standard chemical potential of pure i.

Equation (1.42) is then written as

$$\begin{aligned} G_m^{rg}(T,p,n_1,n_2,\ldots) &= \Sigma n_i \mu_i^{opg\dagger}(T) + \Sigma n_i RT\ln x_i + \int_{p^\dagger}^{p}(\Sigma n_i RT/p)\,dp \\ &\quad + \int_0^{p}(V_m - \Sigma n_i RT/p)\,dp \end{aligned}$$

i.e.

$$\begin{aligned} G_m^{rg}(T,p,n_1,n_2,\ldots) &= \Sigma n_i \mu_i^{opg\dagger}(T) + \Sigma n_i RT\ln x_i + \Sigma n_i RT\ln(p/p^\dagger) \\ &\quad + \int_0^{p}(V_m - \Sigma n_i RT/p)\,dp \end{aligned} \tag{1.44}$$

1-2.1 Development of an Expression for H_m^E

The excess heat of mixing is related to the excess Gibbs free energy of mixing via the relation,

$$H^E = G^E + TS^E$$

$$= G^E - T(\partial G^E/\partial T)_p \qquad (1.45)$$

The excess Gibbs free energy of mixing can be defined as, (Williamson, (1967)),

$$G^E = \Delta_m G^{rg} - \Delta_m G^{pg} \qquad (1.46)$$

where $\Delta_m G^{rg}$ is the Gibbs free energy change on mixing for the real gas mixture and $\Delta_m G^{pg}$ the corresponding change for the perfect gas mixture and for a binary mixture,

$$\Delta_m G = G_m - (G_1 + G_2) \qquad (1.47)$$

The Gibbs free energies of the mixture and of the pure components can be obtained from Equation (1.44) and hence for a binary mixture of components 1 and 2,

$$G_m^{rg}(T,p,n_1n_2) = n_1\mu_1^{opg\dagger}(T) + n_2\mu_2^{opg\dagger}(T) + n_1RT\ln x_1 + n_2RT\ln x_2 + (n_1 + n_2)RT\ln(p/p^\dagger) + \int_o^p (V_m - (n_1 + n_2)RT/p)dp \qquad (1.48)$$

$$G_1^{rg}(T,p,n_1) = n_1\mu_1^{opg\dagger}(T) + n_1RT\ln(p/p^\dagger) + \int_o^p (V_1 - n_1RT/p)dp \qquad (1.49)$$

and $$G_2^{rg}(T,p,n_2) = n_2\mu_2^{opg\dagger}(T) + n_2RT\ln(p/p^\dagger) + \int_o^p (V_2 - n_2RT/p)dp \qquad (1.50)$$

Combining (1.48), (1.49), and (1.50) an expression for $\Delta_m G^{rg}$ is obtained,

$$\Delta_m G^{rg} = G_m^{rg}(T,p,n_1n_2) - G_1^{rg}(T,p,n_1) - G_2^{rg}(T,p,n_2)$$

$$= n_1RT\ln x_1 + n_2RT\ln x_2 + \int_o^p (V_m - (V_1 + V_2))dp \qquad (1.51)$$

Similarly the Gibbs free energy change on mixing for perfect gases is

$$\Delta_m G^{pg} = n_1RT\ln x_1 + n_2RT\ln x_2 \qquad (1.52)$$

and excess Gibbs free energy of mixing is,

$$G^E = \int_o^p (V_m - (V_1 + V_2))dp$$

$$= \int_o^p V^E \, dp \qquad (1.53)$$

writing

$$V^E = V_m - (V_1 + V_2) \qquad (1.54)$$

Using Equation (1.53) in Equation (1.45) gives,

$$H^E = \int_o^p (V^E - T(\partial V^E/\partial T)_p)dp \qquad (1.55)$$

Using the pressure series virial equation of state (1.2) we can derive an expression for V^E where

$$V^E = V_m - V_1 - V_2$$

$$= (n_1 + n_2)RT/p + (n_1 + n_2)\, B'_m + (n_1 + n_2)C'_m p + \ldots - (n_1 RT/p + n_1 B'_{11}$$

$$+ n_1 C'_{111} p + \ldots) - (n_2 RT/p + n_2 B'_{22} + n_2 C'_{222}\, p + \ldots)$$

$$= ((n_1 + n_2)B'_m - n_1 B'_{11} - n_2 B'_{22}) + ((n_1 + n_2)C'_m - n_1 C'_{111} - n_2 C'_{222})p + \ldots$$

and dividing by $(n_1 + n_2)$ we get

$$v^E = (B'_m - x_1 B'_{11} - x_2 B'_{22}) + (C'_m - x_1 C'_{111} - x_2 C'_{222})p + \ldots \qquad (1.56)$$

Substituting Equation (1.56) into Equation (1.55) yields

$$H^E_m = \int_o^p ((B'_m - x_1 B'_{11} - x_2 B'_{22}) + (C'_m - x_1 C'_{111} - x_2 C'_{222})p + \ldots$$

$$-T((dB'_m/dT - x_1 dB'_{11}/dT - x_2 dB'_{22}/dT) + (dC'_m/dT - x_1 dC'_{111}/dT$$

$$- x_2 dC'_{222}/dT)p + \ldots))dp$$

$$= \int_o^p ((B'_m - x_1B'_{11} - x_2B'_{22}) - Td(B'_m - x_1B'_{11} - x_2B'_{22})/dT +$$

$$p(C'_m - x_1C'_{111} - x_2C'_{222}) - Tpd(C'_m - x_1C'_{111} - x_2C'_{222})/dT + \ldots)dp$$

$$= ((B'_m - x_1B'_{11} - x_2B'_{22}) - Td(B'_m - x_1B'_{11} - x_2B'_{22})/dT)p +$$

$$((C'_m - x_1C'_{111} - x_2C'_{222}) - Td(C'_m - x_1C'_{111} - x_2C'_{222})/dT)p^2/2 + \ldots \quad (1.57)$$

Now using Equations (1.3) and (1.4) in (1.57) and rearranging we get

$$H^E_m = ((B_m - x_1B_{11} - x_2B_{22}) - Td(B_m - x_1B_{11} - x_2B_{22})/dT)p +$$

$$((C_m - x_1C_{111} - x_2C_{222}) - (B^2_m - x_1B^2_{11} - x_2B^2_{22}) - Td((C_m - x_1C_{111}$$

$$- x_2C_{222}) - (B^2_m - x_1B^2_{11} - x_2B^2_{22}))/dT)p^2/2RT + \ldots \quad (1.58)$$

and since from Equations (1.14) and (1.15)

$$B_m - x_1B_{11} - x_2B_{22} = 2x_1x_2\varepsilon \quad (1.59)$$

and $$C_m - x_1C_{111} - x_2C_{222} = 3x_1x_2(x_1F_1 + x_2F_2) \quad (1.60)$$

we can write

$$B^2_m - x_1B^2_{11} - x_2B^2_{22} = x_1B^2_{11}(x_1 - 1) + 2x_1x_2B_{11}B_{22} + x_2B^2_{22}(x_2 - 1) +$$

$$4x_1x_2\varepsilon(x_1B_{11} + x_2B_{22} + x_1x_2\varepsilon)$$

$$= 4x_1x_2\varepsilon(x_1B_{11} + x_2B_{22} + x_1x_2\varepsilon) - x_1x_2(B^2_{11} -$$

$$2B_{11}B_{22} + B^2_{22})$$

$$= x_1x_2(4\varepsilon(x_1B_{11} + x_2B_{22} + x_1x_2\varepsilon) - (B_{11} - B_{22})^2). \quad (1.61)$$

Following Knobler (1978) and combining Equations (1.60) and (1.61) we see that

$$(C_m - x_1C_{111} - x_2C_{222}) - (B^2_m - x_1B^2_{11} - x_2B^2_{22}) = x_1x_2(3(x_1F_1 + x_2F_2)$$

$$+ (B_{11} - B_{22})^2 - 4\varepsilon(x_1B_{11} + x_2B_{22} + x_1x_2\varepsilon))$$

$$= x_1x_2\beta \quad (1.62)$$

where $\beta = (B_{11} - B_{22})^2 + 3(x_1F_1 + x_2F_2) - 4\varepsilon(x_1B_{11} + x_2B_{22} + x_1x_2\varepsilon)$ (1.63)

Finally substituting Equations (1.59) and (1.62) into (1.58) we arrive at an expression for H_m^E as a power series in p

$$H_m^E = 2x_1x_2(\varepsilon - Td\varepsilon/dT)p + x_1x_2(\beta - Td\beta/dT)p^2/2RT + \ldots \quad (1.64)$$

In the limit as the pressure tends to zero,

$$\lim_{p\to 0} H_m^E/p = 2x_1x_2(\varepsilon - Td\varepsilon/dT) \quad (1.24)$$

1-2.2 Joule-Thomson Coefficients

The Joule-Thomson coefficient μ_{J-T} is defined by the relation,

$$\mu_{J-T} = (\partial T/\partial p)_H \quad (1.65)$$

This can be expressed in terms of equation of state via the relations

$$(\partial T/\partial p)_H = -(\partial H/\partial p)_T/(\partial H/\partial T)_p = -\frac{1}{C_p}(\partial H/\partial p)_T \quad (1.66)$$

and $$(\partial H/\partial p)_T = V - T(\partial V/\partial T)_p \quad (1.67)$$

which give,

$$\mu_{J-T} = -\frac{1}{C_p}(V - T(\partial V/\partial T)_p)$$

Substitution for V from an equation of state gives the Joule-Thomson coefficient in terms of T and P. For the case of the pressure series virial equation this is as follows. With

$$v = RT/p + B' + C'p + \ldots \quad (1.68)$$

and $$(\partial v/\partial T)_p = R/p + dB'/dT + pdC'/dT + \ldots \quad (1.69)$$

$$v - T(\partial v/\partial T)_p = (RT/p + B' + C'p + \ldots) - T(R/p + dB'/dT + pdC'/dT + \ldots)$$

$$= B' - TdB'/dT + (C' - TdC'/dT)p + \ldots \quad (1.70)$$

Using the relations

$$B' = B \tag{1.3}$$

$$C' = (C - B^2)/RT \tag{1.4}$$

Equation (1.70) becomes

$$v - T(\partial v/\partial T)_p = B - TdB/dT + (2(C - B^2) - TdC/dT + 2TBdB/dT)p/RT + \ldots \tag{1.71}$$

In the limit as the pressure tends to zero the Joule-Thomson coefficient is given by

$$\lim_{p\to 0} \mu_{J-T} = -\frac{1}{C_p}(B - TdB/dT) \tag{1.72}$$

1-2.3 Chemical Equilibria

For the generalized chemical reaction

$$\nu_A A + \nu_B B \rightleftharpoons \nu_C C + \nu_D D \tag{1.73}$$

the Gibbs free energy change ΔG, is given by

$$\Delta G = \nu_C \mu_C + \nu_D \mu_D - \nu_A \mu_A - \nu_B \mu_B \tag{1.74}$$

The chemical potential of a species is then found using Equation (1.44) namely

$$G_m^{rg}(T,p,n_1,n_2, \ldots) = \Sigma n_i \mu_i^{opg\dagger}(T) + \Sigma n_i RT \ln x_i + \Sigma n_i RT \ln(p/p^\dagger) + \int_o^p (V_m - \Sigma n_i RT/p)\,dp \tag{1.44}$$

and the relation,

$$\mu_i(T,p) = \partial G_m^{rg}(T,p,n_1,n_2,\ldots)/\partial n_i \tag{1.75}$$

Hence Equation (1.74) can be written in the form

$$\Delta G = (\nu_C \mu_C^{opg\dagger} + \nu_D \mu_D^{opg\dagger} - \nu_A \mu_A^{opg\dagger} - \nu_B \mu_B^{opg\dagger}) + RT(\nu_C \ln x_C +$$

$$\nu_D \ln x_D - \nu_A \ln x_A - \nu_B \ln x_B) + RT(\nu_C + \nu_D - \nu_A - \nu_B)\ln(p/p^\dagger) +$$

$$\nu_C \int_o^p \frac{\partial}{\partial n_C}(V_m - \Sigma n_i RT/p)dp + \nu_D \int_o^p \frac{\partial}{\partial n_D}(V_m - \Sigma n_i RT/p)dp -$$

$$\nu_A \int_o^p \frac{\partial}{\partial n_A}(V_m - \Sigma n_i RT/p)dp - \nu_B \int_o^p \frac{\partial}{\partial n_B}(V_m - \Sigma n_i RT/p)dp$$

$$= \Delta G^\dagger + RT \ln \frac{(p_C/p^\dagger)^{\nu_C}(p_D/p^\dagger)^{\nu_D}}{(P_A/p^\dagger)^{\nu_A}(P_B/p^\dagger)^{\nu_B}} +$$

$$\int_o^p ((\nu_C \partial/\partial n_C + \nu_D \partial/\partial n_D - \nu_A \partial/\partial n_A - \nu_B \partial/\partial n_B)(V_m - \Sigma n_i RT/p))dp \quad (1.76)$$

and writing

$$\theta(B) = (\nu_C \frac{\partial}{\partial n_C} + \nu_D \frac{\partial}{\partial n_D} - \nu_A \frac{\partial}{\partial n_A} - \nu_B \frac{\partial}{\partial n_B})(V_m - \Sigma n_i RT/p) \quad (1.77)$$

gives $\Delta G = \Delta G^\dagger + RT\ln K_p + \int_o^p \theta(B)dp$ (1.78)

where $\Delta G^\dagger$ is the standard Gibbs free energy change of the reaction.

At equilibrium the Gibbs free energy is at a minimum and $\Delta G = 0$, consequently,

$$-\Delta G^\dagger/T = R\ln K_p + \frac{1}{T}\int_o^p \theta(B)dp \quad (1.79)$$

Differentiating $\Delta G^\dagger/T$ with respect to $\frac{1}{T}$ yields

$$\partial(\Delta G^\dagger/T)/\partial(1/T) = \Delta G^\dagger + \frac{1}{T}\partial(\Delta G^\dagger)/\partial(1/T)$$

$$= \Delta G^\dagger - \frac{T^2}{T}\partial(\Delta G^\dagger)/\partial T$$

$$= \Delta G^\dagger - T\partial\Delta G^\dagger/\partial T \quad (1.80)$$

Hence the standard heat of reaction $\Delta H^{\dagger}$ is given by

$$-\Delta H^{\dagger} = -\partial(\Delta G^{\dagger}/T)/\partial(1/T)$$

$$= R\partial(\ln K_p)/\partial(1/T) + \int_o^p \theta(B)\,dp + \frac{1}{T}\,\frac{\partial}{\partial(1/T)}\left(\int_o^p \theta(B)\,dp\right)$$

i.e. $$-\Delta H^{\dagger} = R\,\partial(\ln K_p)/\partial(1/T) + \int_o^p \theta(B)\,dp + T\,\frac{\partial}{\partial T}\int_o^p \theta(B)\,dp \qquad (1.81)$$

For the specific case of the formation of a complex

$$A + B \rightleftharpoons AB \qquad (1.32)$$

with n_1 moles of A, n_2 moles of B, and n_3 moles of AB at equilibrium, then using a truncated virial equation

$$pV_m = \Sigma n_i RT + \Sigma n_i B_m p \qquad (1.82)$$

gives $$V_m - \Sigma n_i RT = \Sigma n_i B_m p \qquad (1.83)$$

and from Equation (1.77)

$$\theta(B) = \frac{\partial}{\partial n_3}(\Sigma n_i B_m) - \frac{\partial}{\partial n_1}(\Sigma n_i B_m) - \frac{\partial}{\partial n_2}(\Sigma n_i B_m) \qquad (1.84)$$

Writing n_T for Σn_i and using Equation (1.7) for B_m

$$n_T B_m = n_T \Sigma\Sigma x_i x_j B_{ij}$$

$$= n_1^2 B_{11}/n_T + n_2^2 B_{22}/n_T + n_3^2 B_{33}/n_T + 2n_1 n_2 B_{12}/n_T + 2n_1 n_3 B_{13}/n_T$$

$$+ 2n_2 n_3 B_{23}/n_T \qquad (1.85)$$

Hence

$$\partial(n_T B_m)/\partial n_3 = -n_1^2 B_{11}/n_T^2 - n_2^2 B_{22}/n_T^2 + 2n_3 B_{33}/n_T - n_3^2 B_{33}/n_T^2$$

$$-2n_1 n_2 B_{12}/n_T^2 + 2n_1 B_{13}/n_T - 2n_1 n_3 B_{13}/n_T^2 + 2n_2 B_{23}/n_T$$

$$-2n_2 n_3 B_{23}/n_T^2$$

$$= -x_1^2 B_{11} - x_2^2 B_{22} - x_3^2 B_{33} + 2x_3 B_{33}$$

$$- 2x_1x_2B_{12} + 2x_1B_{13} - 2x_1x_3B_{13} + 2x_2B_{23} - 2x_2x_3B_{23} \qquad (1.86)$$

Similarly

$$\partial(n_TB_m)/\partial n_1 = -x_1^2B_{11} - x_2^2B_{22} - x_3^2B_{33} + 2x_1B_{11} + 2x_2B_{12}$$

$$+ 2x_2B_{13} - 2x_1x_2B_{12} - 2x_1x_2B_{13} - 2x_2x_3B_{23} \qquad (1.87)$$

and

$$\partial(n_TB_m)/\partial n_2 = -x_1^2B_{11} - x_2^2B_{22} - x_3^2B_{33} + 2x_2B_{22} + 2x_1B_{12}$$

$$+ 2x_3B_{23} - 2x_1x_2B_{12} - 2x_1x_3B_{13} - 2x_2x_3B_{23} \qquad (1.88)$$

Consequently substituting (1.86), (1.87) and (1.88) into Equation (1.84) gives,

$$\theta(B) = \partial(n_TB_m)/\partial n_3 - \partial(n_TB_m)/\partial n_1 - \partial(n_TB_m)/\partial n_2$$

$$= x_1^2B_{11} + x_2^2B_{22} + x_3^2B_{33} + 2x_1x_2B_{12} + 2x_2x_3B_{23} + 2x_1x_3B_{13}$$

$$+ 2x_3B_{33} - 2x_3B_{23} - 2x_3B_{13} + 2x_1B_{13} - 2x_1B_{11} - 2x_1B_{12}$$

$$+ 2x_2B_{23} - 2x_2B_{12} - 2x_2B_{22}$$

$$= B_m + 2x_3(B_{33} - B_{23} - B_{13}) + 2x_1(B_{13} - B_{11} - B_{12})$$

$$+ 2x_2(B_{23} - B_{12} - B_{22}) \qquad (1.89)$$

Consequently for the formation of the complex AB, equation (1.81) can be written

$$-\Delta H^{\dagger} = R\,\partial(\ln K_p)/\partial(1/T) + \int_o^p \theta(B)dp + T\,\frac{d}{dT}\int_o^p \theta(B)\,dp$$

$$= R\,\partial(\ln K_p)/\partial(1/T) + \theta(B)p + Tpd\theta(B)/dT$$

$$= R\,\partial(\ln K_p)/\partial(1/T) + (\theta(B) + T\,d\theta(B)/dT)p \qquad (1.90)$$

The question now arises of how much the term $(\theta(B) + Td\theta(B)/dT)_P$ contributes to the value of $\Delta H^{\dagger}$. We can estimate an approximate value for $\theta(B)$ by making the following assumptions:-

(1) The concentration of the complex is small and the term in x_3 can be neglected.

(2) The cross virial coefficients B_{13} and B_{23} can be approximated by the relations

$$B_{13} \simeq (B_{11} + B_{33})/2 \tag{1.91}$$

and $$B_{23} \simeq (B_{22} + B_{33})/2 \tag{1.92}$$

(3) The second virial coefficient of the complex can be approximated by

$$B_{33} \simeq B_{11} + B_{22} \tag{1.93}$$

(4) The second virial coefficient of the mixture B_m due to the first assumption above is given by

$$B_m = x_1^2 B_{11} + 2x_1x_2B_{12} + x_2^2B_{22} \tag{1.9}$$

Applying these assumptions, i.e. substituting Equations (1.91), (1.92), (1.93), and (1.9) into the expression for $\theta(B)$, (1.89) yields

$$\theta(B) \simeq x_1^2B_{11} + 2x_1x_2B_{12} + x_2^2B_{22} + 2x_1(B_{22}/2 - B_{12}) + 2x_2(B_{11}/2 - B_{12})$$

i.e. $$\theta(B) \simeq B_{11}(x_1^2 + x_2) + B_{12}(2x_1x_2 - 2x_1 - 2x_2) + B_{22}(x_2^2 + x_1)$$

and making the further assumption that $x_1 = x_2 = 0.5$ gives,

$$\theta(B) \simeq 0.75\ B_{11} - 1.5B_{12} + 0.75\ B_{22}$$

$$\simeq -1.5(B_{12} - \tfrac{1}{2}(B_{11} + B_{22}))$$

$$\simeq -1.5\varepsilon. \tag{1.94}$$

Using this approximation for $\theta(B)$ in Equation (1.90) yields

$$-\Delta H^{\dagger} \simeq R\partial(\ln K_p)/\partial(1/T) - 1.5(\varepsilon + Td\varepsilon/dT)p \qquad (1.95)$$

It must be recognised that the term $(\theta(B) + Td\theta(B)/dT)_p$ represents the contribution to $\Delta H^{\dagger}$ of the nonideality of mixing and as such is a 'physical' interaction. A study of systems with solely 'physical' interactions shows that for a pressure of p = 100 kPa the 'physical term' is of the order of 300 J mol^{-1}. On the other hand the term $(\partial(\ln K_p)/\partial(1/T)$, in hydrogen bonding systems, involves values of typically around 20 $kJmol^{-1}$ with uncertainties of ±2 kJ mol^{-1}. Effectively the 'physical term' can be neglected for pressures below 100 kPa (though for higher pressures it may become more significant) and Equation (1.81) can be written

$$\lim_{p\to 0} \partial(\ln K_p)/\partial(1/T) = -\Delta H^{\dagger}/R \qquad (1.35)$$

1-3 VAPOUR PHASE COMPLEXES

1-3.1 Review of Previous Work

Chemical association has been postulated as the cause of deviations from ideal behaviour in both liquid and gaseous systems. Lambert et al (1949) assumed the dimerization of a pure vapour

$$2A \rightleftharpoons A_2 \qquad (1.27)$$

to explain the experimental values of the second virial coefficient, B in Equation (1.1), which were more negative than expected. They treated the second virial coefficient as consisting of two contributions

$$B(expt) = B(phys) + B(chem) \qquad (1.28)$$

where $B(chem) = -RT\,K_p$ (1.30)

K_p being the formation constant of the dimer.

This hypothesis was extended to binary mixtures of A + B where three possible equilibria can be considered,

$$\text{I} \quad 2A \rightleftharpoons A_2 \tag{1.27}$$

$$\text{II} \quad 2B \rightleftharpoons B_2 \tag{1.31}$$

$$\text{III} \quad A+B \rightleftharpoons AB \tag{1.32}$$

Fox and Lambert (1951) studied mixtures of chloroform and diethyl-ether in which the equilibrium (III) above was assumed, while Lambert Murray and Sanday (1954) investigated the binary mixtures of a non-polar substance, chloroform, with the polar gases diethylamine, acetone and acetronitrile in which the first equilibrium was assumed. Lambert et al (1959) extended the studies to include consideration of the first and third equilibria operating at the same time. This was done by measuring the second virial coefficients of chloroform with methyl formate, methyl acetate, ethyl acetate and diethylamine. These workers assumed that the esters and amine were partially dimerized and were also involved in hydrogen bonding with the chloroform. Prausnitz and Carter (1960) studied the formation of a complex from mixtures of acetaldehyde and acetronitrile, which both dimerize to some extent, so that all three equilibria were present. Chen, O'Connell and Prausnitz (1966) studied complex formation in ammonia-acetylene mixtures while Rätzsch and Freydank (1971) inferred the existence of vapour phase complexes, of ethylene with ammonia, and methanol and of methanol with pentane, from virial coefficient data. Dantzler and Knobler (1969) reported complex formation in benzene and hexafluorobenzene vapour mixtures while King and coworkers (1966), (1971), (1972), (1973), and (1973) have obtained association constants for CO_2 with naphthalene (1966), methanol (1972), ethanol (1973), and diethyl ether, (1973) and for H_2O with CO_2 and N_2O (1971).

A list of systems in which chemical association has been used to explain abnormal behaviour appears in Appendix 2.

1.3.2 Basic Relationships

Consider the case of a binary mixture of associating, but otherwise perfect, gases A and B represented by the equilibrium,

$$A + B \rightleftharpoons AB \tag{1.27}$$

with initially n_1 moles of A and n_2 moles of C. Then if n_3 moles of AB were formed at equilibrium the formation constant

$$K_p = p_{AB}/p_A p_B \tag{1.95}$$

$$= (n_3 RT/V_m)(V_m/(n_1 - n_3)RT)(V_m/(n_2 - n_3)RT)$$

$$= n_3 V_m/RT\,(n_1 - n_3)(n_2 - n_3) \tag{1.96}$$

If the concentration of the complex is assumed to be small, (i.e. $n_3 << n_1, n_2$) then Equation (1.96) becomes,

$$K_p \simeq V_m n_3/n_1 n_2 RT \tag{1.97}$$

Applying the virial equation of state to the mixture and allowing for the change in the number of moles due to complex formation gives,

$$pV_m/RT = (n_1 + n_2 - n_3)(1 + B_m/v_m + \ldots)$$

$$= (n_1 + n_2)(1 - n_3/(n_1 + n_2)) + (n_1 + n_2 - n_3)B_m/v_m + \ldots$$

and since it is assumed that $n_3 << n_1 + n_2$, using Equation (1.97) as an expression for n_3 we can write

$$pV_m/RT = (n_1 + n_2)(1 - n_1 n_2 RTK_p/V_m(n_1 + n_2)) + (n_1 + n_2)B_m/v_m + \ldots$$

The equation can be rewritten in the form,

$$pv_m/RT = 1 - x_1 x_2 RTK_p/v_m + B_m/v_m + \ldots \tag{1.98}$$

Now B_m is given by Equation (1.7) namely

$$B_m = \sum_i \sum_j x_i x_j B_{ij} \qquad (1.7)$$

$$= x_1^2 B_{11} + x_2^2 B_{22} + x_3^2 B_{33} + 2x_1x_2B_{12} + 2x_1x_3B_{13} + 2x_2x_3B_{23} \qquad (1.99)$$

As the concentration of the complex has been assumed to be small, i.e. $n_3 \ll (n_1 + n_2)$ and therefore $x_3 \ll 1$, B_m can be approximated by,

$$B_m \simeq x_1^2 B_{11} + 2x_1x_2B_{12} + x_2^2 B_{22} \qquad (1.100)$$

where the contribution to the binary interactions by the complex has been assumed to be negligible. Equation (1.98) then becomes,

$$pv_m/RT = 1 + (x_1^2 B_{11} + 2x_1x_2B_{12} - x_1x_2RTK_p + x_2^2 B_{22})/v_m + \ldots$$

$$= 1 + (x_1^2 B_{11} + 2x_1x_2(B_{12} - RTK_p/2) + x_2^2 B_{22})/v_m + \ldots \qquad (1.101)$$

The simple virial equation for the gas mixture would be

$$pv_m/RT = 1 + (x_1^2 B_{11} + 2x_1x_2B_{12}^o + x_2^2 B_{22})/v_m + \ldots \qquad (1.102)$$

where B_{12}^o the observed interaction second virial coefficient resulting from the separate contributions of 'physical interactions', $B_{12}(\text{phys})$, and 'chemical interactions', $B_{12}(\text{chem})$, is given by the relation,

$$B_{12}^o = B_{12}(\text{phys}) - RTK_p/2 \qquad (1.103)$$

with $B_{12}(\text{chem}) = -RTK_p/2 \qquad (1.34)$

If B_{12}^o has been measured and $B_{12}(\text{phys})$ is calculated using some set of combining rules then $B_{12}(\text{chem})$ and hence K_p can be found. The basic assumption inherent in this argument is that the effect of the complex on B_m is such that it can be neglected.

The next step is to determine the standard enthalpy of formation of the complex. This can be found using the relation,

$$\lim_{p \to 0} \partial \ln K_p / \partial(1/T) = -\Delta H^\dagger/R \qquad (1.35)$$

and plotting ln K_p against (1/T).

The question also arises of how to determine $\Delta H^{\dagger}$ from calorimetric measurements of the heat of mixing. The overall process, that occurs in the calorimeter, can be represented by

$$A^{o}(T,p) + B^{o}(T,p) \longrightarrow (1-\alpha)A(T,p) + (1-\alpha)B(T,p) + \alpha\, C(T,p) \qquad (1.104)$$

where pure A and pure B are mixed to give a mixture of A, B and C at temperature T, and pressure p. The process represented by Equation (1.104) can be broken down into a series of single step processes each with an associated enthalpy change. They are:-

I $\quad \alpha\, A^{o}(T,p=0) + \alpha B^{o}(T,p=0) \longrightarrow \alpha C^{o}(T,p=0)$

with $\Delta H_I = \alpha \Delta H^{\dagger}$

II $\quad \alpha\, C^{o}(T,p=0) + (1-\alpha)A^{o}(T,p=0) + (1-\alpha)B^{o}(T,p=0) \longrightarrow (1-\alpha)A(T,p=0) + (1-\alpha)B(T,p=0) + \alpha C(T,p=0)$

with $\Delta H_{II} = 0$

III $\quad A^{o}(T,p=0) \longrightarrow A^{o}(T,p)$

with $\Delta H_{III} = \int_o^p (\partial H_A^o/dp)_T dp$

$= \int_o^p (V_A^o - T(\partial V_A^o/\partial T)_p) dp$

IV $\quad B^{o}(T,p=0) \longrightarrow B^{o}(T,p)$

with $\Delta H_{IV} = \int_o^p (V_B^o - T(\partial V_B^o/\partial T)_p) dp$

V $\quad (1-\alpha)A(T,p=0) + (1-\alpha)B(T,p=0) + \alpha C(T,p=0) \longrightarrow (1-\alpha)A(T,p) + (1-\alpha)B(T,p) + \alpha C(T,p)$

with $\Delta H_V = \int_o^p (V_m - T(\partial V_m/\partial T)_p) dp$

where V_m is the volume of the mixture. The overall process can be seen to be given by the summation of the single step processes,

$$\text{Overall} = \text{I} + \text{II} - \text{III} - \text{IV} + \text{V} \tag{1.105}$$

with the resulting enthalpy change,

$$\begin{aligned}\Delta H(\text{overall}) &= \Delta H_I + \Delta H_{II} - \Delta H_{III} - \Delta H_{IV} + \Delta H_V \\ &= \alpha\Delta H^{\dagger} - \int_o^p (V_A^o - T(\partial V_A/\partial T)_p)dp - \int_o^p (V_B^o - T(\partial V_B^o/\partial T)_p)dp \\ &\quad + \int_o^p (V_m - T(\partial V_m/\partial T)_p)dp \\ &= \alpha\Delta H^{\dagger} + \int_o^p ((V_m - V_A^o - V_B^o) - T(\partial(V_m - V_A^o - V_B^o)/\partial T)_p)dp\end{aligned} \tag{1.106}$$

If it is assumed that the concentration of the complex is small then the contribution of the complex to the volume of the mixture can be neglected and the mixture assumed to consist of only A and B. The term $(V_m - V_A^o - V_B^o)$ then takes a special significance. From Equation (1.54)

$$V_p^E = V_m - (V_A^o + V_B^o) \tag{1.107}$$

is the hypothetical excess volume on mixing due to the 'physical interactions' between A and B only. Equation (1.106) can now be written as,

$$\begin{aligned}\Delta H(\text{overall}) &= \alpha\Delta H^{\dagger} + \int_o^p (V_p^E - T(\partial V_p^E/\partial T)_p)dp \\ &= \alpha\Delta H^{\dagger} + H^E(\text{phys})\end{aligned} \tag{1.108}$$

where $H^E(\text{phys})$ is the heat of mixing due to the 'physical interactions' between A and B. The term $\alpha\Delta H^{\dagger}$ can be seen as the 'heat of mixing' due to the formation of the complex AB and Equation (1.108) can thus be written in the form,

$$H^E(\text{overall}) = H^E(\text{chem}) + H^E(\text{phys}) \tag{1.109}$$

Consequently if $H^E(\text{overall})$ is measured and $H^E(\text{phys})$ can be calculated then the standard enthalpy of formation can be found from the value of $H^E(\text{chem})$.

For the case where there are initially n_1 moles of A, n_2 moles of B and n_3 moles of AB formed at equilibrium

$$H^E(\text{chem}) = n_3 \Delta H^\dagger \tag{1.110}$$

or $$H_m^E(\text{chem}) = n_3 \Delta H^\dagger/(n_1 + n_2)$$

$$= z_3 \Delta H^\dagger \tag{1.111}$$

where $$z_3 = n_3/(n_1 + n_2) \tag{1.112}$$

To determine z_3 note that the equilibrium constant can be written,

$$K_x = n_3(n_1 + n_2 - n_3)/(n_1 - n_3)(n_2 - n_3)$$

$$= n_3(n_1 + n_2)(1 - z_3)/(n_1 - n_3)(n_2 - n_3) \tag{1.113}$$

whence

$$z_3(1 - z_3) = K_x(x_1 - z_3)(x_2 - z_3)$$

$$= K_x(x_1x_2 - z_3(x_1 + x_2) + z_3^2)$$

$$= x_1x_2K_x - z_3(1 - z_3)K_x$$

and $$z_3(1 - z_3) = x_1x_2K_x/(1 + K_x) \tag{1.114}$$

As it has been assumed that the concentration of the complex is small, i.e. $n_3 \ll n_1 + n_2$ and $z_3 \ll 1$ Equation (1.114) can be written

$$z_3 \simeq x_1x_2K_x/(1 + K_x) \tag{1.115}$$

Using the general relation,

$$K_p = pn_3(n_1 + n_2 - n_3)/p(n_1 - n_3)p(n_2 - n_3)$$

$$= K_x/p \tag{1.116}$$

Equation (1.115) becomes

$$z_3 = pK_p x_1 x_2/(1 + pK_p) \tag{1.117}$$

and substituting for z_3 in Equation (1.111) gives the expression,

$$(H_m^E/p)(\text{chem}) = \Delta H^\dagger x_1 x_2 K_p/(1 + pKp) \tag{1.118}$$

The next step is to determine the heat of mixing due to the physical interactions $H_m^E(\text{phys})$. From Equation (1.24), it can be seen that,

$$(H_m^E/p)(\text{phys}) = 2x_1 x_2(\varepsilon(\text{phys}) - Td\varepsilon(\text{phys})/dT) \tag{1.119}$$

$$\text{with } \varepsilon(\text{phys}) = B_{12}(\text{phys}) - (B_{11}^o + B_{22}^o)/2 \tag{1.120}$$

and where $B_{12}(\text{phys})$, the interaction second virial coefficient due to the 'physical interactions' is calculated using some set of combining rules, and B_{11}^o; B_{22}^o are the observed second virial coefficients for the pure components.

Once $(H_m^E/p)(\text{phys})$ is known and $(H_m^E/p)(\text{overall})$ has been measured $(H_m^E/p)(\text{chem})$ is then found by difference. From a knowledge of the equilibrium constant K_p the standard heat of formation of the complex can be found using Equation (1.118).

2. EXPERIMENTAL METHOD

2-1 REVIEW OF PREVIOUS HEATS OF MIXING OF GASES MEASUREMENTS

Direct measurements of the heat of mixing of gases fall into two well defined categories, those performed at high pressures ($p>10^3$ kPa), and those at low pressures ($p<100$ kPa). A summary of the systems studied at high pressures can be found in Appendix 1. The low pressure work is listed in Table 2-1.

2-1.1 High Pressure Heats of Mixing

Pioneering work on the heats of mixing of gases at high pressures was done at the Kamerlingh-Onnes Laboratory where Beenakker and Coremans reported some preliminary results in 1962. This was followed by the work of Beenakker et al (1965), Knoester, Taconis and Beenakker (1967), and Van Eijnsbergen and Beenakker (1968), who extended the range of systems studied. Later authors included Lee, and Mather (1970), Klein, Bennett and Dodge (1971), and Hejmadi, Katz, and Powers (1971). The latest results come from Wormald and co-workers (1977) who have investigated the pressure dependence of the enthalpy of mixing with measurements ranging from the gas phase, through the two phase, and supercritical regions, into the liquid region as the pressure was increased.

2-1.2 Low Pressure Heats of Mixing

Very few low pressure heats of mixing of gases have been reported. Williamson (1966) first investigated the use of a flow calorimeter for studying the low pressure heat of mixing for Benzene and Cyclohexane vapours. This work was extended by Judd (1969) while Wormald, (1969), presented results for six systems over a range of temperatures. The latest reported results come from Wormald (1977).

TABLE 2-1

LOW PRESSURE HEAT OF MIXING OF GASES,

SYSTEMS STUDIED TO DATE.

Source	System	Temperature/K	Pressure/kPa
Williamson (1966)	Benzene-Cyclohexane	359	101.3
Judd (1969)	Benzene-Cyclohexane	358	101.3
Wormald (1969)	Nitrogen-Benzene	363, 373, 383	101.3
	Nitrogen-Cyclohexane	363, 373, 383	101.3
	Benzene-Cyclohexane	373	101.3
	Nitrogen-Acetone	343, 353, 363	101.3
	Nitrogen-Chloroform	343, 353, 363	101.3
	Acetone-Chloroform	343, 353, 363	101.3
Wormald (1977)	Benzene-Methane	363 to 413 Step 10*	101.3
	Cyclohexane-Methane	363 to 413 Step 10	101.3
	Benzene-Cyclohexane	363 to 413 Step 10	101.3
This Work	Benzene-Cyclohexane	358	101.3
	Benzene-Cyclohexane	323	21
	Benzene-Cyclohexane	315	19
	Benzene-Cyclohexane	305	14
	Acetone-Chloroform	343	20, 53, 87
	Acetone-Chloroform	323	53

* This indicates that this system was studied at 363 K, 373 K, 383 K, 393 K, 403 K, and 413 K, i.e. at intervals of 10 K.

2-2 REVIEW OF EXPERIMENTAL METHODS

The measurement, to any reasonable degree of accuracy, of the thermal properties of systems with low heat capacities, and in which the energy effects are small, is best carried out by flow calorimetry. In such methods the heat capacity of the calorimeter is not involved once steady state operation has been reached.

For measurements done at high pressure all workers so far have measured the heat of mixing of gases with a single observation. Once the gas streams have mixed the temperature of the gas stream is bought back up to that of the inlet gas streams by means of an electrical heater. When isothermal operation has been reached the heat of mixing is calculated from measurements of the flow rates, heater power, inlet and outlet gas composition, pressures, and temperatures.

The conditions existing in the calorimeter have been such that the heat leakage to the surroundings from the calorimeter can be assumed to be negligible.

Because few measurements of the heat of mixing of gases have been performed at low pressures, it was decided to base the calorimeter design on those used for vapour heat capacity measurements. A review of such calorimeters has been carried out by McCullough and Waddington (1968). For such flow calorimeters it is possible to differentiate between the various types of general calorimeter design according to the functional form of the heat exchange with the surroundings. The three main types of calorimeter are those in which:

(1) Heat exchange is proportional to the inverse of the flowrate squared. This approach, first described by Scheele and Heuse (1912), has not been further developed into a modern precision method.

(2) Heat exchange is proportional to the inverse of the flow rate. This design was initiated by Pitzer (1941) and is known as the 'non-adiabatic' method.

(3) Heat exchange is reduced to a very low level by the use of heated shielding. This is known as the 'nearly-adiabatic' flow calorimeter, as small corrections for heat loss must still be made. This design is exemplified by the work of Scott and Mellors (1945).

Of the three types of calorimeter the 'non-adiabatic' type is the only one which has been used widely and consequently it was decided to construct a calorimeter of the 'non-adiabatic' type for the low pressure measurements of the heats of mixing of gases.

2-3 CALORIMETER LAYOUT

The layout of the calorimeter and thermocouples is shown schematically in Figures 2-1 and 2-2.

All temperature differences are expressed as the emfs generated by the thermocouples.

For the arrangement in Fig. 2-2 we can define two temperature differences

$$\Delta T1 = TC1 - TC2 \qquad (2.1)$$

and

$$\Delta T2 = TC3 - TC2 \qquad (2.2)$$

where $\Delta T1$ is the temperature difference between the inlet gas streams and $\Delta T2$ is the temperature difference across the heater. Both $\Delta T1$ and $\Delta T2$ are expressed in μV and are associated with temperature differentials $\Delta t1$ and $\Delta t2$.

When the calorimeter is in an isothermal state (i.e. no gas flow) Δt is zero but ΔT may not be zero due to strain in the thermocouple arrangement arising from its construction. This residual emf is known as the point of zero temperature difference $\Delta T_o/\mu V$. Hence $\Delta T1_o$ corresponds to a zero temperature difference between TC1 and TC2 and $\Delta T2_o$ corresponds to a zero temperature difference between TC2 and TC3.

2.3.1 Joule-Thomson Effects in Flow Calorimeters

A problem that can arise in flow calorimetry is the Joule-Thomson cooling of a gas due to the pressure drop through the calorimeter. For a calorimeter used in measuring heat capacities such cooling can be compensated for by measuring the temperature difference across the heater $\Delta T2$, for the energized state (heater power turned on) and the non-energized state. The temperature rise for a set power input is then taken as the difference between $\Delta T2$ (energized) and $\Delta T2$ (non-energized). However no such compensation can be made in a heat of mixing calorimeter as in the non-energized state there exists a temperature difference due to the mixing of the gases and any Joule-Thomson cooling can not be detected.

As a consequence the pressure drop through the calorimeter must be kept as low as possible. This desire for a low pressure drop conflicts with the need for complete mixing of the two gases, which can only be achieved by having a sufficiently high linear velocity, to establish a turbulent flow regime, and implies a high pressure drop.

A characteristic of any fluid flow is the dimensionless Reynolds number given by (Perry(1963))

$$N_{Re} = D\bar{V}\rho/\mu \qquad (2.3)$$

where D is the equivalent diameter of the flow path, $\bar{V}$ is the linear flow velocity, ρ is the fluid density and μ the viscosity.

The Reynolds number is a ratio of the inertial forces in the fluid to the viscous forces which retard the fluid elements from slipping over each other.

For a value of $N_{Re} < 2100$ the fluid flow is said to be laminar and there is very little mixing of the fluid elements, and any mixing that occurs will occur by diffusion. For a $N_{Re} > 4000$ the flow is said to be turbulent with violent eddying causing rapid mixing of the fluid elements. Consequently as a criterion for mixing N_{Re} must be > 4000.

The pressure drop for fluid flow is given by the relation (Perry 1963))

$$\Delta P = 4f L \bar{V}^2/D\rho \qquad (2.4)$$

where D, $\bar{V}$ and ρ are as before, L is the fluid path length over which the pressure drop is calculated, and f is the 'friction factor' which depends on the relative magnitude of the inertial forces in the fluid to the viscous forces which retard the fluid elements from slipping over each other. As the Reynolds number is a ratio of these forces a plot of ln f against ln N_{Re} yields in practice two lines

(1) $N_{Re} \leqslant 2100$ i.e. streamline or laminar flow

(2) $N_{Re} \geqslant 4000$ i.e. turbulent flow.

The design of the flow calorimeter geometry is a compromise between the two effects, turbulent flow required for mixing and the minimising of Joule-Thomson cooling. The procedure adopted was to design the heater section with a N_{Re} of 5000 to promote mixing over the heater and a N_{Re} of 1600 elsewhere to minimise the pressure drop through the calorimeter. Once the design pressure drop is known an estimate of Joule-Thomson cooling can be found using the known Joule-Thomson coefficient data.

2-4 EXPERIMENTAL METHOD AND PROCEDURE

This section will outline the method and procedure used in determining the heat of mixing of two gases. The method followed depends in detail on whether the heat of mixing is endothermic or exothermic but the procedure is essentially the same in both cases.

It has been shown, Section 1-2, that the heat of mixing of gases can be expressed as a power series in pressure

$$H_m^E = 2x_1x_2\ (\varepsilon - Td\varepsilon/dT)p \ + \text{higher terms} \qquad (1.64)$$

and $$\lim_{p\to 0} H_m^E/p = 2x_1x_2\ (\varepsilon - Td\varepsilon/dT) \qquad (1.24)$$

which is independent of pressure. Consequently we are interested not just in measuring H_m^E but in determining H_m^E/p.

2-4.1 Endothermic Mixing

In this case the temperature falls on mixing and $\Delta T2$ is negative. With no gas flow and the calorimeter in an isothermal state $\Delta T2_o$ is measured. The gas flows are then established at a given total flowrate and composition.

Once the apparatus is at steady state the heater is switched on and readings of heater power (W_h) and $\Delta T2$ are made. A plot of $\Delta T2$ vs W_h is drawn and W_{ho}, the heater power required to bring the gas temperature back to its input temperature and thus compensate for the heat of mixing, is found by interpolation as shown in Figure 2-3.

From this and knowledge of the total flowrate, f_T, and pressure p, an 'apparent heat of mixing', $H_m^{E'}$ can be found

$$H_m^{E'}/p = W_{ho}/f_T\ p \qquad (2.5)$$

In a 'non adiabatic' calorimeter heat losses to the surroundings, which are proportional to $1/f_T$, determine the value of the 'apparent heat of mixing'. To obtain the true heat of mixing, H_m^E, these heat losses must be reduced to zero and this is assumed to happen at infinite gas

flow rate.

To do this the procedure described above is repeated for at least four different flowrates and a plot of $H_m^{E'}/p$ vs $1/f_T$ is obtained, Figure 2-4.

The heat of mixing, corrected for heat exchange, is then found by extrapolation to infinite gas flow rate (i.e. $1/f_T = 0$). The range of flowrates is chosen such that the extrapolation is kept as small as possible.

2-4.2 Exothermic Mixing

In this case the gas temperature rises on mixing. Initially $\Delta T2_o$, the point of zero temperature difference, is measured and the gas flows are then established at a given total flowrate and composition. Once steady state operation has been reached the temperature rise across the heater ($\Delta T2_m$), due to the energy release (W_o) on the mixing of the gases only, is measured.

Finally the heater is switched on and a plot of $\Delta T2$ vs W_h is obtained as before.

The quantity desired is W_o the amount of energy released on the mixing of the gases. This can be found by extrapolating the curve obtained back to the point of zero temperature difference ($\Delta T2_o$), Fig. 2-5. The apparent heat of mixing $H_m^{E'}$, is then found from W_o and measurements of pressure (p), and total flowrate (f_T)

$$H_m^{E'}/p = W_o/f_T\ p \qquad (2.6)$$

This procedure is repeated for at least four different flowrates and the true heat of mixing found as before from a plot of $H_m^{E'}/p$ vs $1/f_T$.

2-5 ANALYSIS OF ERRORS

The heat of mixing is not calculated directly from a single set of measurement but involves several sets of measurements and evolves from the use of a graphical extrapolation. It is not possible, therefore, to do a direct error analysis. An indirect analysis can be done by analysing the two steps involved, in determining the heat of mixing, separately. These two steps are:-

(1) The calculation of the apparent heat of mixing $H_m^{E'}/p$ and

(2) The determination of the true heat of mixing H_m^E/p.

2-5.1 Apparent Heat of Mixing

The calculation of $H_m^{E'}/p$ involves a graphical interpolation of the $\Delta T2$ vs W_h plot and is given by the relation

$$H_M^{E'}/p = W_{ho}/f_T\, p \tag{2.5}$$

where W_{ho} is given by the equation of the regression of W_h on $\Delta T2$, namely

$$W_{ho} = A\Delta T2_o + B \tag{2.7}$$

A and B are the regression coefficients and are calculated by the method of least squares (Topping (1955)), details of which can be found in Appendix 5. Equation (2.5) then becomes

$$H_m^{E'}/p = (A\Delta T2_o + B)/f_T\, p \tag{2.8}$$

Using the δ notation for errors equation (2.8) becomes

$$\frac{\delta(H_m^{E'}/p)}{H_m^{E'}/p} = \frac{A\delta\Delta T2_o + \Delta T2_o\,\delta A + \delta B}{A\Delta T2_o + B} + \frac{\delta f_T}{f_T} + \frac{\delta p}{p} \tag{2.9}$$

Hence the error in the apparent heat of mixing can be determined from equation (2.9). Having obtained sufficient values of $H_m^{E'}/p$ a plot of $H_m^{E'}/p$ vs $1/f_T$ is used to determine the true heat of mixing H_m^E/p.

2-5.2 True Heat of Mixing

This involves a graphical extrapolation of the apparent heat of mixing $H_m^{E'}/p$ vs the reciprocal of the flowrate, $1/f_T$, to the point where $1/f_T = o$, i.e. $f_T \to \infty$. The regression of $H_m^{E'}/p$ on $1/f_T$ is calculated (Topping (1955)) where

$$H_m^{E'}/p = C/f_T + D \qquad (2.10)$$

The true heat of mixing is then given by the value of the coefficient D. The error in D is only a measure of the scatter in the points $(H_m^{E'}/p,\ 1/f_T)_i$ used to calculate the coefficients and does not take into account the errors in the actual values of $H_m^{E'}/p$. Consequently when determining the error $\delta(H_m^E/p)$, of the true heat of mixing, the errors $\delta(H_m^{E'}/p)$ in the apparent heat of mixing results must be considered. Hence the error in H_m^E/p is given by

$$\delta(H_m^E/p) = \delta D + \overline{\delta(H_m^{E'}/p)} \qquad (2.9)$$

where $\overline{\delta(H_m^{E'}/p)}$ is the average of the errors of the $H_m^{E'}/p$ values used to determine H_m^E/p.

3. APPARATUS

This Chapter will describe the apparatus needed for flow calorimetry, its operation, and the tests carried out on it.

3-1. THE FLOW SYSTEM

The flow system is shown in Figure 3-1. The syringe pumps provide, through the flow control network, stable liquid flows which are vaporized in the boiler and brought to the thermostat temperature before they enter the calorimeter, where the inlet gas temperatures are compared. Mixing then occurs and the mixture flows over the heater and remaining thermocouples before it leaves the calorimeter. The mixture then passes through a length of spiral tubing which protects the calorimeter from changes in the ambient air temperature. The gas mixture travels via a line, kept just above thermostat temperature by means of a heating tape, to the vapour collection system where it is condensed and collected. The pressure of the boiler, calorimeter and vapour collection system is maintained by the pressure controller and measured by a mercury in glass manometer mounted on a boxwood scale.

3-2. CALORIMETER PUMPS

These pumps, designed and built by Judd (1969), are of the syringe type. The main body of the pump is shown in Figure 3-2.

A brass piston (8) is driven by a precision lead screw (12) up a brass cylinder. A liquid tight seal between the cylinder and piston is provided by means of a teflon rope gland (9) whose tightness is adjusted by means of the nuts (10). The outlet of the pump is a standard Q.V.F. blank end modified as shown.

The pump was designed so that a lead screw speed of approximately one rpm, which corresponds to a liquid flow of 1.96 ml/min, was required. This was achieved by using a Philips stepping motor, AU5105/81, in conjunction with a Philips gear box, AU5300/80 DP, which had a gear reduction of 75:1. The motor speed range was stated to be 0 to 200 rpm and the use of the gear box produced a lead screw speed range of approximately 0 to 3 rpm, as well as increasing the torque supplied by the motor, to the value required to drive the pumps. Even so, at the higher speeds the torque was still insufficient to drive the pumps and consequently the motors were operated with a speed range of 0 to 125 rpm, which corresponds to a liquid flow rate range of 0 to 3.3 ml/min.

The speed of the stepping motors is controlled by the electrical pulse rate fed to the motor driving circuits, (Philips Electronic Switch 2P 727 86). The rotor of the stepping motor turns through an angle of 7.5^{o} for each pulse supplied to the driving circuits. Consequently if a pulse rate of 100 Hz is fed into the driving circuits, the motor will have a speed of 100 x (7.5/360) x 60 rpm or 125 rpm. Provided that the pulse rate is kept constant, the rotor speed is constant but quantised in units of 7.5^{o}. This small pulsation is reduced to negligible proportions by the high ratio of the gear box.

The motor speed, and therefore the liquid flow rate, is determined by the pulse rate fed to the motor driving circuits. In order to be able to obtain flow rates which can be reproduced accurately at a later date, the pulse rate must be able to be repeated easily. This was achieved by means of a pulse generator, described in Appendix 3, which can produce a quantised series of pulse rates. The pulse rates available can be described by the equation,

$$P/(Hz) = 300/N \qquad (3.1)$$

where P is the pulse rate and N = 1, 255. Consequently any one flow rate can be reproduced on demand but the values of N used in practice ranged from 2 to 6.

3-2.1 Flow Control

Because of their construction the operating pressure of the pumps must fall within the range 0 to 5 cm Hg gauge pressure. At pressures higher than this there was a tendency for the seals to leak. This was solved by use of the system shown in Figure 3-3.

As the pressure in the calorimetric system is often sub-atmospheric, it was necessary to have an adjustable non-return valve to prevent the pressure falling in the pumps. This non-return valve was constructed by taking a long barrelled 6 mm Youngs tap and lightly grinding the seat of the tap to fit a 5/16" ball bearing. A short 'Youngs tap' barrel, along with a spring, kept the ball bearing against the seat of the tap as shown in Figure 3-4.

3-3 HEAT OF MIXING CALORIMETER

The construction of the calorimeter is shown in Figure 3-5. The U tube which contains the calorimeter and the vacuum jacket are made of glass. The inlet gas tubes are each 5 mm i.d. and the U tube and gas outlets are both 10 mm i.d. Both ends of the U tube are fitted with 25 mm Glass to Metal seals and two eleven pin electrode seals are used to take heater and thermocouple leads out of the calorimeter. A 22 mm 'Soveril' joint is used to 'break' the U tube and facilitate the assembly of the calorimeter. The incoming gases flow over the thermocouples (6)

and mix prior to entering the heater channel. The mixed gases flow down the spiral heater channel which has an effective path length of 150 mm. This is designed to slightly increase turbulence and promote complete mixing. The gas mixture then passes the thermocouples (8) which compare its temperature to that of the inlet gas streams. The mixture then leaves the calorimeter via the outlet tube (10).

3-3.1 Thermocouple Arrangement

There are four thermocouples in the calorimeter connected as shown schematically in Figure 3-6. The thermocouples are made up of 36 gauge copper-constantan wire and are each soldered to a copper cylinder, 4 mm dia. by 6 mm, to ensure better thermal contact and stability. With this arrangement it is possible to compare the inlet gas temperatures, and obtain two values of the temperature difference across the heater, i.e. on mixing.

This provides a check and back-up system if either of TC3 or TC4 fails. The thermocouple leads leave the calorimeter by the right hand electrode seal. From there the leads, in fibreglass sheaths, are taken through the oil bath to a junction box on top of the thermostat. From the junction box coaxial cable leads are taken to a Croydon Thermocouple switch (model number SP1) via which any one of the following temperature differences can be selected.

(1) $\Delta T1 = TC1 - TC2$

(2) $\Delta T2 = TC3 - TC2$

(3) $\Delta T3 = TC4 - TC1$

The temperature difference is monitored by use of a Hewlett-Packard, Model 419A, DC Null Voltmeter which can be read to ± 0.1 μV. The signal is amplified by the voltmeter and fed to a Toa chart recorder, model EPR-2TC.

3-3.2 Calorimeter Heater

A 26 Ω heater was constructed from 29 gauge nichrome wire. It was initially wound into a coil of 2 mm dia. and then wound round a spiral teflon former. The teflon former shown in Figure 3 - 7 provides a channel through which the gas mixture must travel. The dimensions of the former are chosen such that the gas flow turbulence is increased to promote mixing but not such that the pressure drop becomes so large that significant Joule-Thomson effects would occur.

Using the design pressure drop and the Joule-Thomson data available (Lindsay and Brown (1935)) it was verified that no significant Joule-Thomson effect should occur.

The heater wire is laid in the channel of the teflon former and the heater leads taken out in the opposite direction to the gas flow, leaving the calorimeter by the left hand electrode seal. The heater circuit diagram is shown in Figure 3-8.

The power dissipated in the heater W_h is given by the relation

$$W_h = v_h \, i_h \qquad (3.2)$$

where the current i_h is determined by measuring the potential drop across a 10Ω Standard Resistance, (Croydon Type RS1). The power supply to the heater consisted of two 1.2V Nickel-Cadmium cells with alkaline electrolyte. The potentials V_s and V_h are measured using a Pye Universal decade potentiometer, Model No. 7595, which can be read to ± 1 μV. The potentiometer has two Ni-Cd alkaline cells for a power supply and uses a Cambridge Weston Normal cell (No. L-228232). A Kipp and Zonen Microva **AL** 4 Galvanometer is used in conjunction with the potentiometer.

3-4. VAPOUR COLLECTION SYSTEM

The main requirement for a vapour collection system is that it should be able to collect and condense vapour from the calorimeter in such a manner that constant pressure can be maintained throughout an experiment. The system shown in Figure 3-9 serves this purpose.

Incoming vapour is condensed by the first condenser and is initially collected in the reflux flask. Liquid accumulates in the collection flask as it over flows from the reflux flask via the U tube, which provides a liquid seal to prevent any vapour passing into the collection side. A constant pressure can be maintained, without excessive pressure controller action, by the refluxing carried out in the reflux side. When the equipment is at atmospheric pressure at the end of a run the liquid mixture, in the collection flask, is drawn off through the drain valve.

3-5. PRESSURE CONTROLLER

The unit shown in Figure 3-10 was able to maintain a constant pressure in the calorimetric system to better than ± 1 mmHg, for sub-atmospheric operation.

Operation of the Controller

With all four taps open the system is pumped down by means of a water vacuum pump and, once the desired pressure has been reached, the reference pressure vessel is isolated by closing tap 6. Tap 3 is also closed at this time, leaving only taps 4 and 5 open. Consequently, as the pressure is lowered in the calorimetric system the mercury level in the left hand side of the U tube rises to cover the sinter, thus cutting off the action of the pump. If the pressure should rise in the system,

the mercury level in the left hand side of the U tube drops exposing part of the sinter and enabling the system to be pumped down again until the mercury level rises and covers the sinter.

The pressure controller was found to be very effective, as the action of the vapour collection system in condensing the effluent vapour was such, that the pressure controller had very little work to do in coping with any small leaks that occurred from time to time. The pressure was measured within ± 1 mm Hg using a mercury in glass manometer mounted on a one metre boxwood scale.

3-6 BOILER AND EQUILIBRATOR

This consists of two 15 m copper tubes (6 mm dia.) wound together into a 250 mm diameter coil and immersed in the thermostat. The tubes are soldered together to ensure good thermal contact. The first 300 mm of each tube is packed with copper turnings, to smooth out the flow of liquid, which arrives as small drops, and to ensure rapid vaporization with the ensuing good thermal contact. Heat transfer calculations (detailed in Appendix 4) have shown that complete vaporization of the feed can be expected to take place within the first metre of tubing and that the difference between the temperature of the inlet vapour to the calorimenter, and the temperature of the thermostat would not be able to be measured.

3-7 VACUUM PUMPS

The calorimeter vacuum jacket was evacuated by an Edwards Mercury Vapour Diffusion pump, model number EM1, backed by a conventional, oil sealed, rotary pump, model number 25, from the Precision Scientific Company. An Edwards B5 Pirani gauge, with an M6A head was used to check the jacket vacuum.

3-8 THERMOSTAT

The thermostat consisted of a 97.5 litre stainless steel tank, 460 mm x 460 mm x 460 mm, insulated with 50 mm of fibreglass. Shell 'Thermia 933' oil was used as the bath fluid as this oil can stand a maximum temperature of 290^{o} C.

The thermostat was stirred by a six bladed propeller powered by a 200 W motor. This gave vigorous fluid movement and very good thermal stability (± 0.003 K), which was checked using a thermistor D.C. bridge, throughout the thermostat.

The thermostat was covered by a lid made in two sections from sheet asbestos. The calorimeter and boiler were suspended from one section while the stirrer motor, thermostat heaters, and a cooling coil were attached to the other section.

The thermostat was heated by two 36 Ω 'pyrotenax' heaters each 17 m long. Thermostat cooling was achieved by passing water from a constant head supply through 8 m of 9 mm O.D. copper tubing. A metric series 7 'rotameter' was used to set and monitor the cooling water flow rate.

Thermostat temperature control was initially achieved by using a Bayley Model 122 temperature controller with a platinum resistance sensor. However it became apparent that, for low pressure operation of the calorimeter, the temperature control was not good enough and variations in bath temperature were affecting the thermocouple readouts. It was then decided to change to a S.C.R. proportional controller (Martin (1968)) with the appropriate thermistor sensor. This gave better long and short term control with temperature stability of ± 0.004 K for periods of up to five hours.

3-9 TEMPERATURE MEASUREMENT

The primary temperature measurement was done using a Rosemount platinum resistance thermometer (model No. WS104) and Rosemount comparator bridge (model No. VLF51A-150). The resistance thermometer was used to set the bath temperature initially, and a Beckmann Thermometer was subsequently used to check long term temperature drift.

To check the short term temperature control and enable more precise controller tuning, a thermistor D.C. bridge, Figure 3-11, was used. With the appropriate thermistor sensor in the bath the output from the bridge was fed into the H.P. 419A D.C. Null Voltmeter which amplified it and a record was kept on the 'Toa' chart recorder.

The thermistor D.C. bridge has a sensitivity of 5700 $\mu V\ K^{-1}$ (Beath (1967)). The bridge was used to check the thermal stability throughout the thermostat and also the degree of long term temperature control (up to five hours).

3-10 TESTING OF EQUIPMENT

This section will discuss tests carried out on the calorimeter pumps and the calorimeter itself.

3-10.1 Calorimeter Pumps

The pumps were initially calibrated using toluene. They were then tested for flow stability as the pump's piston moved up the cylinder and for reproduceability of flow rate from day to day.

Results showed that the pumps were stable to ± 0.1% over their complete movement, starting from a full cylinder until the pump piston

could travel no further. This involved periods of time ranging from 2.5 to 6 hours. The pumps were able to reproduce the same flow rate to within ± 0.3% from day to day.

Once the pump's characteristics were known for toluene it was a simple exercise using density data to predict the flow rates for other liquids. This was done for Benzene and Cyclohexane and subsequent checks with these liquids verified the predicted flow rates. Consequently any one flow rate selected was known to ± 0.3%.

3-10.2 Calorimeter

The tests carried out on the calorimeter comprised the following:

(a) Determination of pressure drop for various gas flows across the heater and subsequent estimation of Joule-Thomson effect.

(b) Test for Joule-Thomson effect using benzene in both streams.

(c) Determination of the heat capacity of benzene vapour at 358 K.

The results were as follows:

(a) Using propane as a test gas the pressure drop across the heater was measured using a Dwyer, Model number 400, pressure gauge. For a gas Reynolds number of 5000, across the heater the pressure drop was 45 ± 1 Pa. The design of the calorimeter heater was based on a maximum Reynolds number of 5000. Lindsay and Brown (1935) have reported a Joule-Thomson coefficient for benzene, at 358 K, of 3.75×10^{-5} K Pa^{-1} which implies, for a pressure drop of 45 Pa, a temperature drop across the heater of 1.4×10^{-3} K. For a copper constantan thermocouple arrangement a temperature difference of $1.4\ 10^{-3}$ K results in an emf of 0.06 μV, which cannot be resolved by the equipment used to monitor the thermocouples.

(b) To check for any possible Joule-Thomson effect a run using benzene in both streams was performed at the maximum flow rate available of 1.2 10^{-3} mol s^{-1}. No temperature drop could be discerned over the heater/mixer section indicating that the Joule-Thomson effect could not be detected.

(c) The calorimeter was then used to determine the heat capacity of benzene vapour at 358 K. The 'apparent' heat capacity was determined for four different flow rates using

$$C_p(app) = W_h/f\ \Delta T \qquad (3.3)$$

where W_h is the power dissipated in the heater to produce a temperature rise ΔT in the vapour with a flow rate f.

A plot of $C_p(app)$ against 1/f was extrapolated to infinite flow rate, where heat losses are assumed zero, to obtain a value for the true heat capacity of benzene of 93 ± 4 J mol^{-1} K^{-1} which compares favourably with the literature value of 99 J mol^{-1} K^{-1}, Rossini (1952).

3-11 MATERIALS

3-11.1 Benzene and Cyclohexane

Benzene and Cyclohexane from the May and Baker range of chemicals were used. The Benzene was of their 'Pronalys' grade while the Cyclohexane was of their 'laboratory' grade. The cyclohexane showed traces of benzene when checked with a U.V. Spectrophotometer, but investigation on a gas chromatograph with a 20% carbowax 600 on celite column at 100^{o} C showed this to be less than 0.1%. The benzene when checked on the gas chromatograph showed only one peak.

Judd (1969) showed that the heat of mixing was dependent on composition according to the relation

$$H_m^E = A\, x_1\, x_2 \qquad (3.3)$$

For an equimolar feed of pure benzene and pure cyclohexane this means that

$$H_m^E = 0.25A \qquad (3.4)$$

As the cyclohexane has 0.1% benzene the effect of this benzene is shown by the fact that for an equimolar feed of benzene and cyclohexane (with 0.1% benzene)

$$H_m^E = (0.5005)(0.4995)\ A.$$

$$= 0.249\ A. \qquad (3.4)$$

Thus the 0.1% benzene trace in the cyclohexane will have an effect of 0.4% or less on the value of H_m^E .

3-11.2 Acetone and Chloroform

The Acetone used was from the Fisher certified A.C.S. range while the Chloroform was of the B.D.H. 'Analar' grade of chemicals.

4. RESULTS, CALCULATIONS AND DISCUSSION

This chapter will present and discuss the results obtained in this work.

4-1 CALCULATION DETAILS

The results tabulated in section 4-2 were calculated using the procedures outlined in section 2-4. An example of an endothermic heat of mixing experimental run, at a given flowrate, is shown in Figure 4-1 as a plot of temperature difference across the heater, $\Delta T2$, against heater power W_h. The line of best fit is found by using a weighted linear least squares method (Topping (1955)). This method, outlined in Appendix 5, determines the coefficients A, B in the relation,

$$\Delta T2 = AW_h + B \tag{4.1}$$

and their standard errors. The power W_{ho}, required to compensate for the heat of mixing and hence the 'apparent' heat of mixing $H_m^{E'}/p$, is found by interpolation. After four such runs covering a range of total flowrates, the 'true' heat of mixing is found by extrapolation as shown in Figure 4-2. The line of best fit is again found by the method of least squares (Topping (1955)).

Once the true heat of mixing (H_m^E/p), at the experimental composition, is known it is corrected to a composition of x = 0.5 using the relation (Judd (1969))

$$H_m^E/p = Ax_1x_2 \tag{4.2}$$

4-2 RESULTS

This section will list both raw data and the calculated results.

4-2.1 Raw Data

Table 4-1 details the apparent heat of mixing for Benzene and Cyclohexane for different flowrates, and the pressure at which the apparent heat of mixing was determined.

TABLE 4-1 Apparent Heat of Mixing for Benzene and Cyclohexane, ($x_{Benzene} = 0.549$)

T/K	$1/f_T/(s.mol^{-1})$	p/kPa	$(H_m^{E'}/p)/10^{-6} m^3 mol^{-1}$
358	896	101.3 ± 0.1	45 ± 2
	1496	101.3 ± 0.1	39 ± 3
	2076	101.3 ± 0.1	40 ± 2
	2680	101.3 ± 0.1	33 ± 3
323	896	20.7 ± 0.1	130 ± 20
	1192	20.9 ± 0.1	91 ± 9
	1490	22.5 ± 0.1	60 ± 20
	2087	21.6 ± 0.1	20 ± 20
315	896	20.1 ± 0.1	130 ± 30
	1192	19.9 ± 0.1	100 ± 30
	1490	19.3 ± 0.1	80 ± 30
	2087	19.3 ± 0.1	40 ± 20
305	896	14.8 ± 0.1	130 ± 40
	1192	14.7 ± 0.1	100 ± 20
	1490	13.6 ± 0.1	60 ± 40

Table 4-2 details, the apparent heat of mixing against flowrate for Acetone and Chloroform, and the pressure at which $H_m^{E'}/P$ was determined.

TABLE 4-2 Apparent Heat of Mixing for Acetone and Chloroform

($x_{Acetone}$ = 0.525)

T/K	$1/f_T/(s\,mol^{-1})$	p/kPa	$-(H_m^{E'}/p)/10^{-3}\,m^3\,mol^{-1}$
343	705	87.2 ± 0.1	1.34 ± 0.07
	940	86.9 ± 0.1	1.27 ± 0.05
	1190	88.7 ± 0.1	1.22 ± 0.05
	1412	87.2 ± 0.1	1.18 ± 0.06
343	705	50.8 ± 0.1	1.25 ± 0.06
	940	52.7 ± 0.1	1.21 ± 0.08
	1190	51.8 ± 0.1	1.14 ± 0.07
	1412	52.5 ± 0.1	1.12 ± 0.08
343	705	20.3 ± 0.1	1.18 ± 0.04
	940	20.1 ± 0.1	1.14 ± 0.05
	1190	19.8 ± 0.1	1.07 ± 0.06
	1412	19.6 ± 0.1	1.02 ± 0.07
323	705	53.3 ± 0.1	2.28 ± 0.07
	940	52.3 ± 0.1	2.32 ± 0.08
	940	52.3 ± 0.1	2.12 ± 0.06
	1190	52.7 ± 0.1	1.98 ± 0.06
	1412	52.1 ± 0.1	1.7 ± 0.1

4-2.2 Calculated Results

Table 4-3 shows the true heat of mixing for Benzene and Cyclohexane versus temperature corrected to a mole fraction x = 0.5

TABLE 4-3 Heat of Mixing Benzene and Cyclohexane (x = 0.5)

T/K	p/kPa	$(H_m^E/p)/10^{-6} m^3 mol^{-1}$
358	101.3 ± 0.2	50 ± 8
323	21.4 ± 0.9	200 ± 40
315	19.7 ± 0.5	220 ± 40
305	14.4 ± 0.8	240 ± 50

Table 4-4 shows the true heat of mixing for Acetone and Chloroform versus temperature and pressure corrected to a mole fraction x = 0.5

TABLE 4-4 Heat of Mixing of Acetone and Chloroform (x = 0.5)

T/K	p/kPa	$-(H_m^E/p)/10^{-3} m^3 mol^{-1}$
343	87.5 ± 0.9	1.49 ± 0.08
343	52 ± 1	1.39 ± 0.09
343	20.0 ± 0.4	1.35 ± 0.07
323	52.5 ± 0.5	2.9 ± 0.3

4-3 COMPARISON OF RESULTS WITH PUBLISHED VALUES

This section will compare and discuss the results obtained in this work with those values previously measured.

4.3.1 Benzene and Cyclohexane

Table 4-5 sets out the comparison of the heat of mixing of Benzene and Cyclohexane from this work with values previously measured.

TABLE 4-5 Comparison of Heat of Mixing for Benzene and Cyclohexane ($x = 0.5$)

T/K	$(H_m^E/p)/10^{-6} m^3 mol^{-1}$	Source
359	55 ± 3	Williamson (1966)
358	53 ± 3	Judd (1969)
358	50 ± 8	This Work
363 to 383	40 ± 10	Wormald (1969)
363	4 ± 2	Wormald (1977)
373	4 ± 2	Wormald (1977)

Table 4-6 illustrates the shape of the H_m^E/p curve with composition, indicating that it follows the relation

$$H_m^E/p = Ax_1x_2 \qquad (4.2)$$

TABLE 4-6 Comparison of H_m^E/p for Benzene and Cyclohexane with Composition at T = 358K. (Judd 1969)

$x_{Benzene}$	$(H_m^E/p)/10^{-6} m^3 mol^{-1}$	$(H_m^E/px_1x_2)/10^{-6} m^3 mol^{-1}$
0.3	44 ± 3	210 ± 10
0.4	48 ± 3	200 ± 10
0.5	53 ± 3	210 ± 10
0.6	47 ± 3	200 ± 10
0.7	42 ± 3	200 ± 10

The only result, from this work, which can be compared directly to a calorimetric value previously measured is that at 358 K. This result ($50 \pm 8\ 10^{-6} m^3 mol^{-1}$) is in good agreement with those of Williamson (1966) ($55 \pm 3\ 10^{-6} m^3 mol^{-1}$) and Judd (1969) ($53 \pm 3\ 10^{-6} m^3 mol^{-1}$). The closest other calorimetrically obtained result is that of Wormald (1969) who gives a value for H_m^E/p over the range 363 K to 383 K as $40 \pm 10\ 10^{-6}$ $m^3 mol^{-1}$. These results suggest that the value for 358 K obtained in this work is probably correct.

However no direct calorimetric values of H_m^E/p for temperatures below 358 K have been previously reported and consequently the values for H_m^E/p at 305 K, 315 K and 323 K reported here can be compared only with values predicted from a smooth fit to the excess second virial coefficient data available. From Equation (1.24) it can be seen that

$$H_m^E/2x_1x_2p = \varepsilon - T d\varepsilon/dT \qquad (4.3)$$

and if a smooth curve is fitted to the values of ε then the experimental values of $H_m^E/2x_1x_2p$ can be compared with a smooth curve for $H_m^E/2x_1x_2p$ as predicted by Equation (4.3).

The values of ε have in fact been fitted to a function of the form (this work),

$$\varepsilon = a + b \exp(c/T) \qquad (4.4)$$

details of which are in Section 4-4. Equation (4.3) now becomes

$$H_m^E/2x_1x_2p = a + b(1+c/T)\exp(c/T) \qquad (4.5)$$

and a plot of Equation (4.5) for two different fits appears on Figure 4-3 along with the experimental values of $H_m^E/2x_1x_2p$ from Tables 4-3 and 4-5. Fit number two uses all the known ε data when determining the constants a, b and c, while fit number one does not include the ε values at 298 K and 300 K due to reservations previously expressed (Shannon 1976), about the values obtained for these two points, which are discussed in Section 4-4.1.

The result at 305 K is lower than that predicted by Equation (4.5) while the result at 323 K is slightly on the high side. The result at 315 K agrees well with the predicted value.

The latest reported results come from Wormald (1977) whose results at 363 K and 373 K for H_m^E/p of 4 ± 2 $10^{-6} m^3 mol^{-1}$ are a factor of ten lower than all others previously reported. The resultant value of 8 ± 4 $10^{-6} m^3 mol^{-1}$ for $H_m^E/2x_1x_2p$ is also a factor of ten lower than that predicted by Equation (4.5).

In a recent private communication Wormald (1978) states that his 1977 values might be too small and that a value of H_m^E/p of 10 ± 5 $10^{-6} m^3 mol^{-1}$ at 363 K would be about right. However once translated onto Figure 4-3 it can be seen that this value also does not agree with that predicted by the ε data. It is apparent therefore that the H_m^E/p results of Wormald (1977) are suspect and they will not be used in any subsequent analysis.

4-3.2 Acetone and Chloroform

The only previous calorimetric result which can be used for comparative purposes is that of Wormald (1969) at 343 K. Knobler and Pasco (1975) have measured the excess second virial coefficient of acetone and chloroform over the temperature range 298 K to 373 K. From a plot of ε vs T and using Equation (1.24),

$$\lim_{p \to 0} H_m^E/p = 2x_1x_2(\varepsilon - T d\varepsilon/dT) \qquad (1.24)$$

expected values of H_m^E/p can be calculated and are set out in Table 4-7 along with that of Wormald (1969) and those measured in this work.

TABLE 4-7 Comparison of H_m^E/p for Acetone and Chloroform

T/K	p/kPa	$-(H_m^E/p)/10^{-3}m^3mol^{-1}$	Source
343	20.0 ± 0.4	1.35 ± 0.07	This Work
	52 ± 1	1.39 ± 0.09	This Work
	87.5 ± 0.9	1.49 ± 0.08	This Work
	101.3 ± 0.2	1.11 ± 0.03	Wormald (1969)
		1.4 ± 0.2	Knobler and Pasco (1975)
323	52 ± 1	2.9 ± 0.3	This Work
		2.4 ± 0.3	Knobler and Pasco (1975)

As can be seen from Table 4-7 the general trend, observed in this work, of increasing H_m^E/p for increasing pressure is not followed by the result of Wormald (1969). The only other way of comparison is by using the ε data of Knobler and Pasco (1975) and Equation (1.24) which predicts values of H_m^E/p which agree with the results obtained in this work.

4-4 CORRELATION OF THE EXCESS SECOND VIRIAL COEFFICIENT DATA AND HEATS OF MIXING DATA

It has been shown, in Section 1-2, that the heats of mixing of gases at low pressures can be simply related to the excess second virial coefficient of those gases by the relation

$$H_m^E/p = 2x_1x_2(\varepsilon - T d\varepsilon/dT) \qquad (1.24)$$

The question now arises of how best to utilise the measurements of H_m^E/p to help define the shape of the plot of ε vs T.

Francis et al (1969) fitted measurements of the second virial coefficient together with values of (B-TdB/dT) derived from Joule-Thomson coefficient measurements to an equation for B(T) of the 'square well' form,

$$B(T) = A + B \exp(c/T) \tag{1.26}$$

An analogous treatment for the excess second virial coefficient data, leads one to the suggestion that the available data for ε should be fitted along with the measurements of H_m^E/p to a function of the form

$$\varepsilon(T) = a + b \exp(c/T) \tag{4.4}$$

4-4.1 Fitting of Excess Second Virial Coefficient Data and Heats of Mixing Data.

Jordan (1978) has developed a multi-variable curve fitting program (described in Appendix 6) which uses the method of least squares in minimising the sum of squares of deviations of the data from the smooth curve. The analysis was performed in two ways as follows:

(a) The ε data only (Table 4-8) were fitted by the function (4.4) and

(b) The ε data and the H_m^E/p data were both fitted by the function (4.4)

Fitting Using (ε_i, T_i) Data Only

The sum of squares of deviations of the data from the smooth curve is given by

$$Y1 = \sum_i w_i (\varepsilon_i - \varepsilon(T_i))^2 \tag{4.6}$$

where w_i is the weighting assigned to the experimental point (ε_i, T_i). The weighting of a point is inversely proportional to the error, assigned to it by the workers who measured it, and scaled such that the experimental point with the largest error has a weighting of one.

Of all the data to be fitted to Equation (4.4) the values for ε at 298 K (Knobler and Pasco (1975)) and 300 K (Shannon (1976)) appear to be too large. Shannon (1976) has expressed reservations about these points, mainly because of his suspicions about adsorption in the apparatus. Consequently the curve fitting was done in two parts,

TABLE 4-8 Literature Values of the Excess Second Virial Coefficient, of Benzene and Cyclohexane with Weighting w.

T/K	$\varepsilon/10^{-6}\,m^3\,mol^{-1}$	w	Source
373	21 ± 3	26.7	Shannon (1976)
	22 ± 2	40	Knobler and Pasco (1975)
	22 ± 1	80	Knobler and Handa (1976)
348	19 ± 3	26.7	Shannon (1976)
	25 ± 2	40	Knobler and Handa (1976)
333	14 ± 15	5.3	McElroy (1968)
323	35 ± 10	8	McElroy (1968)
	44 ± 1	80	Shannon (1976)
	29 ± 2	40	Knobler and Handa (1976)
318	45 ± 20	4	McElroy (1968)
315	38 ± 16	5	Shannon (1976)
313	30 ± 45	1.8	McElroy (1968)
308	57 ± 10	8	Knobler and Handa (1976)
300	175 ± 50	1.6	Shannon (1976)
298	135 ± 80	1	Knobler and Pasco (1975)

(i) Disregarding the values for ε at 298 K and 300 K and fitting the remaining 13 points, and

(ii) Fitting all 15 points.

The best overall fit for each case is given in Table 4-9 and shown on Figure 4-4.

TABLE 4-9 Best Fits of (ε_i, T_i) Data to the Function $\varepsilon(T) = a + b \exp(c/T)$

Fit No.	$a/10^{-6}\ m^3\ mol^{-1}$	$b/10^{-10}\ m^3\ mol^{-1}$	$c/10^3$ K	$Y1/10^{-8}\ m^6\ mol^{-2}$
1 (13 points)	16.77 ± 0.09	1.00 ± 0.001	3.955 ± 0.025	1
2 (15 points)	13.77 ± 0.08	1.00 ± 0.001	4.039 ± 0.025	2.8

Fitting Using Both (ε_i, T_i) and $(H^E_m/p_j, T_j)$ Data

The next approach was to incorporate the heats of mixing data. Writing H for $H^E_m/2x_1x_2p$ Equation (4.5) becomes

$$H(T) = a + b(1+c/T)\exp(c/T) \qquad (4.7)$$

where a, b, and c are the coefficients in function (4.4)

$$\varepsilon(T) = a + b \exp(c/T) \qquad (4.4)$$

Hence Equation (4-7) can be used to determine a sum of squares of deviations of the heat of mixing data from that predicted from the curve for ε. The total sum of squares of deviations to be minimised now consists of two terms,

(1) The contribution Y1 from the $(\varepsilon_i T_i)$ data as defined by Equation (4.6), and

(2) The contribution Y2 from the heat of mixing data (H_j, T_j) where

$$Y2 = \sum_j w_j (H_j - H(T_j))^2 \qquad (4.8)$$

where w_j, the weighting of the (H_j, T_j) point, is inversely proportional to the experimental error of that point and scaled such that the (H_j, T_j)

point with the largest error has a weighting of one.

TABLE 4-10 Values of the Heat of Mixing of Benzene and Cyclohexane With Weighting w.

T/K	$(H_m^E/2x_1x_2p)/10^{-6}m^3mol^{-1}$	w	Source
359	110 ± 6	16.7	Williamson (1966)
358	100 ± 16	6.3	This Work
	105 ± 5	20	Judd (1969)
	105 ± 5	20	Judd (1969)
	100 ± 5	20	Judd (1969)
	100 ± 5	20	Judd (1969)
	100 ± 5	20	Judd (1969)
323	400 ± 80	1.3	This Work
315	440 ± 80	1.3	This Work
305	480 ± 100	1	This Work

The total sum of squares of deviations is now given by

$$Y = P \times Y1 + Q \times Y2 \qquad (4.9)$$

where P and Q are the weightings of the two types of data with respect to each other. To determine the values to be assigned to P and Q values of H_m^E/p were calculated using Equation (4.10),

$$H_m^E/p = 2x_1x_2(a+b(1+c/T)\exp(c/T)) \qquad (4.10)$$

which follows from Equation (4.5). Values for a, b and c were taken from Table 4-9. The expected errors for these values were determined and compared with the experimental errors of the heats of mixing data.

The results, Table 4-11, showed that the calculated errors were of the same order of magnitude and consequently P and Q were each assigned a value of one.

TABLE 4-11 Expected and Experimental Errors of Heats of Mixing Data.

T/K	∂(expected)/10^{-6} m^3 mol^{-1}	∂(experimental)/10^{-6} m^3 mol^{-1}
358	7	8
323	25	40
315	35	40
305	55	50

The curve fitting was again carried out in two parts,

(i) Disregarding the values for ε at 298 K and 300 K and fitting the remaining 13 points along with the $H_m^E/2x_1x_2p$ values

(ii) Using all 15 (ε_i, T_i) points along with the $H_m^E/2x_1x_2p$ values.

The best overall fit for each case is given in Table 4-12 and shown on Figure 4-4.

TABLE 4-12 Best Fits of (ε_i, T_i) Data and (H_j, T_j) Data Together to Function $\varepsilon = a + b \exp(c/T)$

Fit No.	a/10^{-6} m^3 mol^{-1}	b/10^{-10} m^3 mol^{-1}	c/10^3 K	Y/10^{-8} m^6 mol^{-2}
3 (13$\varepsilon_i$pts+$H_j$pts)	13.52 ± 0.08	6.37 ± 0.03	3.412 ± 0.025	4.5
4 (15$\varepsilon_i$pts+$H_j$pts)	14.17 ± 0.09	5.57 ± 0.02	3.454 ± 0.025	6.7

4.4.2 Effect of the Use of the Heats of Mixing Data on the Correlation of the Excess Second Virial Coefficient for Benzene and Cyclohexane.

It can be seen from Figure 4-4, the plot of ε vs T, that curve fits numbers 1, 3 and 4 are almost identical. Curve fit number 2 using

all 15 (ε_i, T_i) points alone is, as could be expected, different in so far as it predicts a higher value for ε at the low end of the temperature scale. A study of the sum of squares of deviations of the ε data from the four curve fits, Table 4-13, verifies this contention.

TABLE 4-13 Sum of Squares of Deviations (SSD) of Curve Fits From 13ε and 15ε Data Points

Fit No.	SSD(13εpts)/10^{-8} m^6 mol^{-2}	SSD(15εpts)/10^{-8} m^6 mol^{-2}
1	1	3.13
2	1.28	2.8
3	1.05	3.23
4	1.05	3.19

Fit numbers 3 and 4 indicate, that the reservations held concerning the low temperature values (298 K and 300 K) of ε (Shannon (1976)) are justified, and that these should be discarded when discussing the behaviour of the excess second virial coefficient. On the other hand fit numbers 1 and 3 indicate that the use of the H_m^E/p data included in correlating the 13 ε values does not improve the quality of the fit to any extent. The heats of mixing data are useful in so far as they have confirmed suspicions about the two low temperature values of ε.

The two types of data are complementary and one type does not precede the other in importance.

4-5 COMPARISON OF LITERATURE AND PREDICTED VALUES OF THE INTERACTION SECOND VIRIAL COEFFICIENT FOR BENZENE AND CYCLOHEXANE.

This section will predict values of B_{12} using the equation for ε derived in the previous section and compare them with values found in the literature.

4-5.1 Prediction of B_{12}

Table 4-14 sets out the known literature values of B_{12}, which are also plotted on Figure 4-5 along with two smooth curves.

The upper curve is calculated using the relation

$$B_{12} = \varepsilon(T) + \tfrac{1}{2}(B_{11} + B_{22}) \tag{4.10}$$

where

$$\varepsilon(T)/10^{-6}\,m^3\,mol^{-1} = 13.52 + 6.37 \times 10^{-4} \exp(3412K/T) \tag{4.11}$$

is curve fit number 3 obtained in Section 4-4 and B_{ii} is taken from the listings of pure second virial coefficient data in Dymond and Smith (1969).

The lower curve is calculated using the McGlashan and Potter (1962) correlation,

$$B_{12}/V^c_{12} = 0.430 - 0.886\,(T^c_{12}/T) - 0.694(T^c_{12}/T)^2 - 0.0375(n_{12} - 1)(T^c_{12}/T)^{4.5} \tag{4.12}$$

where the pseudocritical properties V^c_{12}, T^c_{12}, and chain length n_{12} were calculated using the following combining rules,

$$T^c_{12} = (T^c_{11}\,T^c_{22})^{\frac{1}{2}} \tag{1.17}$$

$$V^c_{12} = \frac{1}{8}(V^{c1/3}_{11} + V^{c1/3}_{22})^3 \tag{1.18}$$

and

$$n_{12} = \tfrac{1}{2}(n_1 + n_2) \tag{4.13}$$

TABLE 4-14 Literature Values of the Interaction Second Virial Coefficient of Benzene and Cyclohexane

T/K	$B_{12}/10^{-6}\ m^3\ mol^{-1}$	Source
298	-1410 ± 130	Knobler and Pasco (1975)
300	-1355 ± 100	Shannon (1976)
308	-1346 ± 70	Bottomley and Coopes (1962)
	-1380 ± 54	Knobler and Handa (1976)
313	-1336 ± 95	McElroy (1968)
315	-1340 ± 60	Shannon (1976)
318	-1272 ± 70	McElroy (1968)
323	-1225 ± 50	Shannon (1976)
	-1210 ± 50	Knobler and Handa (1976)
	-1222 ± 60	McElroy (1968)
	-1215 ± 70	Bottomley and Coopes (1962)
328	-1227 ± 70	Waelbroeck (1955)
333	-1144 ± 65	McElroy (1968)
	-1203 ± 70	Waelbroeck (1955)
343	-1041 ± 70	Bottomley and Coopes (1962)
	-1109 ± 70	Waelbroeck (1955)
348	-1075 ± 70	Waelbroeck (1955)
	-1029 ± 46	Knobler and Handa (1976)
	-1035 ± 47	Shannon (1976)
373	- 910	Cox and Stubley (1960)
	- 844 ± 47	Shannon (1976)
	- 847 ± 47	Knobler and Pasco (1975)
	- 843 ± 47	Knobler and Handa (1976)

The critical properties used for Benzene and Cyclohexane are listed in Table 4-15 (Shannon (1976)).

TABLE 4-15 Critical Properties for Benzene and Cyclohexane

	T^c/K	$V^c/10^{-3} m^3 mol^{-1}$	n
Benzene	562	26.04	4.07
Cyclohexane	553	30.8	3.83

4-5.2 Comparison of Predicted and Experimental B_{12}'s

From Figure 4-5 and as a result of the curve fitting performed in Section 4-4 it can be seen that the values of B_{12} at 298 K and 300 K are too high. However little else of importance can be deduced as B_{12} can be correlated to within experimental error by both the McGlashan Potter equation and the smooth curve which is a result of the curve fit obtained in Section 4-4.

It would seem therefore that the experimental errors of the B_{12} values are too large at present to provide a definitive test of the combining rules and that the present range of data will have to be improved to provide a more precise foundation for such testing.

4-6 ASSOCIATION IN ACETONE-CHLOROFORM VAPOUR MIXTURES

There is strong evidence (Pimental and McClellan (1960)) that acetone and chloroform form a complex due to hydrogen bonding in the vapour phase. Campbell and Kartzmark (1960) have shown, by determining the freezing point diagram, that a stable compound of the formula AB exists in the solid state, and also, through studies of the heats of mixing of the acetone-chloroform and acetone-carbontetrachloride systems, have suggested that the compound also exists in the liquid phase.

TABLE 4-16 Values of Excess and Interaction Second Virial Coefficients for Acetone and Chloroform

T/K	$-\varepsilon/10^{-6}\,m^3\,mol^{-1}$	$-B_{12}^{o}/10^{-6}\,m^3\,mol^{-1}$	$-B_{12}(phys)/10^{-6}\,m^3\,mol^{-1}$	$-B_{12}(chem)/10^{-6}\,m^3\,mol^{-1}$	$K_p/10^{-3}\,kPa^{-1}$
298	1003 ± 60	2623	548	2075 ± 110	1.67 ± 0.04
308	742 ± 16	2179	504	1675 ± 6.6	1.31 ± 0.05
323	486 ± 6	1706	446	1260 ± 60	0.94 ± 0.04
348	265 ± 4	1207	383	824 ± 55	0.57 ± 0.04
373	134 ± 4	896	327	569 ± 55	0.37 ± 0.03

and $\Delta H^{\dagger} = -19 \pm 2\ kJ\ mol^{-1}$

From the behaviour of the heat of mixing, in the vapour phase, with temperature and pressure (Table 4-7) it can be seen that increasing pressure increases the amount of energy released while decreasing the temperature also increases the heat of mixing. This behaviour is consistent for an exothermic reaction of the type,

$$A + B \rightleftharpoons AB \tag{1.27}$$

which has been postulated for acetone and chloroform by Huggins et al (1955).

Several methods can be used to determine the standard heat of formation of the complex in the vapour phase. Knobler and Pasco (1975) have measured the excess second virial coefficient ε, for acetone and chloroform, and from these measurements, following the procedure outlined in Section 1-3, have determined a heat of formation for the complex using the relation,

$$\lim_{p\to 0} d(\ln K_p)/d(1/T) = -\Delta H^{\dagger}/R \tag{1.35}$$

Their results are shown in Table 4-16 and Figure 4-6.

Another method, to calculate $\Delta H^{\dagger}$, using the heat of mixing due to chemical association $(H_m^E/P)(chem)$, and the equilibrium constant K_p, is also outlined in Section 1-3. Using Knobler and Pasco's data for ε, the heat of mixing due to physical interactions $(H_m^E/p)(phys)$, and hence $(H_m^E/p)(chem)$ has been calculated. Using Equation (1.118),

$$(H_m^E/p)(chem) = \Delta H^{\dagger} x_1 x_2 K_p/(1+pK_p) \tag{1.118}$$

with values of K_p from Table 4-16, the standard heat of formation has been calculated and the results are shown in Table 4-17.

TABLE 4-17 Calculation of Heat of Formation of the Complex Between Acetone and Chloroform

T/K	$((H_m^E/p)(phys))/10^{-3}\,m^3\,mol^{-1}$	$((H_m^E/p)(chem))/10^{-3}\,m^3\,mol^{-1}$	$K_p/10^{-3}$ kPa	p/kPa	$\Delta H^{\dagger}$/kJmol^{-1}
323	1.9 ± 0.2	-4.8 ± 0.4	0.988	52 ± 1	-21 ± 3
343	1.5 ± 0.2	-2.9 ± 0.3	0.630	52 ± 1	-19 ± 3

Several other authors (Table 4-18) have also determined the standard heat of formation of the complex.

TABLE 4-18 Heat of Formation of Complex Between Acetone and Chloroform

Source	Phase	$-\Delta H^{\dagger}/kJmol^{-1}$
Moelwyn-Hughes and Sherman (1936)	Gas	17.5
Huggins et al (1955)	Liquid	10.5 ± 4.2
Knobler and Pasco (1975)	Gas	19 ± 2
Campbell and Kartzmark (1960)	Liquid	11.3 ± 0.4
Morcom and Travers (1965)	Liquid	10.8 ± 0.5
Kearns (1961)	Liquid	10.4
This Work	Gas	20 ± 3

Moelwyn-Hughes and Sherman (1935), Huggins et al (1955) and Knobler and Pasco (1975) obtained $\Delta H^{\dagger}$ from measurements of the equilibrium constant via Equation (1.35). Campbell and Kartzmark (1960) obtained their values from studies of the liquid heats of mixing of the acetone-chloroform and acetone-carbon tetrachloride systems, Figure 4-9. Kearns (1961) and Morcom and Travers (1965) calculated their values by postulating the formation of two complexes in the liquid phase namely,

$$A + B \rightleftharpoons AB \qquad (1.21)$$

and

$$A + 2B \rightleftharpoons AB_2 \qquad (4.14)$$

where A represents acetone and B, chloroform. They applied the method of McGlashan and Rastogi (1958) to vapour pressure, and liquid heats of mixing data to derive equilibrium constants and heats of formations for both complexes.

From the studies listed above there can be little doubt that acetone and chloroform form a complex that is consistent with hydrogen bonding theory (Pimental and McClellan (1960)). Whether or not it is one to one complex only as suggested by Huggins et al (1955) or as Morcom and Travers (1965) suggest a complex of the formula AB_2 is also formed may be examined in terms of the plot of H_m^E/p against composition. A solely one to one complex will be expected to give a symmetrical plot. The results of Campbell and Kartzmark (1960) and Morcom and Travers (1965) for H_m^E in the liquid phase are shown in Figure 4-8 along with the liquid H_m^E values for acetone and carbon tetrachloride. The skewed shape of the curves seems to suggest the formation of a complex of the type AB_2 where A represents acetone. The results of Wormald (1969), Figure 4-7, for the gas phase H_m^E/p against composition,while lower than those obtained in this work, show that the plot is symmetrical indicating the formation of a one to one complex only in the gas phase.

5 SUGGESTIONS FOR FURTHER WORK

5-1 IMPROVEMENTS TO APPARATUS AND TECHNIQUE

This section will discuss the main areas where it is felt improvements can be made in the apparatus and experimental technique.

5-1.1 Liquid Pumps and Flow System

The present pumps should be replaced by ones which can operate at higher pressures as the present flow control system, with the limits on pump operating pressure, requires constant attention throughout an experimental run to keep it operating satisfactorily. With a high pressure pump the liquid can be injected straight into the boiler via a suitably designed nozzle, which would maintain a high enough pressure drop across itself, and thus automatically maintain a constant pressure in the pump. As a result the present flow system would be able to be discarded. Several types of High Pressure Liquid Chromotography pumps would be suitable as they have the desired flow stability.

5-1.2 Calorimeter

The basic design of the calorimeter seems to work satisfactorily although there is a need to extend the flow range to enable the distance of the final extrapolation in the determination of H_m^E/p (Figure 4-2) to be shortened with respect to the flow range covered. With only one calorimeter there is a limit on the flow range available due to the physical size of the calorimeter U tube and heater former. This is particularly the case for low pressure operation when it is difficult to get meaningful results at relatively high flowrates. The flow range could be improved by having two calorimeters in parallel, so that either could be used at any one time, with different size U tubes and heater

formers, designed however to the same Reynolds number and, consequently, pressure drop across the heater.

5.3.1 Temperature Control

At present when operating at very low pressures (<15 kPa) variations in the thermostat temperature affect the thermocouple readouts. Hence improvements in temperature control to eliminate this effect would be desirable. This could be achieved by developing a more sophisticated temperature controller or by improving the thermal properties of the thermostat by increasing the stirrer power and improving the thermostat insulation.

5.2 SUGGESTIONS FOR FURTHER WORK

The system, benzene and cyclohexane should be investigated in the temperature range 325 K to 360 K and below 305 K. This is dependent on better temperature control, as the thermostat's rest temperature with only the stirrer going is in the range 330 K to 340 K, and a dual calorimeter setup to enable the lower flowrates for the low pressure runs necessary at the lower temperatures.

Further measurements on the acetone and chloroform system could also be done over a range of compositions to check whether only a one to one complex is formed or a one to two complex is formed as well. As a check a system known to form a two to one complex would be interesting to study.

APPENDIX 1

HIGH PRESSURE HEATS OF MIXING OF GASES

Source	System	Temp. Range/K	Pressure Range/MPa
Beenakker, and Coremans (1962)	$H_2 + N_2$	293	3 - 8.1
Beenakker, et al. (1965)	$H_2 + N_2$	147 - 293	0.8 - 13.2
	$H_2 + Ar$	169 - 293	2 - 13.2
	$N_2 + Ar$	169 - 293	2 - 13
	$CH_4 + H_2$	230 - 293	1.5 - 13
	$CH_4 + Ar$	201 - 293	1.5 - 12
Knoester, et al. (1967)	$H_2 + N_2$	147 - 293	3 - 13.2
	$N_2 + Ar$	169 - 293	3 - 13.2
	$H_2 + Ar$	169 - 293	3 - 13.2
Van Eijnsbergen, and Beenakker (1968)	$H_2 + CH_4$	201 - 293	1 - 12.1
	$He + CH_4$	201 - 293	1 - 12.1
	$N_2 + CH_4$	201 - 293	1 - 12.1
	He + Ar	169 - 293	1 - 12.1
	$CH_4 + Ar$	201 - 293	1 - 12.1
Lee, and Mather (1970)	$N_2 + CO_2$	313	0.4 - 13.1
Klein, et al. (1971)	$CH_4 + N_2$	195 - 313	1.7 - 10.3
Hejmadi, et al. (1971)	$N_2 + CO_2$	304 and 313	3.4 and 6.5

Source	System	Temp. Range/K	Pressure Range/MPa
Wormald, Lewis, and Mosedale (1977)	$H_2 + CH_4$	201 and 298	2 - 10.2
	$H_2 + N_2$	201 and 298	2 - 10.2
	$N_2 + CH_4$	201 and 298	2 - 10.2
	$Ar + CH_4$	201 and 298	2 - 10.2
	$Ar + N_2$	201 and 298	2 - 10.2
* Lewis, Mosedale and Wormald (1977)	$N_2 + Ar$	123 - 298	0.8 - 10.2

* This reference involves the study of the heats of mixing in the two phase, supercritical, and liquid regions as well. The conditions reported here are for the gas and gas region only.

APPENDIX 2

VAPOUR PHASE ASSOCIATION

The following table lists those systems where association in the vapour phase, be it dimerization or otherwise, has been postulated to explain departures from non-ideality.

The studies can be split into two types:-

(1) Where dimerization of a pure vapour, C has been studied with the equilibrium

$$\text{I} \quad 2\,C \rightleftharpoons C_2 \qquad \text{(A2.1)}$$

(2) Where association in a vapour mixture, A + B has been studied with one or more of three possible equilibria present -

$$\text{II} \quad 2\,A \rightleftharpoons A_2 \qquad (1.27)$$

$$\text{III} \quad 2\,B \rightleftharpoons B_2 \qquad (1.31)$$

$$\text{IV} \quad A + B \rightleftharpoons AB \qquad (1.32)$$

The table will show the system studied and which of the four equilibria above (I, II, III, and IV) were considered by the authors.

TABLE A2-1

VAPOUR PHASE ASSOCIATION SYSTEMS

Source	System	Equilibrium Studied
Alexander and Lambert (1941)	Acetaldehyde	I
Lambert et al (1949)	Acetone	I
	Acetonitrile	I
	Methanol	I
Lambert and Strong (1950)	Ammonia	I
	Methylamine	I
	Dimethylamine	I
	Ethylamine	I
	Diethylamine	I
Fox and Lambert (1951)	Chloroform + Diethyl ether	IV
Lambert et al. (1954)	Cyclohexane + Diethylamine	III
	Cyclohexane + Acetone	III
	Cyclohexane + Acetonitrile	III
Lambert et al. (1959)	Chloroform + methyl formate	III & IV
	Chloroform + n-propyl formate	III & IV
	Chloroform + methyl acetate	III & IV
	Chloroform + ethyl acetate	III & IV
	Chloroform + diethylamine	III & IV
Prausnitz and Carter (1960)	Acetonitrile + Acetaldehyde	II, III & IV
Chen et al. (1966)	Ammonia + Acetylene	IV
Guggenheim (1966)	Nitric Oxide	I
Scott (1966)	Nitric Oxide	I

Source	System	Equilibrium Studied
Najour and King (1966)	CO_2 + naphthalene	IV
Dantzler and Knobler (1969)	Benzene + Hexafluorobenzene	IV
Rätzsch and Freydank (1971)	Ethylene + Ammonia	IV
	Ethylene + Methanol	IV
	n-Pentane + Methanol	IV
Coan and King (1971)	H_2O + CO_2	IV
	H_2O + N_2O	IV
Hemmaplardh and King (1972)	CO_2 + Methanol	IV
Gupta et al. (1973)	CO_2 + Ethanol	IV
Millen and Mines (1974)	Methanol + Methylamine	IV
	Methanol + Dimethylamine	IV
	Methanol + Trimethylamine	IV
	Methanol + Triethylamine	IV

APPENDIX 3

PUMP STEPPING MOTOR DRIVE

A3-1 DESCRIPTION OF STEPPING MOTOR DRIVE

In order to drive the stepping motors a pulse generator, capable of producing an output suitable for the stepping motors, was designed and used. A variable output ranging from 0 to 150 Hz was needed to produce a suitable wide range of flowrates.

The major problem was one of being able to select a flowrate and repeat it at a later date without having to measure it each time. Consequently a 'discrete' range of output pulse rates was needed. This was achieved by use of the circuit shown in Figure A-1.

The pulse generator takes the 50 Hz signal from the mains power supply and transforms it into a 300 Hz signal. In doing this the sine wave form of the mains signal is transformed into a positive square shaped pulse.

The 300 Hz signal is then passed through two dividers (74193) in series. These dividers are used to provide the discrete range of final outputs. Each divider has four switches which can be used to alter the pulse rate of the signal.

The first divider can divide the signal by 1, 2, 4 or 8 by activation of the appropriate switch. Any combination of the switches divides the signal by the sum of their individual actions. Hence using the first divider alone the 300 Hz signal can be divided by 1 to 15 to produce an output range of 300 Hz to 20 Hz. The four switches on the second divider divide the signal by 16, 32, 64 or 128 when activated. Combined with the

first divider, the second divider gives a total facility for dividing the 300 Hz signal by an integer N where -

$$N = 1, 255 \qquad (A3.1)$$

and the output pulse rate can be found from the relation -

$$P/Hz = 300/N \qquad (3.1)$$

The resulting output signal then passes through shaping and buffer stages before being fed into the stepping motor drive circuits, Philips Electronic Switch 2P 727 86. A detailed account of these switches can be found in the Philips "Handbook on Stepping Motors".

At a later stage it was necessary to obtain a higher torque from the motors and the electronic switches were modified using the method outlined in the Philips "Handbook on Stepping Motors".

A3-2 PARTS LIST AND NOTES ON CIRCUIT DIAGRAM FOR PULSE GENERATOR AND POWER SUPPLY FOR STEPPING MOTORS

A3-2.1 Parts List

Integrated Circuits

I1	½ 7413
I2	¼ 7426

Rectifier Bridge Diodes

IN4001	4 per bridge

Capacitators

C1	4 x 0.001 µF
C2	1 x 2000 µF
C3	1 x 0.22 µF
C4	1 x 10 µF
C5	2 x 7.5 µF
C6	2 x 0.01 µF

Resistors

R1	25 x 1 K
R2	1 x 310 Ω
R3	1 x 270 Ω
R4	2 x 330 Ω
R5	2 x 100 Ω
R6	16 x 82 Ω
R7	2 x 220 Ω
R8	1 x 470 Ω
R9	1 x 1 K adjustable pot.

A3-2.2 Notes

(1) R9 is adjusted to give a square wave at X.

(2) Adjust Z until voltage at Y is 0.25 V or less.

(3) Adjust C5 until there is 300 Hz free running at W.

(4) All 74193 have identical wiring and resistor networks on the loading gates.

(5) Outputs, U, go to the Stepping Motor driving circuits.

(6) There are a number of decoupling capacitors scattered around the +5 V power supply rail.

(7) The -24 V and + 12 V power supplies are used to drive the stepping motors.

APPENDIX 4

BOILER EFFECTIVENESS

The boiler and equilibrator performs the following three functions:

(1) Heating liquid feeds from room temperature T_a, to vaporizing temperature T_v. The value of T_v depends on the operating pressure.

(2) Vaporization of the liquid feeds.

(3) Heating the vapour feeds up to temperature T_f, before they enter the calorimeter.

The three steps can be summarized as shown in Figure A-2.

To determine the length of tube required for each step we must find the area required for transferring the requisite amount of heat. To do this we use the generalized Fourier equation for heat transfer,

$$q = h\ A\ \overline{\Delta T} \qquad \text{(A4.1)}$$

where q = heat required,

h = heat transfer coefficient

A = area for heat transfer

$\overline{\Delta T}$ = Log mean temperature difference between the feed and thermostat.

An explanation of the derivation of this equation can be found in any text on Heat Transfer, e.g. Kern (1950). To obtain A we need a value for q and an estimate of h.

The Energy required for the three steps can be calculated as follows:

(1) Heating of liquid

$$q_1 = m\ C_{pl}(T_v - T_a) \qquad \text{(A4.2)}$$

(2) $$q_2 = m\lambda \qquad \text{(A4.3)}$$

(3) $$q_3 = m\ C_{pg}(T_f - T_v) \qquad \text{(A4.4)}$$

where m = feed mass flowrate

C_ρ = heat capacity, l-liquid, g-gas,

λ = heat of vaporization

The conditions chosen for the calculations are for sub-atmospheric operation where heat transfer is reduced to a considerable extent due to the low pressure. They were,

T_B = 315 K p = 20 kPa (absolute)

T_v = 308 K m = $4.8 10^{-5}$ kg s^{-1} (maximum)

T_a = 298 K C_{pl} = 1750 J kg^{-1} K^{-1}

λ = 4.4×10^5 J kg^{-1} C_{pg} = 1088 J kg^{-1} K^{-1}

Hence q_1 = 0.8W, q_2 = 21 W and q_3 = 0.4 W.

For Step 1, referring to figure A-2,

$$\overline{\Delta T} = ((T_B-T_a) - (T_B-T_v))/\ln((T_B-T_a)/(T_B-T_v)) \qquad (A4.5)$$

$$= 11.2 \text{ K.}$$

and using h = 200 W $m^{-2}K^{-1}$ as suggested by Perry (1963) this gives A_1 = 10^{-4} m^2. Similarly for Step 2 h = 220 W $m^{-2}K^{-1}$ is used, but as this is an isothermal process $\overline{\Delta T}$ becomes (T_B-T_v) and $A_2 = q_2/h(T_B-T_v) = 1.4 10^{-2}$ m^2. The total area required for vaporisation is therefore 1.4×10^{-2} m^2.

The 6 mm Copper tubing has a heat transfer area of $1.57\ 10^{-2}$ m^2/m of tubing. Thus the liquid feed is completely vaporised in the first metre of tubing leaving 14 m of tubing with a heat transfer area of 0.22 m^2 for step 3.

Using a procedure outlined in Kern (1950) we can calculate a value of the heat transfer coefficient at atmospheric pressure and from that a value for h at a pressure of 20 kPa. The results are:

h (atm) = 20 $Wm^{-2}K^{-1}$

and h (20 kPa) = 10 $Wm^{-2}K^{-1}$.

Hence $\overline{\Delta T} = q_3/hA = 0.18$ K. For Step 3

$$\overline{\Delta T} = ((T_B-T_v) - (T_B-T_f))/\ln((T_B-T_v)/(T_B-T_f)). \quad (A4.6)$$

We want to show that $\Delta T = T_B - T_f$ is small so that $T_f \simeq T_B$.

$$\text{Now } \overline{\Delta T} = (7 - \Delta T)/\ln(7/\Delta T) \quad (A4.7)$$

By trial and error:

ΔT/K	$\overline{\Delta T}$/K
1	3.08
0.5	2.5
0.1	1.6
0.01	1.1
0.001	0.8

To obtain an estimate of the value of ΔT let $\overline{\Delta T} = 0.18 = 7/\ln(7/\Delta T)$ which gives $\Delta T \simeq 10^{-16}$ K, i.e. $T_B = T_f$.

Consequently it can be assumed that the inlet temperature of the vapour feeds to the calorimeter is that of the thermostat.

APPENDIX 5

LINEAR REGRESSION

For the linear regression of y on x where

$$y = a\,x + b \tag{A5.1}$$

the sum of squares of deviations of the data (x_i, y_i) from the fitted line is given by

$$S = \sum_i W_i (y_i - (ax_i + b))^2 \tag{A5.2}$$

where W_i is the weighting of the data point (x_i, y_i). To find the best fit S must be a minimum (Topping (1955)), i.e.

$$\partial S/\partial a = 0 \tag{A5.3}$$

and

$$\partial S/\partial b = 0 \tag{A5.4}$$

Using equations (A5.2), (A5.3) and (A5.4) the regression coefficients are found to be given by

$$a = \frac{\sum W_i \sum W_i x_i y_i - \sum W_i x_i \sum W_i y_i}{\sum W_i \sum W_i x_i^2 - (\sum W_i x_i)^2} \tag{A5.5}$$

and

$$b = \frac{\sum W_i y_i \sum W_i x_i^2 - \sum W_i x_i \sum W_i x_i y_i}{\sum W_i \sum W_i x_i^2 - (\sum W_i x_i)^2} \tag{A5.6}$$

The standard errors of the coefficients a and b are according to Topping (1955) given by the following expressions.

Standard error of a

$$\delta_a^2 = \frac{\sum W_i \sum W_i (y_i - (ax_i + b))^2}{(n-2)(\sum W_i \sum W_i x_i^2 - (\sum W_i x_i)^2)} \tag{A5.7}$$

Standard error of b

$$\delta_b^2 = \frac{\sum W_i x_i^2 \sum W_i (y_i - (ax_i + b))^2}{(n-2)(\sum W_i \sum W_i x_i^2 - (\sum W_i x_i)^2)} \tag{A5.8}$$

where n is the number of data points.

A BASIC program was written and used to calculate a, b, δ_a and δ_b. The program is designed for use with an interactive terminal and is listed below.

```
10 REM-THIS PROG RAM CALCULATES THE COEFICIENTS AND THEIR STANDARD
29 REM-ERPO RS OF THE EQUATION Y(I)=A*X(I)+BWHERE(X(I),Y(I))IS
30 REM-A DATA OINT WITH VEIGHTING W(I)ØTHECALCULATIONISDONE
40 REM-BY THE METHOD OF LEAST SQUARES. INPUTS REQUIRED APE
50 REM-N=NO  OF DATA POINTS
60 REM-X(I),Y(I)ANDW(I)
70 DIM X(20) ,Y(20),W(20),Z(20)
80 PRINT "NO  OF DATA POINTS N "
90 INPUT N
100 PRINT "INP UT X(I),Y(I),& W(I) FOP I=1 TO N"
110 FOR I=1 TO  N
120 INPUT X( I),Y(I),W(I)
130 LET C=W( I)+C
140 LET D=W( I)*X(I)*Y(I)+D
150 LET E=W( I)*X(I)+E
160 LET F=W (I )*Y(I)+F
170 LET G=W (I)*X(I)↑2+G
180 NEXT I
190 LET H=C*G -E*E
200 LET A=( C*D-E*F)/H
210 LET B=(F*G -E*D)/H
220 FOP J=1 TO  N
230 LET Z( J)=A*X(J)+B
240 LET K=W (J)*(Z(J)-Y(J))↑2+K
250 NEXT J
270 LET M=C*K/( (N-2)*H)
280 LET M1=S QP(M)
290 LET O=G*K/ ((N-2)*H)
300 LET O1=SQ R(O)
320 PRINT "A=";A,"B=";B
330 PRINT  \ P PINT
340 PRINT "S TD EPPOP OF A=";M1;"STD EPROR OF B=";O1
345 PRINT  \ P PINT  \ PRINT
350 END
```

APPENDIX 6

CURVE FITTING PROGRAM

This program is for a multi-variable optimisation routine designed to fit a specified function to a set of data by minimising the sum of squares of deviations of the data from the fitted function. The program uses a Hooke and Jeeves pattern search method (Dixon (1972)), to change the value of the constants in the function, in search of the optimum sum of squares of deviations.

This Appendix will list both curve fitting programs used, which were designed for use with an interactive terminal.

A6-1 Program for Fitting (ε_i, T_i) Data Only

The function to be fitted is given in line 75 of the program, namely

$$\varepsilon/10^{-6}\,m^3\,mol^{-1} = a + (b*10^{-4})\ \exp(100C/T) \qquad (A6.1)$$

where the constants in

$$\varepsilon = A + B\ \exp(C/T) \qquad (A6.2)$$

have been scaled so that they are of the same order of magnitude. The inputs required are:

(1) No. of (ε_i T_i) data points to be fitted.

(2) Number of variables (constants) in the function.

(3) Initial step size in the variables for the search method.

(4) Final step size in the variables for the search method.

(5) Step size reduction factor.

(6) Initial values of a, b and c.

The (ε_i, T_i) and weighting W_i, data is already included in the program, by means of a DATA statement lines 6000 to 6002. This enables the program to be rerun rapidly for various initial values of a, b and c.

Statement 4010 in the program is a dummy input which causes the program execution to be stopped once the search has been terminated and the optimum values found. This enables the interim output to be suppressed thus saving time. Upon entering the dummy input (any integer), the final output, which has the following form, is printed:

(1) The optimum value of the sum of squares of deviations.

(2) A listing of the final values of the constants a, b and c.

(3) A listing of the numbers of, explorations, pattern moves, and function evaluations required to find the optimum.

```
20 REM MULTI VARIABLE OPTIMISATION BY HOOKE AND JEEVES
21 REM  PATTERN SEARCH METHOD
40 REM  SEE DIXON "NONLINEAR OPTIMISATION" P 69.
60 REM THE FUNCTION TO BE OPTIMISED IS DEFINED IN A SUBROUTINE
61 REM          AT LINE 5000
75 DEF FNA(A,B,C,T)=A+1.00000E-04*B*EXP(100*C/T)
80 DIM P(20),T(20),W(20)
85 PRINT "NUMBER OF DATA POINTS? "; \ INPUT N9
88 FOR M=1 TO N9
90 READ P( M),T(M),W(M)
95 NEXT M
100 DIM X( 10),X1(10),X2(10),X3(10)
200 PRINT "INPUT NUMBER OF VARIABLES N"
220 INPUT N
300 PRINT "INPUT INITIAL STEP SIZE K"
320 INPUT K
340 PRINT "INPUT FINAL STEP SIZE K1"
360 INPUT K1
380 PRINT "INPUT STEP SIZE REDUCTION FACTOR"
400 INPUT K2
420 LET K9=K
480 REM  INPUT STARTING POINT X
500 FOR I=1 TO N
520 PRINT "X("I")= ", \ INPUT X(I)
540 NEXT I
560 LET K=K9
600 REM  INITIALISE COUNTERS
620 LET J=0 \ LET J1=0 \ LET J2=0
2000 REM  START SEARCH
2020 REM  EVALUATE FUNCTION AT STARTING POINT
2040 FOR I=1 TO N
2060 LET X1( I)=X(I) \ LET X2(I)=X(I)
2080 NEXT I
2100 GOSUB 5000
2120 LET Y=Y1 \ LET Y2=Y1
2140 PRINT "AT INITIAL BASE POINT Y=",Y
```

```
2160 PRINT "X=",
2180 FOR I=1 TO N
2200 PRINT X( I),
2220 NEXT I
2240 PRINT  \ PRINT
2300 REM START EXPLORATION
2320 LET J=J+1
2340 PRINT "EXPLORATION NUMBER "J
2360 FOR I=1 TO N
2380 LET X1(I)=X2(I)+K
2400 GOSUB 5000
2420 LET Z=Y1
2460 IF Z>Y2 THEN 2700
2480 REM  FAILURE . CHANGE SIGN OF STEP.
2520 LET X1(I)=X2(I)-K \ LET K=-K
2540 GOSUB 5000
2560 LET Z=Y1
2600 IF Z>Y2 THEN 2700
2620 REM  FAILURE AGAIN. GO ON TO NEXT DIRECTION
2660 LET X3(I)=X2(I)
2670 LET X1( I)=X2(I)
2680 GO TO 27 80
2700 REM  SUCCESS
2740 LET X3(I)=X1(I)
2760 LET Y2=Z
2780 NEXT I
2800 REM  END OF EXPLORATION
2820 PRINT "AFTER EXPLORATION Y2= ";Y2
2840 PRINT "X3= ";
2860 FOR I=1 TO N
2880 PRINT X3(I);
2900 NEXT I
2920 PRINT
2940 REM  TEST WHETHER EXPLORATION HAS IMPROVED OVER BASE POINT
2960 PRINT "EXP LORATION HAS ";
2980 IF Y2>Y THEN 3000
2990 PRINT "NOT";
3000 PRINT "IMPROVED ON BASE POINT"
3020 IF Y2<=Y THEN 3500
3040 PRINT "MAKE PATTERN MOVE"
3060 FOR I=1 TO N
3080 LET X2(I)=X3(I)*2-X(I)
3100 LET X(I)=X3(I)
3110 LET X1(I)=X2(I)
3120 NEXT I
3140 LET Y=Y2
3160 GOSUB 5000
3180 LET Y2=Y1
3200 LET J2=J2+1
3220 PRINT "PATTERN MOVE "J2" IS TO X2= ";
3260 FOR I=1 TO N
3280 PRINT X2(I);
3300 NEXT I
3320 PRINT  \ PRINT "WHERE Y2=",Y2
3340 PRINT "BASE POINT NUMBER "J2+1" BECOMES"
3350 PRINT "X= ";
3360 FOR I=1 TO N
3380 PRINT X(I);
3400 NEXT I
3420 PRINT  \ PRINT "WHERE Y= "Y
```

```
3440 GO TO 2320
3500 REM  NO IMPROVEMENTFROM EXPLORATION. HAVE WE EXPLORED
3502 REM    FROM THE BASE POINT ?
3520 FOR I=1 TO N
3540 IF X2(I)=X(I) THEN 3580
3560 GO TO 3700
3580 NEXT I
3590 GO TO 3900
3700 PRINT "START NEXT EXPLORATION FROM THE BASE POINT."
3720 FOR I=1 TO N
3740 LET X2(I)=X(I)
3760 NEXT I
3780 LET V2=V
3800 GO TO 2320
3900 PRINT "HAVE ALREADY EXPLORED FROM BASE POINT. DECREASE STEP SIZE"
3920 LET K=K*K2 \ PRINT "K= "K
3940 REM  TEST FOR TERMINATION
3960 IF ABS(K)>=K1 THEN 2320
4000 REM  TERMINATE
4010 INPUT A9
4020 PRINT  \ PRINT "OPTIMUM VALUE IS",Y
4040 FOR I=1 TO N
4060 PRINT "X("I")="X(I)
4080 NEXT I
4100 PRINT J" EXPLORATIONS"
4120 PRINT J2" PATTERN MOVES"
4140 PRINT J1" FUNCTION EVALUATIONS"
4300 STOP
5000 REM SUM OF SQUARES SUBROUTINE
5020 LET V1=0
5040 LET J1=J1+1
5060 FOR M=1 TO N9
5080 V9=P( M)-FNA(X1(1),X1(2),X1(3),T(M))
5100 LET V9=V9*V9
5110 V9=V9*W(M)
5120 LET V1=V1-V9
5140 NEXT M
5160 RETURN
6000 DATA 57,308,8,22,373,80,35,323,8,25,348,40,22,373,40
6001 DATA 38,315,5,21,373,26.7,45,318,4,29,323,40,44,323,80
6002 DATA 19,348,26.7,30,313,1.78,14,333,5.33,135,298,1,175,300,1.6
8191 END
```

A6-2 Program for Fitting Both (ε_i, T_i) and $(H^E_m/p_j, T_j)$ Data

This program is essentially the same as the previous one but is modified to include in the total sum of squares of deviations that contribution attributable to the deviations of the $(H^E_m/p_j, T_j)$ data as outlined in Section 4-4. Additional inputs required are

(1) Overall weighting of the $(H^E_m/p_j, T_j)$ data points.

(2) Overall weighting of the (ε_i, T_i) data points.

The $(H^E_m/p_j, T_j, W_j)$ data is read in as for the $(\varepsilon_i, T_i, W_i)$ data by means of the DATA statements numbers 5998 and 5999 in the program. The final output is the same as for the other program with the addition of the contribution of each set of data to the final sum of squares of deviations.

```
20 REM MULTI VARIABLE OPTIMISATION BY HOOKE AND JEEVES
21 REM  PATTERN SEARCH METHOD
40 REM  SEE DIXON "NONLINEAR OPTIMISATION" P 69.
60 REM THE FUNCTION TO BE OPTIMISED IS DEFINED IN A SUBROUTINE
61 REM          AT LINE 5000
62 DIM R(10),T1(10),W1(10)
63 DEF FNB(A,B,C,T)=A+1.000000E-04*B*EXP(100*C/T)*(1+100*C/T)
64 PRINT "OVERALL WEIGHTING OF HE/P DATA POINTS?"; \ INPUT Q
65 REM N8 IS THE NUMBER OF HE/P DATA POINTS
66 N8=10
67 FOR M1=1 TO N8
68 READ R(M1),T1(M1),W1(M1)
69 NEXT M1
75 DEF FNA(A,B,C,T)=A+1.000000E-04*B*EXP(100*C/T)
80 DIM P(20),T(20),W(20)
81 PRINT "OVERALL WEIGHTING OF DATA POINTS?"; \ INPUT P
85 PRINT "NUMBER OF DATA POINTS? "; \ INPUT N9
88 FOR M=1 TO N9
90 READ P(M),T(M),W(M)
95 NEXT M
100 DIM X(10),X1(10),X2(10),X3(10)
200 PRINT "INPUT NUMBER OF VARIABLES N"
220 INPUT N
300 PRINT "INPUT INITIAL STEP SIZE K"
320 INPUT K
340 PRINT "INPUT FINAL STEP SIZE K1"
360 INPUT K1
380 PRINT "INPUT STEP SIZE REDUCTION FACTOR"
400 INPUT K2
420 LET K9=K
480 REM  INPUT STARTING POINT X
500 FOR I=1 TO N
```

```
520 PRINT "X("I")= ", \ INPUT X(I)
540 NEXT I
560 LET K=K9
600 REM  INITIALISE COUNTERS
620 LET J=0 \ LET J1=0 \ LET J2=0
2000 REM  STAR T SEARCH
2020 REM  EV ALUATE FUNCTION AT STARTING POINT
2040 FOR I=1 TO N
2060 LET X 1( I)=X( I) \ LET X2(I)=X(I)
2080 NEXT I
2100 GOSUB 5000
2120 LET Y=Y 1 \ LET Y2=Y1
2140 PRINT " AT INITIAL BASE POINT Y=",Y
2160 PRINT "X =",
2180 FOR I=1 TO N
2200 PRINT X( I),
2220 NEXT I
2240 PRINT  \ P RINT
2300 REM START  EXPLORATION
2320 LET J=J+1
2340 PRINT "EXP LORATION NUMBER "J
2360 FOR I=1 TO N
2380 LET X 1( I)=X2(I)+K
2400 GOSUB 5000
2420 LET Z=Y 1
2460 IF Z>Y2 THEN 2700
2480 REM  FAILURE . CHANGE SIGN OF STEP.
2520 LET X 1( I)=X2(I)-K \ LET K=-K
2540 GOSUB 5000
2560 LET Z=Y 1
2600 IF Z>Y2  T HEN 2700
2620 REM  FAILURE AGAIN. GO ON TO NEXT DIRECTION
2660 LET X 3(I)=X 2(I)
2670 LET X 1( I)=X2(I)
2680 GO TO  2780
2700 REM  SUCCESS
2740 LET X 3( I)=X 1(I)
2760 LET Y 2=Z
2780 NEXT I
2800 REM  END OF EXPLORATION
2820 PRINT " AFTER EXPLORATION Y2= ";Y2
2840 PRINT "X 3= ";
2860 FOR I=1 TO N
2880 PRINT X 3(I);
2900 NEXT I
2920 PRINT
2940 REM  TEST W HETHER EXPLORATION HAS IMPROVED OVER BASE POINT
2960 PRINT  "EXPLORATION HAS ";
2980 IF Y 2>Y  THEN 3000
2990 PRINT " NOT";
3000 PRINT " IMPROVED ON BASE POINT"
3020 IF Y2<=Y  THEN 3500
3040 PRINT "MAKE P ATTERN MOVE"
3060 FOR I=1 TO N
3080 LET X 2( I)=X 3( I)*2-X(I)
3100 LET X( I)=X 3( I)
3110 LET X 1( I)=X2(I)
3120 NEXT I
3140 LET Y=Y 2
3160 GOSUB 5000
3180 LET Y 2=Y 1
3200 LET J2=J2+1
3220 PRINT "PATTERN MOVE "J2" IS TO X2= ";
```

```
3260 FOR I=1 TO N
3280 PRINT X 2(I);
3300 NEXT I
3320 PRINT  \ PRINT "WHERE Y2=",Y2
3340 PRINT "BASE P OINT NUMBER "J2+1" BECOMES"
3350 PRINT "X = ";
3360 FOR I=1 TO N
3380 PRINT X (I);
3400 NEXT I
3420 PRINT  \ PRINT "WHERE Y= "Y
3440 GO TO 2320
3500 REM  NO  IMPROVEMENTFROM EXPLORATION. HAVE WE EXPLORED
3502 REM     F RO M THE BASE POINT ?
3520 FOR I=1 TO N
3540 IF X2( I)=X(I) THEN 3580
3560 GO TO 37 00
3580 NEXT I
3590 GO TO 3900
3700 PRINT "START NEXT EXPLORATION FROM THE BASE POINT."
3720 FOR I=1 TO  N
3740 LET X2( I)=X( I)
3760 NEXT I
3780 LET Y2=Y
3800 GO TO 2320
3900 PRINT "HAVE ALREADY EXPLORED FROM BASE POINT. DECREASE STEP SIZE"
3920 LET K=K*K2 \ PRINT "K= "K
3940 REM  TEST FOR TERMINATION
3960 IF ABS(K)>=K1 THEN 2320
4000 REM  TERMINATE
4010 INPUT A9
4020 PRINT  \ PRINT "OPTIMUM VALUE IS",Y
4030 PRINT  \ PRINT "S1=";S1,"S2=";S2
4040 FOR I=1 TO N
4060 PRINT "X ("I")="X(I)
4080 NEXT I
4100 PRINT J" EX PLORATIONS"
4120 PRINT J2"  PATTERN MOVES"
4140 PRINT J1" FUNCTION EVALUATIONS"
4300 STOP
5000 REM SUM O F SQUARES SUBROUTINE
5020 LET Y1=0
5030 S1=0 \ S2=0
5040 LET J1=J1+1
5060 FOR M=1 TO N9
5080 Y9=P( M)-FNA(X1(1),X1(2),X1(3),T(M))
5100 LET Y9=Y9*Y9
5120 S1=W(M)*Y9+S1
5140 NEXT M
5160 FOR M1=1 TO N8
5180 Y8=P(M1)-FNB(X1(1),X1(2),X1(3),T1(M1))
5200 Y8=Y8*Y8
5220 S2=W1(M1)*Y 8+S2
5240 NEXT M1
5260 S=P*S 1+Q*S2
5280 Y1=Y 1-S
5300 RETURN
5998 DATA  110,359,16.7,105,358,20,100,358,20,105,358,20,100,358,20
5999 DATA  100,358,20,100,358,6.3,400,323,1.3,440,315,1.33,480,305,1
6000 DATA  57,308,8,22,373,80,35,323,8,25,348,40,22,373,40
6001 DATA  38,315,5,21,373,26.7,45,318,4,29,323,40,44,323,80
6002 DATA  19,348,26.7,30,313,1.78,14,333,5.33,135,298,1,175,300,1.6
8191 END
```

APPENDIX VII THERMOSTAT BATH PROPORTIONAL TEMPERATURE CONTROLLER

after M.L. Martin, Adelaide University, South Australia

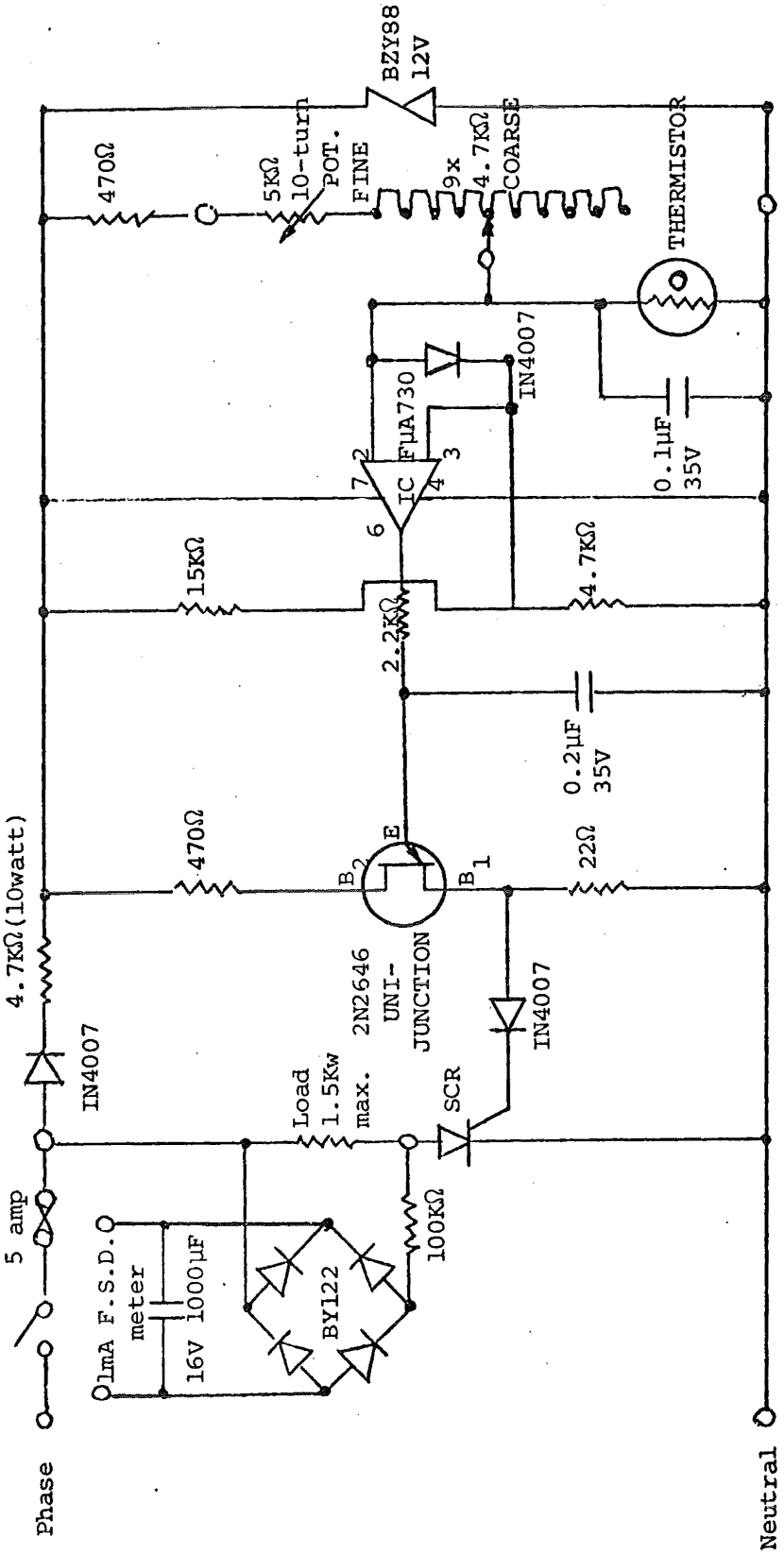

APPENDIX 8

REFERENCES

Alexander, E. A., and Lambert J. D., Trans. Faraday Soc., 1941, 37, 421.

Beath, L. A., Ph.D. Thesis, University of Otago, 1967.

Beenakker, J. J. M., and Coremans J. M. J., Symp. Thermophys. Props., A.S.M.E. 2nd, Princeton, N.J., 1962, p.2.

Beenakker, J. J. M., Van Eijnsbergen, B., Knoester, M., Taconis, K. W., and Zanbergen, P., Symp. Thermophys. Props., A.S.M.E. 3rd, Lafayette Ind., 1965, p.114.

Bottomley, G. A. and Coopes, I. H., Nature, 1962, 193, 268.

Campbell, A. N., and Kartzmark, E. M., Can. J. Chem., 1960, 38, 652.

Chen, H. Y., O'Connell, J. P., and Prausnitz, J. M., Can. J. Chem., 1966, 44, 429.

Coan, C. R. and King, A. D. Jun., J. Amer. Chem. Soc., 1971, 93, 1857.

Cox, J. D. and Stubley, D., Appendix to Partington et. al., Trans. Far. Soc., 1960, 56, 484.

Dantzler, E. M., and Knobler, C. M., J. Phys. Chem., 1969, 73, 1602.

Dixon, L. C. W., Nonlinear Optimisation, The English Universities Press Ltd., London, 1972.

Dymond, J. H. and Smith E. B., The Virial Coefficients of Gases, Clarendon Press, Oxford, 1969.

Edwards, A. E., and Roseveare, W. E., J. Amer. Chem. Soc., 1942, 64, 2816.

Fox, J. H. P., and Lambert, J. D., Proc. Roy. Soc., 1954, A226, 394.

Francis, P. G., McGlashan, M. L., and Wormald, C. J., J. Chem. Thermodynamics, 1969, 1, 441.

Guggenheim, E. A., Thermodynamics, North-Holland Publishing Co., 1950.

Guggenheim, E. A. Rev. Pure Appl. Chem, 1953, R. Australian Chem. Inst.

Guggenheim, E. A. Mol. Phys., 1966, 10, 401.

Gupta, S. K., Leslie, R. D., and King, A. D. Jun., J. Phys. Chem., 1973, 77, 2011.

Hejmadi, A. V., Katz, D. L., and Powers, J. E., J. Chem. Thermodynamics, 1971, 3, 483.

Hemmaplardh, B., and King, A. D. Jun., J. Phys. Chem., 1972, 76, 2170.

Hill, T. L., Introduction to Statistical Thermodynamics, Addison Wesley, Reading, 1960.

Hirschfelder, J. O., Curtiss, C. F., and Bird, R. B., Molecular Theory of Gases and Liquids, Wiley, New York, 1954.

Huggins, C. M., Pimentel, G. C., and Shoolery, J. N., J. Chem. Phys., 1955, 23, 1244.

Jordan, P. J., University of Canterbury, 1978, Private Communication.

Judd, N., 1969, Private Communication.

Kearns, E. R., J. Physical Chem., 1961, 65, 314.

Kern, D. Q., Process Heat Transfer, McGraw-Hill, 1950.

Klein, R. R., Bennett, C. O., and Dodge, B. F., A.I.Ch.E., 1971, 17, 958.

Knobler, C. M., Chemical Thermodynamics (Specialist Periodical Reports), The Chemical Society, London, 1978, Vol.2, Chap. 7.

Knobler, C. M., Beenakker, J. J. M., and Knapp, H. F. P., Physica, 1959, 25, 909.

Knobler, C. M. and Handa, P., 1976, Private Communication.

Knobler, C. M. and Pasco, N., 1975, Private Communication.

Knoester, M., Taconis, K. W., and Beenakker, J. J. M., Physica, 1967, 33, 389.

Lambert, J. D., Clarke, J. S., Duke, J. F., Hicks, C. L., Lawrence, S. D., Morris, D. H., and Stone, M. G. T., Proc. Roy. Soc., 1959, A249, 414.

Lambert, J. D., Murray, S. J. and Sanday, J. P., Proc. Roy. Soc., 1954, A226, 394.

Lambert, J. D., Roberts, G. A. H., Rowlinson, J. S., and Wilkinson, V. J., Proc. Roy. Soc., 1949, A196, 113.

Lambert, J. D., and Strong, E. D. T., Proc. Roy. Soc., 1950, A200, 566.

Lee, J. I., and Mather, A. E., J. Chem. Thermodynamics, 1970, 2, 881.

Lewis, K. L., Mosedale, S. E., and Wormald, C. J., J. Chem. Thermodynamics, 1977, 9, 221.

Lindsay, J. D., and Brown G. G., Ind. Eng. Chem., 1935, 27, 817.

McCullough, J. P., and Waddington, G., "Vapour Flow Calorimetry" Experimental Thermodynamics, Vol. 1, Plenum Press, N.Y., 1968.

McElroy, P. J., Ph.D. Thesis, University of Otago, N.Z., 1968.

McGlashan, M. L., and Potter, D. J. B., Proc. Roy. Soc., 1962, A267, 214.

McGlashan, M. L., and Rastogi, R. P., Trans. Faraday Soc., 1958, 54, 496.

Martin, M. L., University of Adelaide, 1968, Private Communication.

Mason, E. A., and Spurling, T. H., The Virial Equation of State, Pergamon Press, Oxford, 1969.

Massoudi, R., and King, A. D. Jun., J. Phys. Chem., 1973, 77, 2016.

Millen, D. J., and Mines, G. W., Trans. Faraday Soc., 1974, 70, 693.

Moelwyn-Hughes, E. A., and Sherman, A., J. Chem. Soc., 1936, 101.

Morcom, K. W., and Travers, D. N., Trans. Faraday Soc., 1965, 61, 235.

Najor, G. J., and King, A. D. Jun., J. Chem. Phys., 1966, 45, 1915.

Perry, J. H. (Ed.), Chemical Engineers Handbook, 4th Edn., McGraw-Hill, 1963.

Pimentel, G. C., and McClellan, A. L., The Hydrogen Bond, W. H. Freeman and Co., San Francisco and London, 1960.

Pitzer, K. S., J. Amer. Chem. Soc., 1941, 63, 2413.

Prausnitz, J. M., Molecular Thermodynamics of Fluid Phase Equilibria, Prentice-Hall, Englewood Cliffs, New Jersey, 1969.

Prausnitz, J. M., and Carter, W. B., J. Amer. Inst. Chem. Eng., 1960, 6, 611.

Philips, Stepping Motors, Industrial Components and Materials Division, 32.087 B/E 12-64, Holland.

Rätzsch, M., and Freydank, H., J. Chem. Thermodynamics, 1971, 3, 861.

Rossini, Ed., Amer. Petrol Inst. Project 44 Tables, 1952.

Scheele, K., and Heuse, W., Ann. Physik., 1912, 37, 79.

Scott, R. B., and Mellors, J. W., J. Res. Natl. Bur. Stand., 1945, 34, 243.

Scott, R. L., Mol. Phys., 1966, 11, 399.

Shannon, T. W., Ph.D. Thesis, University of Canterbury, 1976.

Topping, J., Errors of Observation and Their Treatment, Institute of Physics, London, 1955.

Van Eijnsbergen, B., and Beenakker, J. J. M., Physica, 1968, 39, 499.

Waelbroeck, F. G., J. Chem. Phys., 1955, 23, 749.

Williamson, A. G., 1966, Private Communication.

Williamson, A. G., An Introduction to Non-Electrolyte Systems., Oliver and Boyd, London, 1967.

Wormald, C. J., Proc. 1st Intern. Conf. Calorimetry and Thermodynamics, Warsaw, 1969, 601.

Wormald, C. J., J. Chem. Thermodynamics, 1977, 9, 901.

Wormald, C. J., Lewis, K. L. and Mosedale, S. J., J. Chem. Thermodynamics, 1977, 9, 27.

Wormald, C. J. 1978, Private Communication.

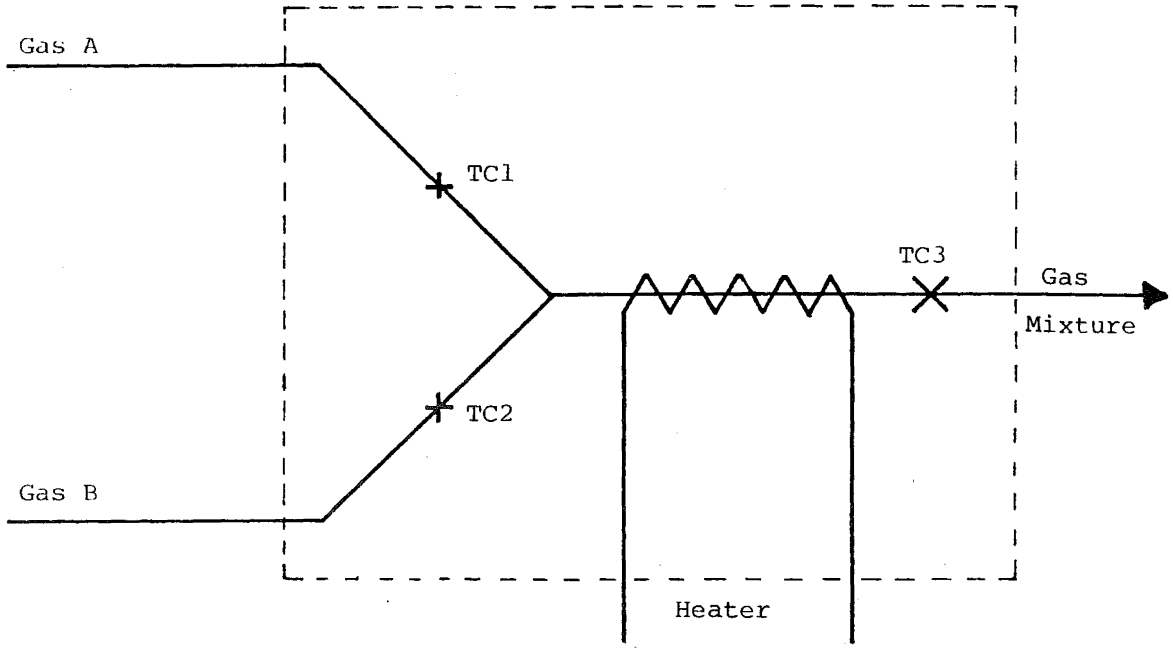

FIGURE 2-1 Calorimeter Layout

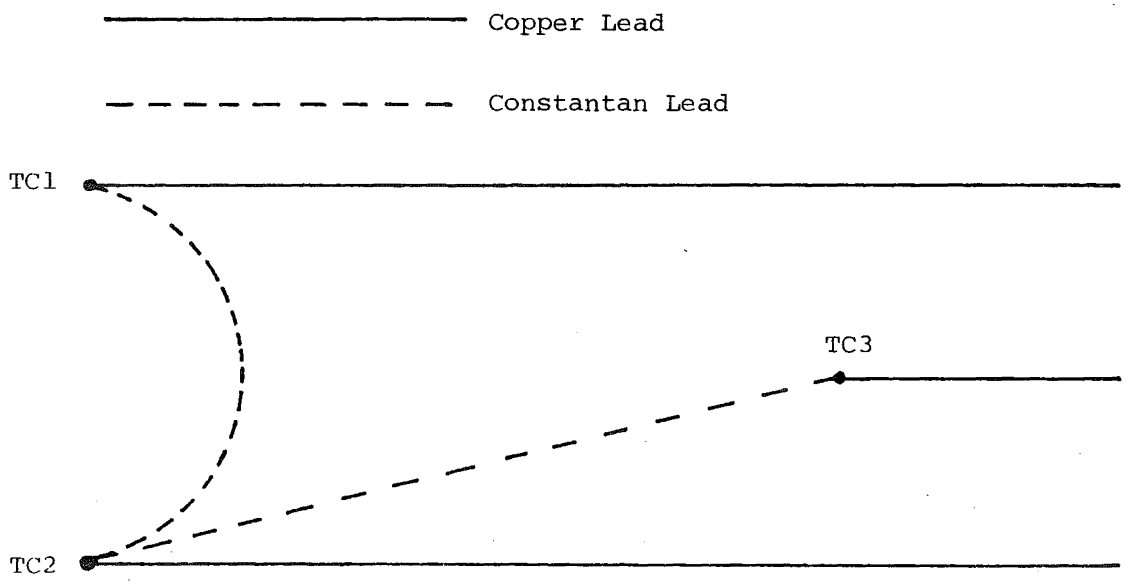

FIGURE 2-2 Thermocouple Arrangement

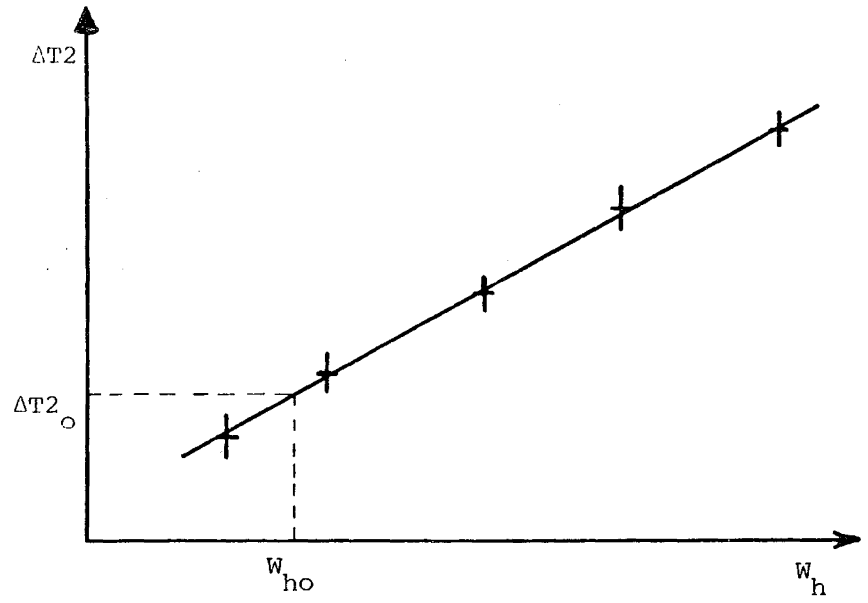

FIGURE 2-3 Plot of ΔT2 Against W_h for Endothermic Mixing

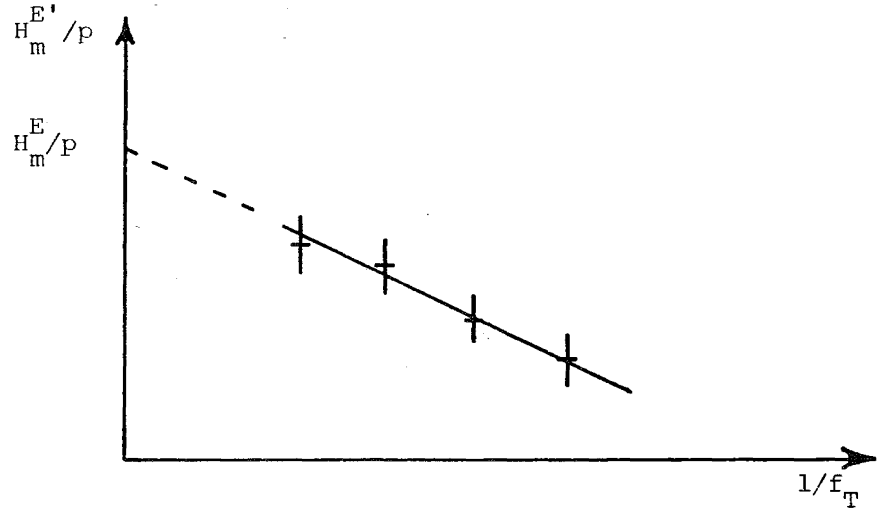

FIGURE 2-4 Determination of True Heat of Mixing H_m^E/p

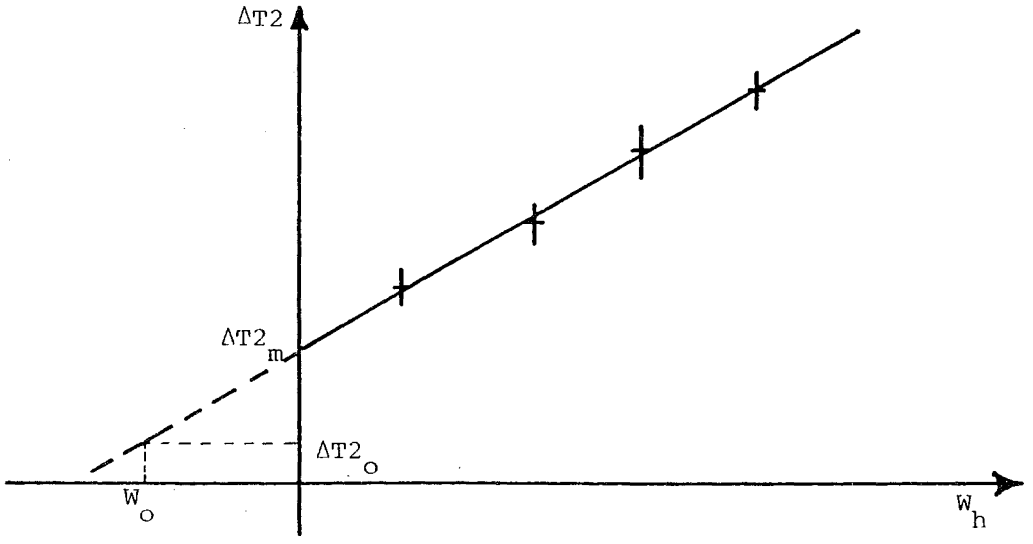

FIGURE 2-5 Plot of ΔT2 Against W_h for Exothermic Mixing

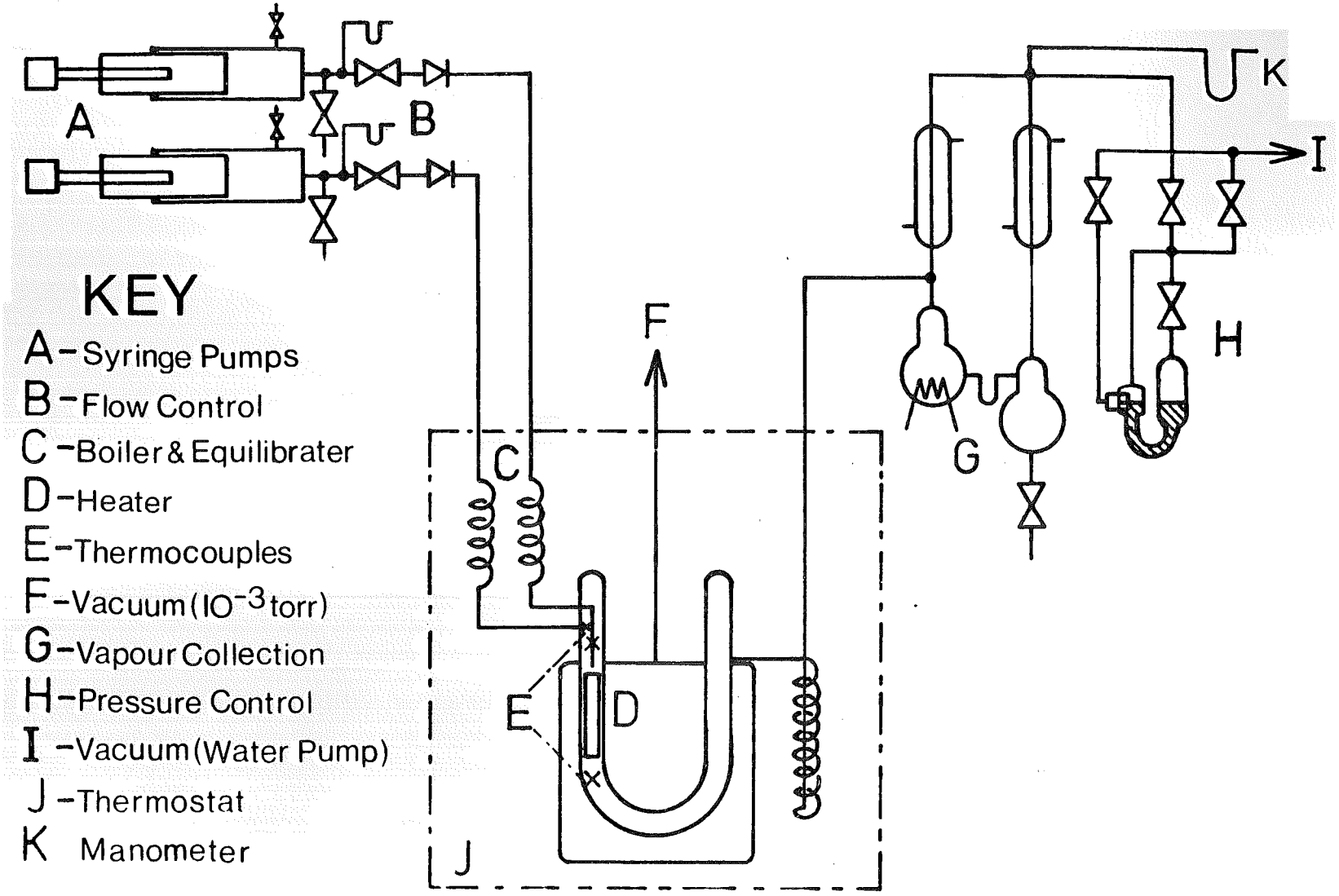

FIG. 3-1 CALORIMETER FLOW DIAGRAM.

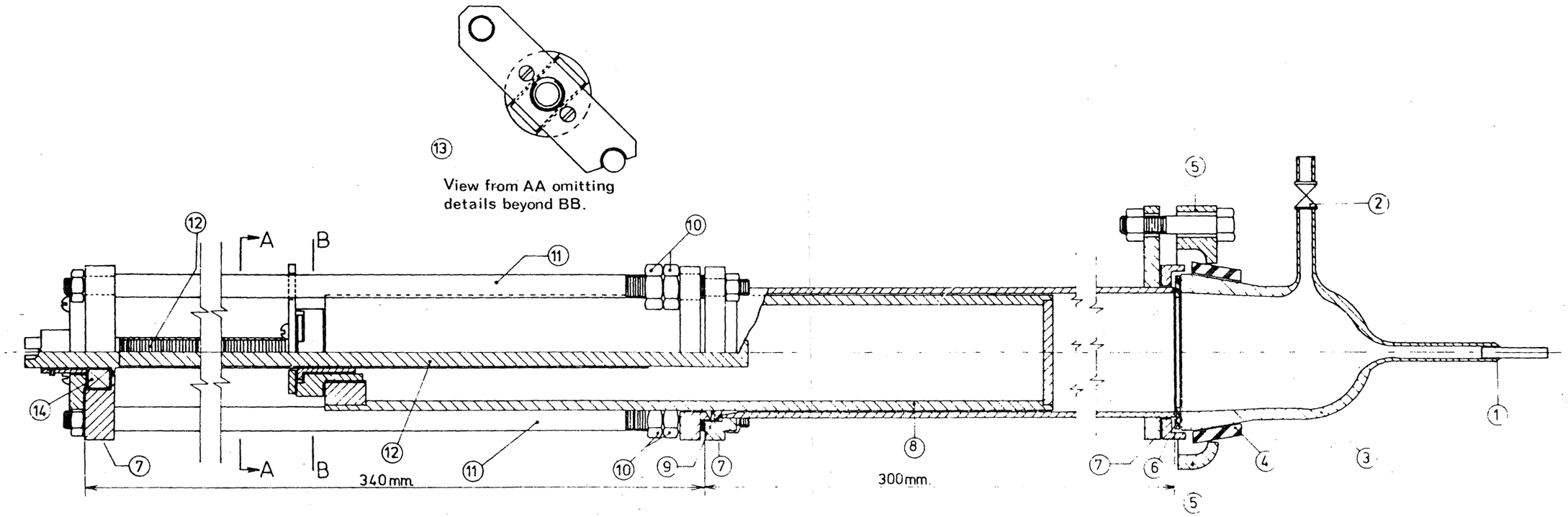

FIG 3-2 CALORIMETER PUMP

KEY

1 - 1/4" glass to metal (Kovar) Seal
2 - 6 mm Youngs Tap
3 - 2" QVF Blank End (modified)
4 - 2" QVF Rubber Gasket
5 - QVF Backing Flange
6 - Teflon-coated Gasket
7 - Pump Frame Mounting Points
8 - Pump Piston
9 - Teflon Rope Seal
10 - Seal Adjustment Nuts
11 - Guide Rods
12 - Lead Screw (½" dia., 28 T.P.I.)
13 - Drive Transmission Assembly
14 - ½" x 15/16" x 3/8" Thrust Ball Race

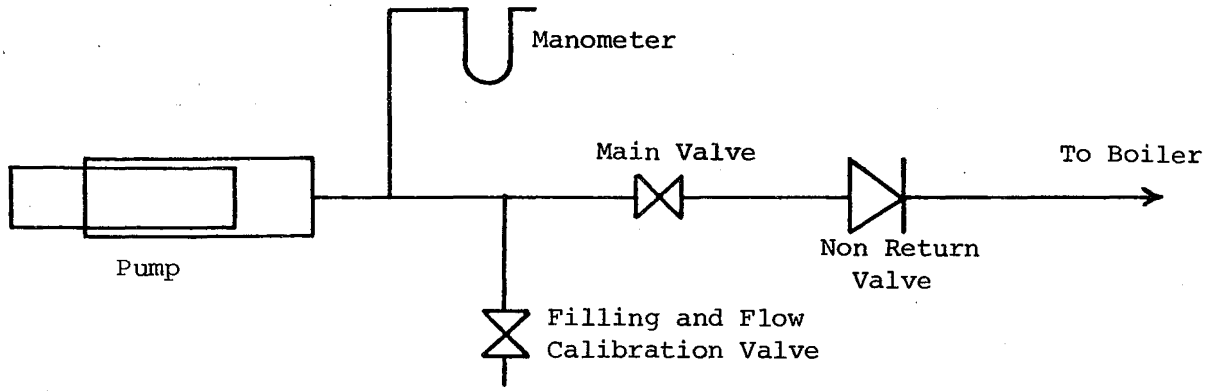

FIGURE 3-3 Flow Control System

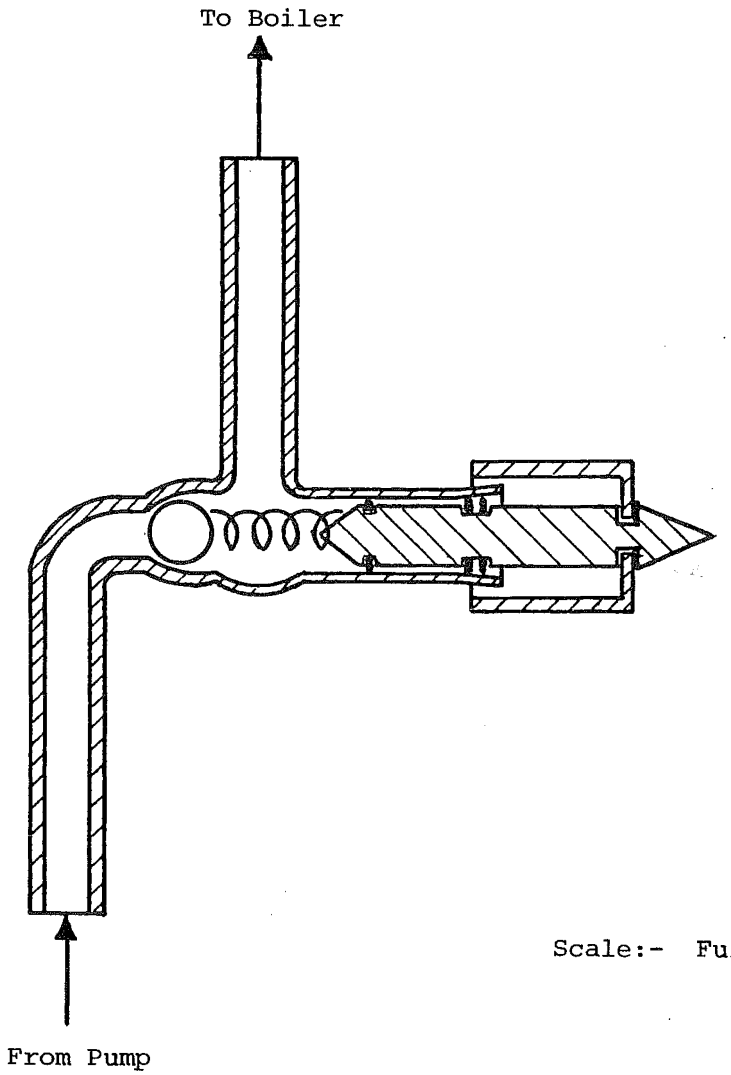

Scale:- Full Size.

FIGURE 3-4 Adjustable Non-Return Valve

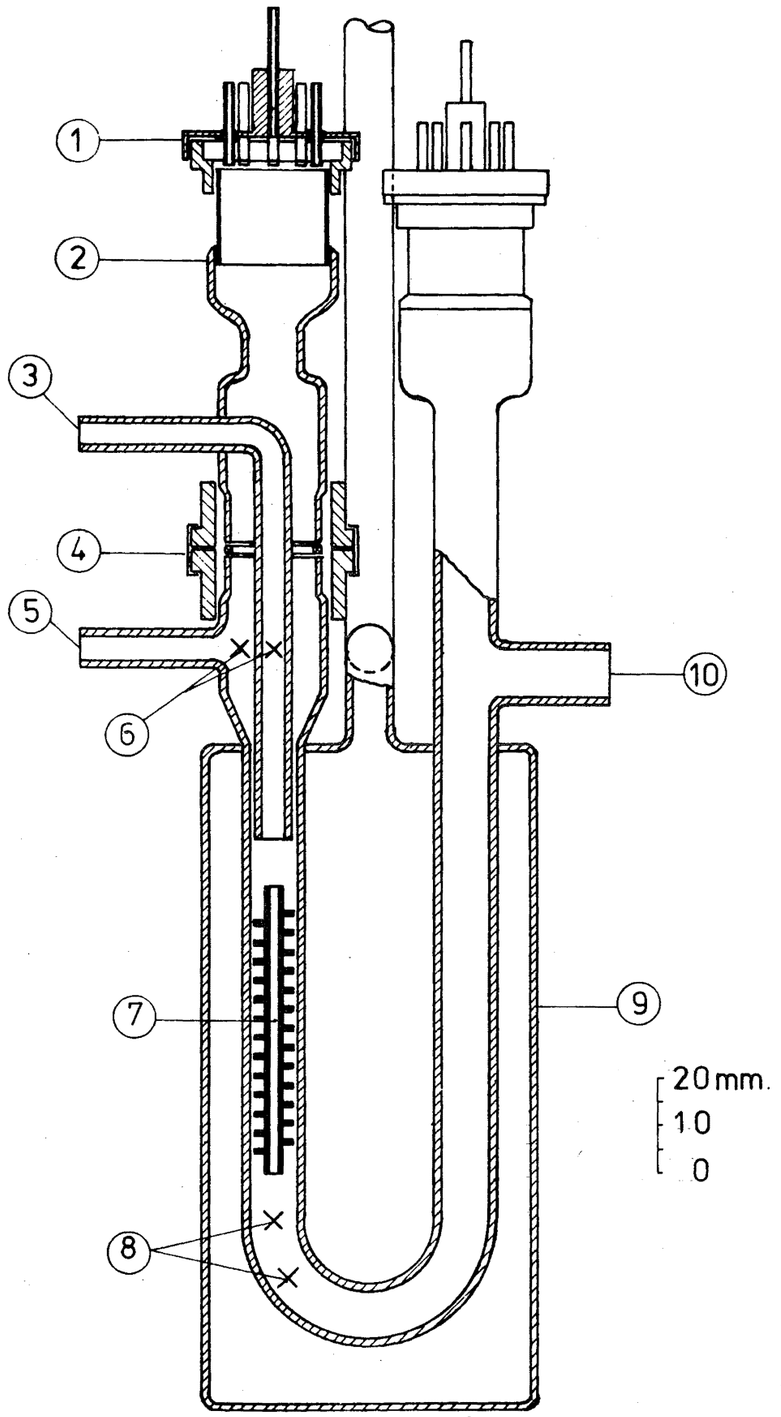

FIG. 3-5 HEATS OF MIXING CALORIMETER.

KEY

(1) 11 Pin Electrode Seal for Heater Leads

(2) 25 mm Glass to Metal (Kovar) Seal

(3) Vapour/Gas Inlet

(4) 22 mm 'Soveril' Joint

(5) Vapour/Gas Inlet

(6) Thermocouples

(7) Heater

(8) Thermocouples

(9) Vacuum Jacket

(10) Mixture Outlet

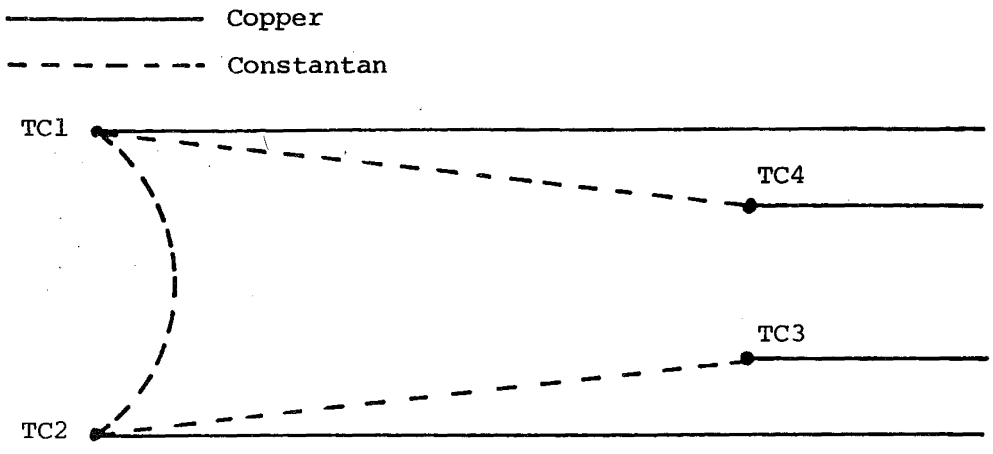

FIGURE 3-6 Thermocouple Arrangement

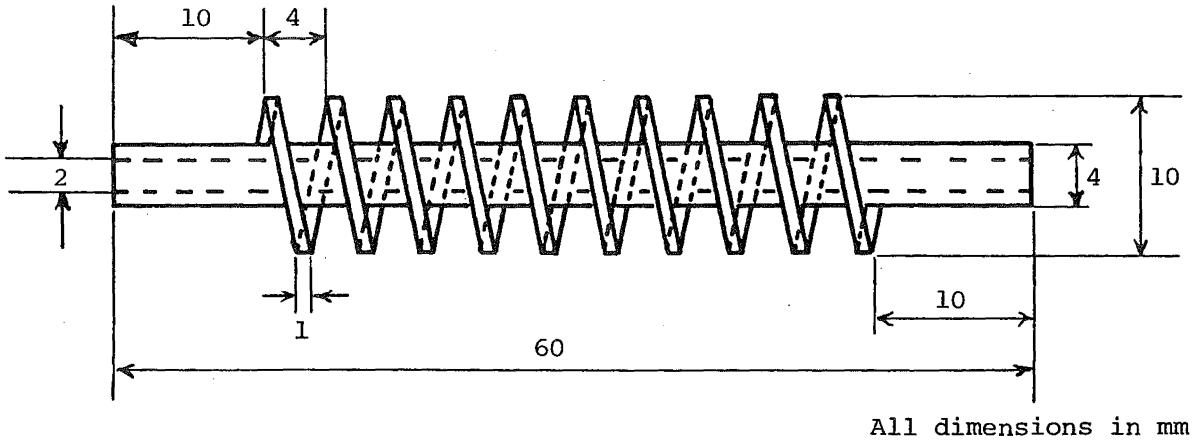

FIGURE 3-7 Teflon Former for Heater

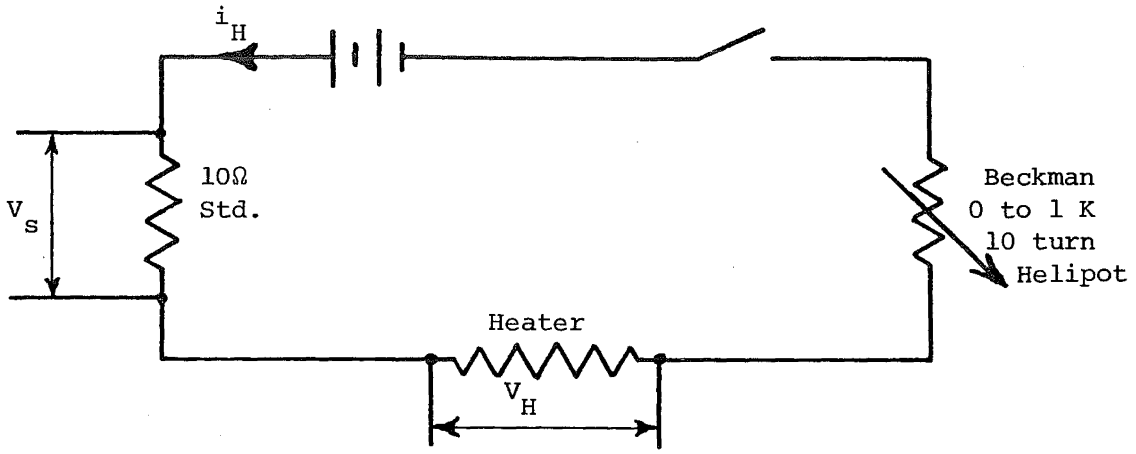

FIGURE 3-8 Calorimeter Heater Circuit Diagram

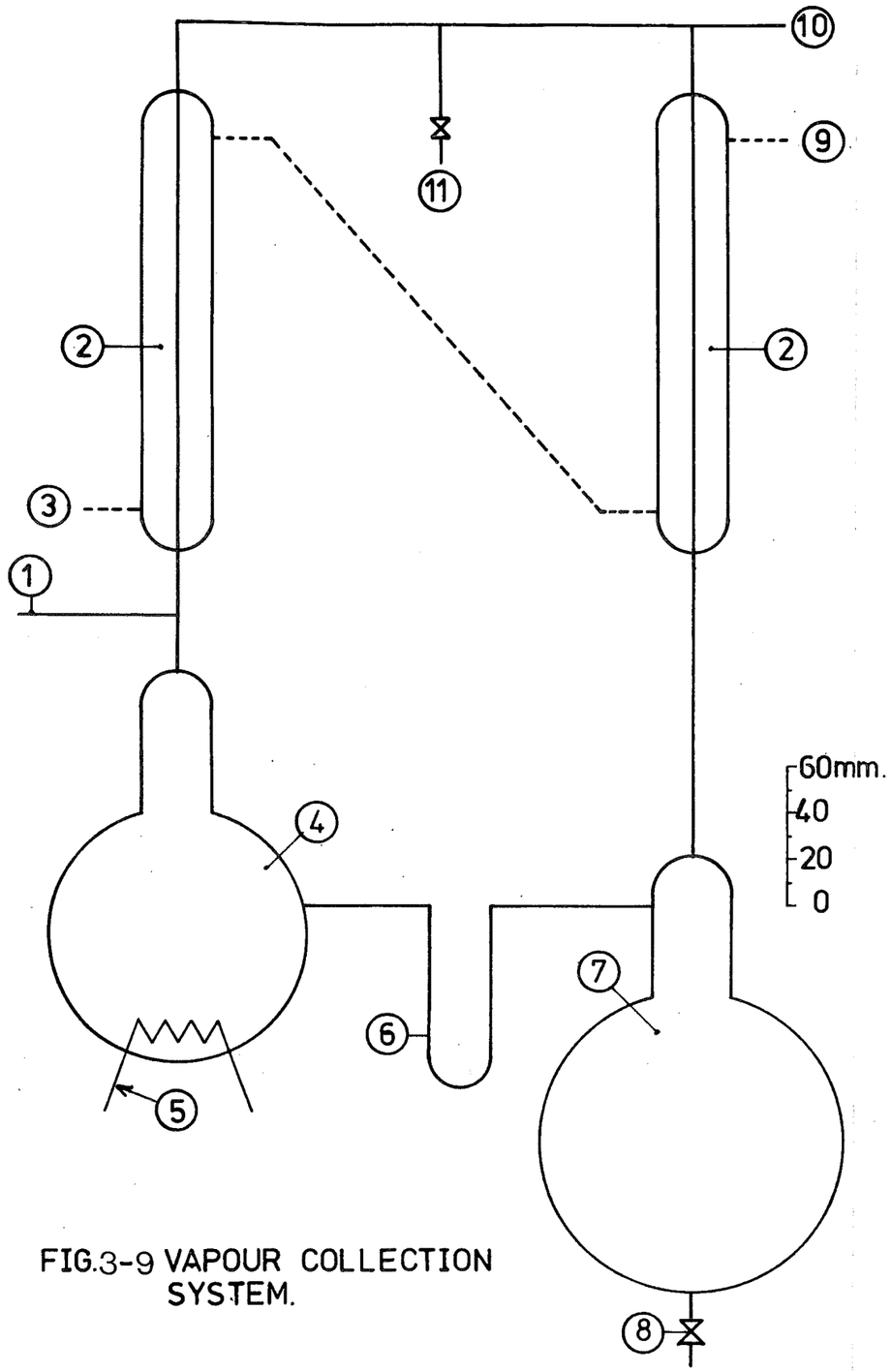

FIG.3-9 VAPOUR COLLECTION SYSTEM.

KEY

(1) Gas Mixture from Calorimeter

(2) Double Surface Condenser

(3) Cooling Water Inlet

(4) Reflux Flask

(5) Reflux Heater (Electrothermal m103 Heating Mantle with Electrothermal mc221 Controller)

(6) Liquid-Vapour Seal U Tube

(7) Collection Flask

(8) Drain (10 mm Young's Tap)

(9) Cooling Water Outlet

(10) To Pressure Controller

(11) To Pressure Measurement

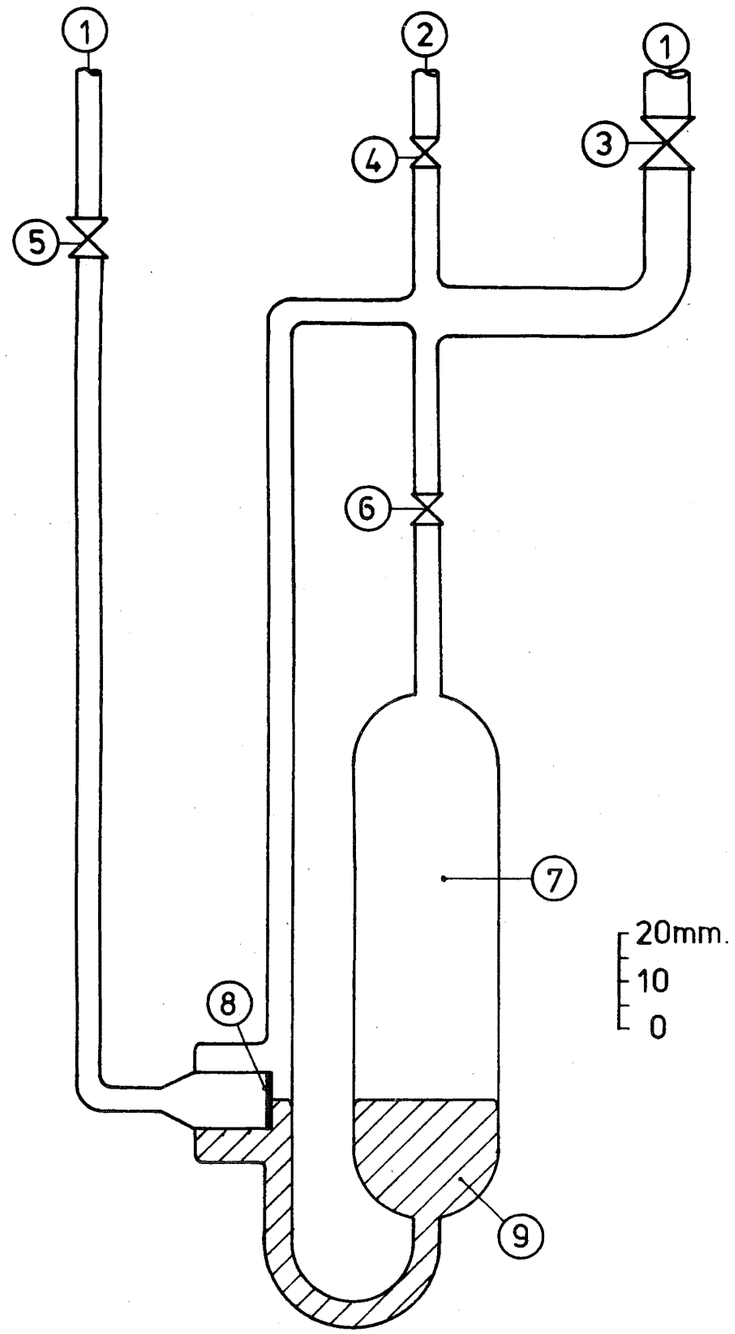

FIG 3-10 PRESSURE CONTROLLER.

KEY

(1) Low Vacuum Line (Water Pump)

(2) To Calorimetric System (Vapour Collection - Calorimeter - Boiler)

(3) 10 mm Young's Tap

(4) 6 mm Young's Tap

(5) 6 mm Young's Tap

(6) 6 mm Young's Tap

(7) Pressure Reference Vessel

(8) Grade Four Sinter

(9) Mercury

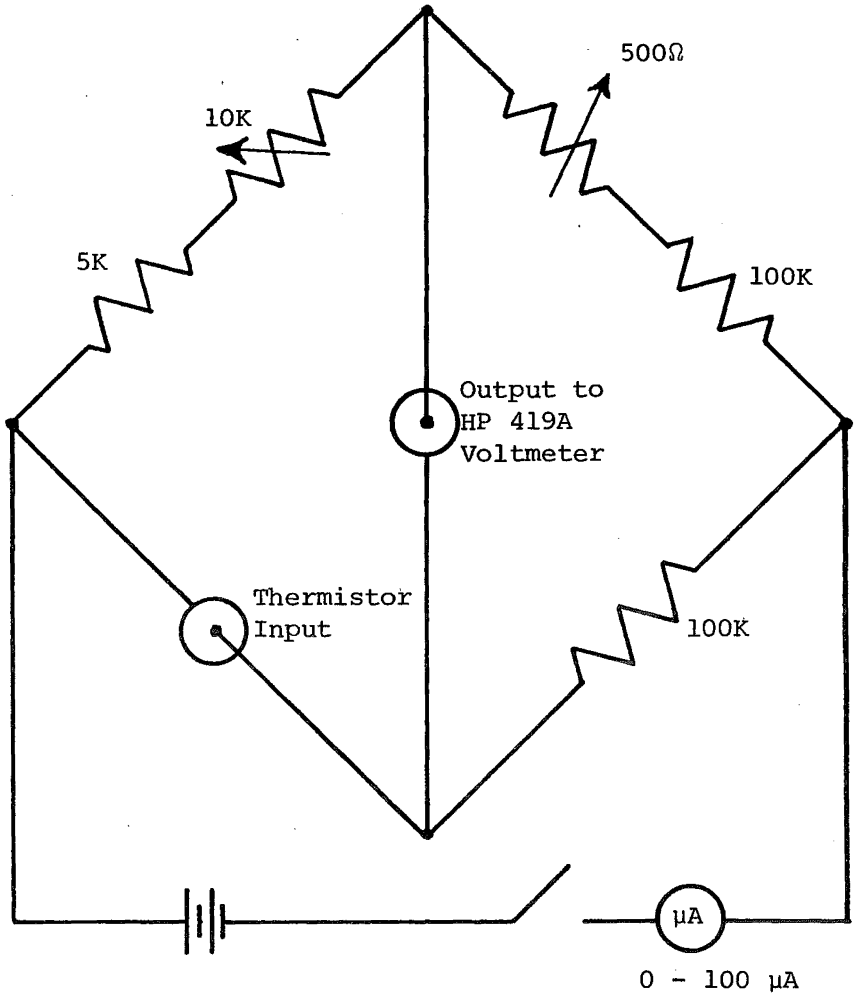

FIGURE 3-11 D.C. Thermistor Bridge

Notes

(1) The power supply consists of two Eveready Mercury Cells No. E42N.

(2) The fixed resistors are from the high stability (0.01%) 'Vishay' range.

(3) Two ten turn Beckmann Helipots are used for the variable resistors.

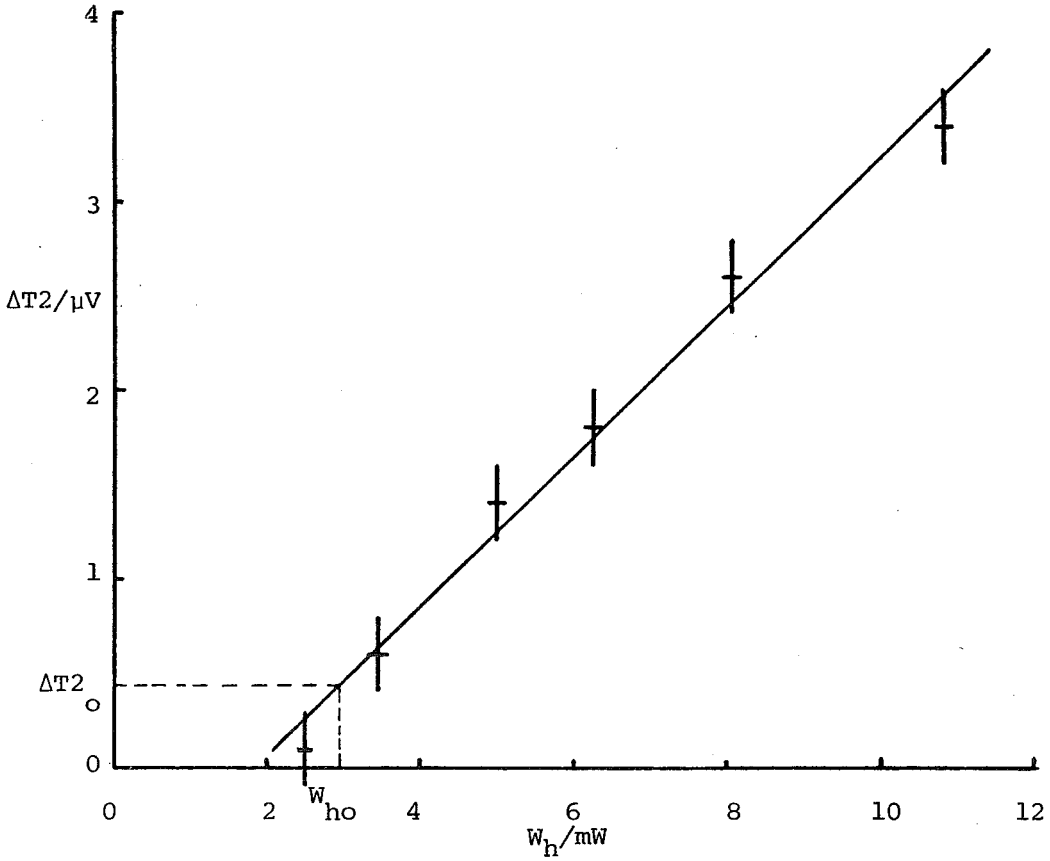

FIGURE 4-1 Plot of ΔT2 Against W_h for Benzene and Cyclohexane, f_T = 1.117 10^{-3} mol s^{-1}, T = 315K

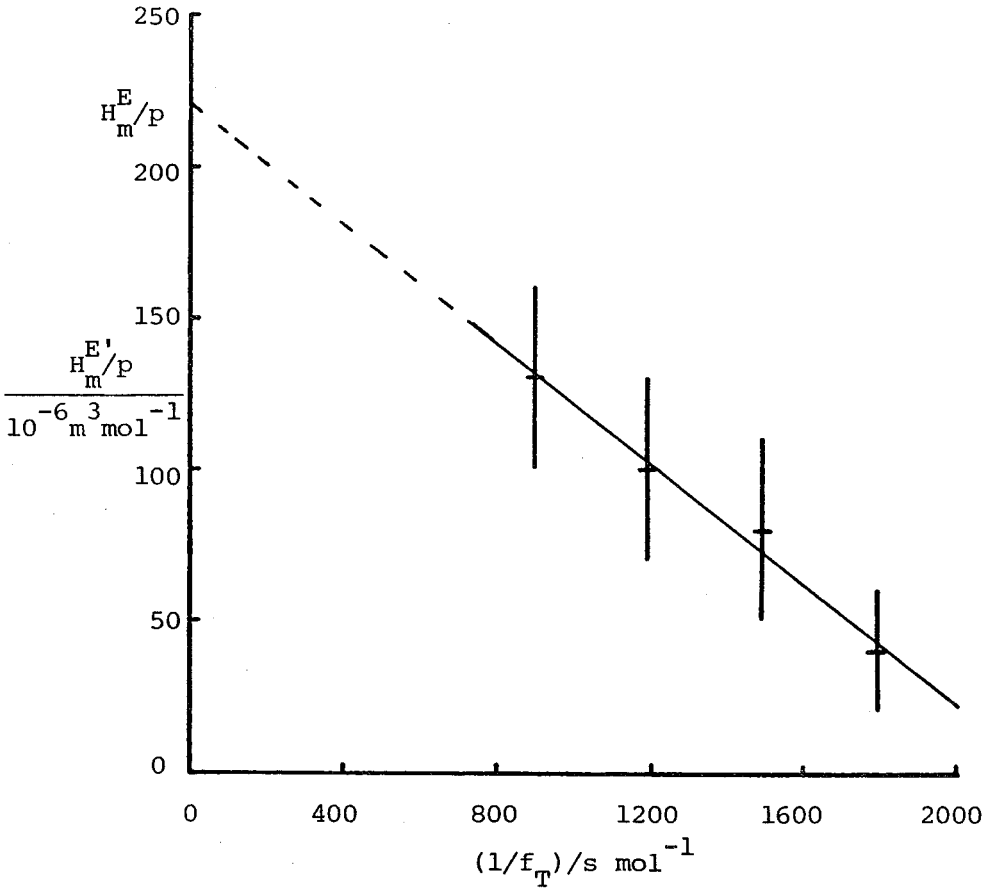

FIGURE 4-2 Plot of $H_m^{E'}/p$ Against $1/f_T$ for Benzene and Cyclohexane, T-315 K

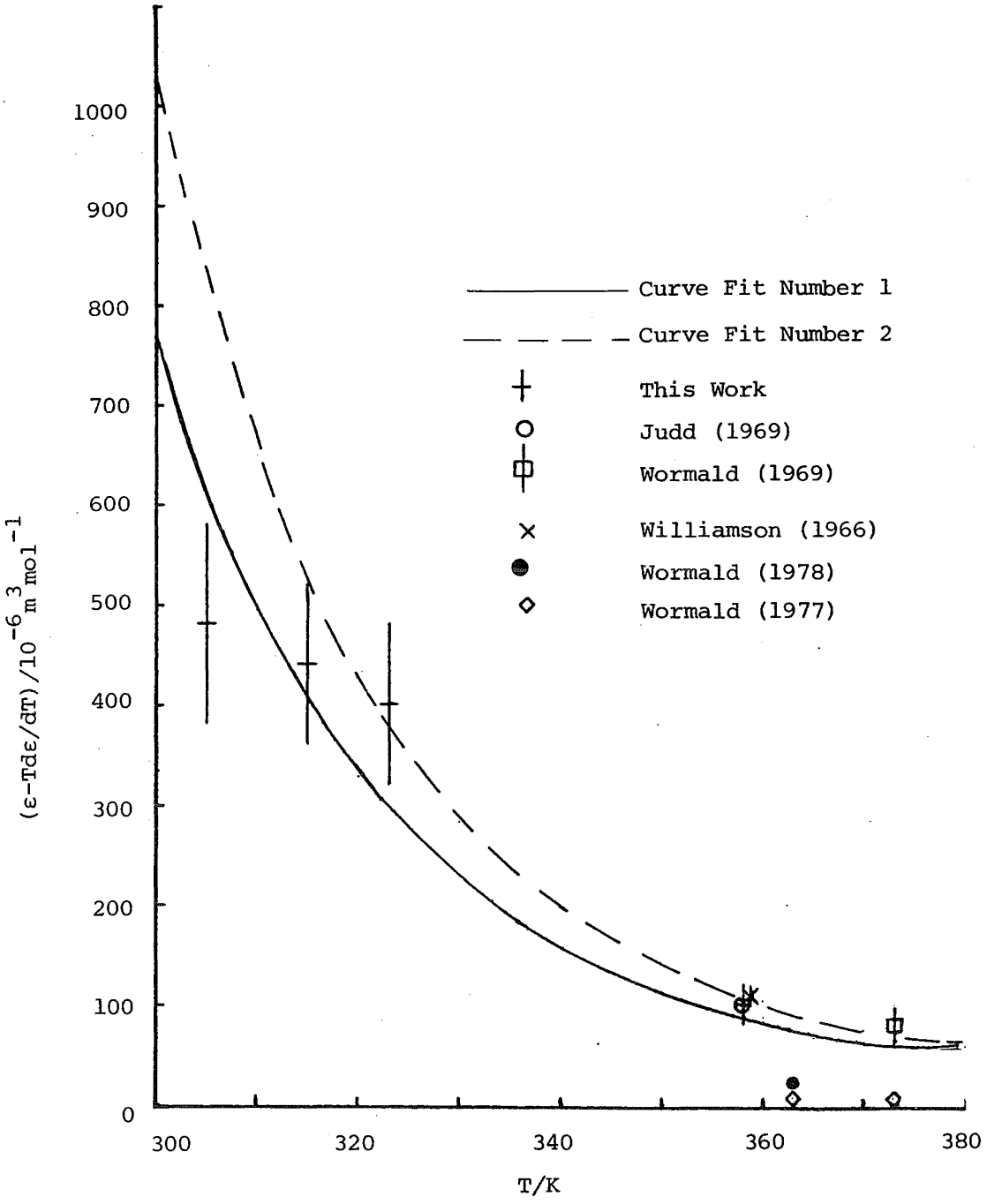

FIGURE 4-3 Plot of ε-Tdε/dT Against Temperature for Benzene and Cyclohexane. The Smooth Curves are those Calculated using Equation (4.5) with Coefficients from Curve Fit Numbers 1 and 2.

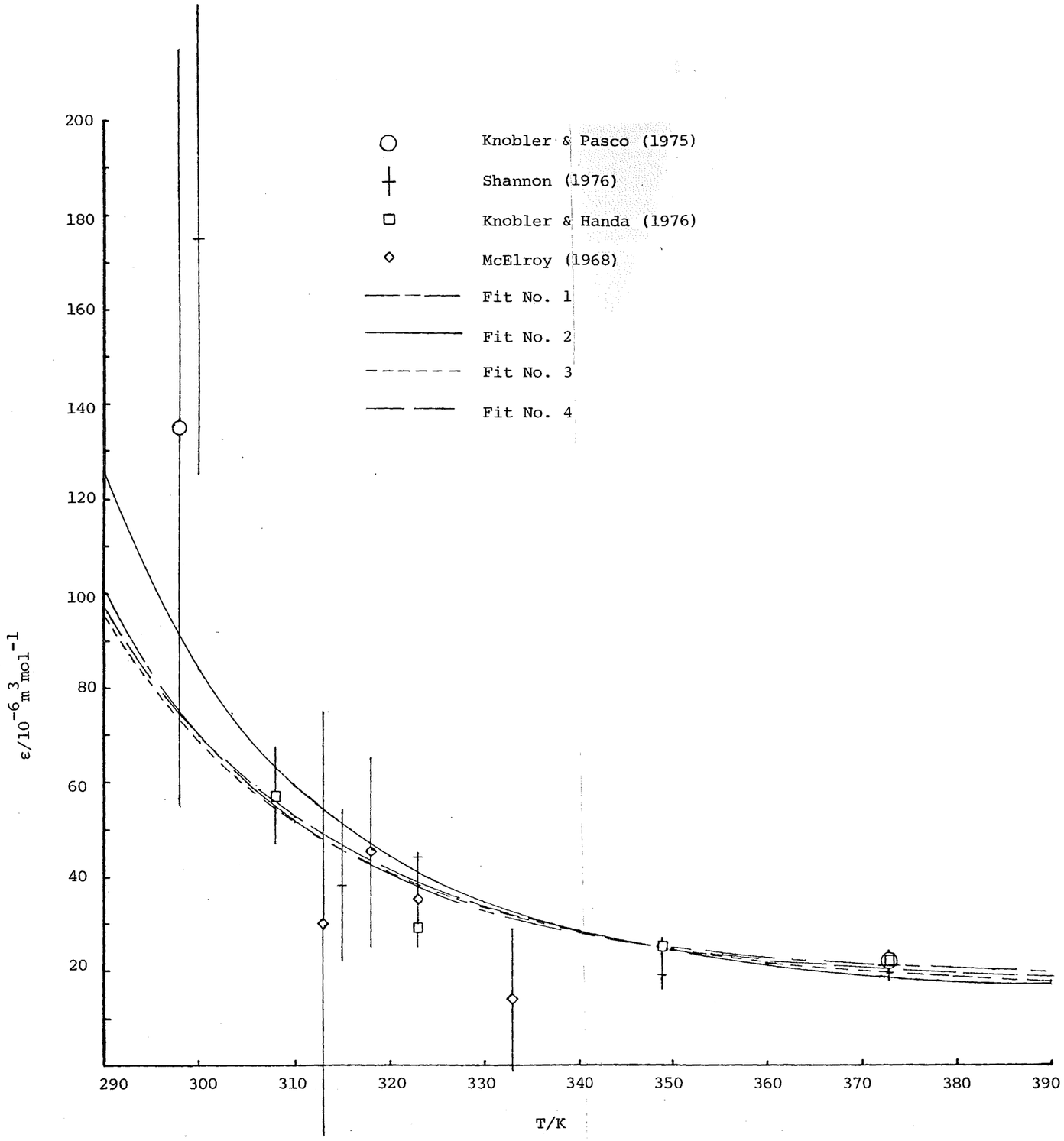

FIGURE 4-4 Excess Second Virial Coefficient for Benzene and Cyclohexane with Temperature

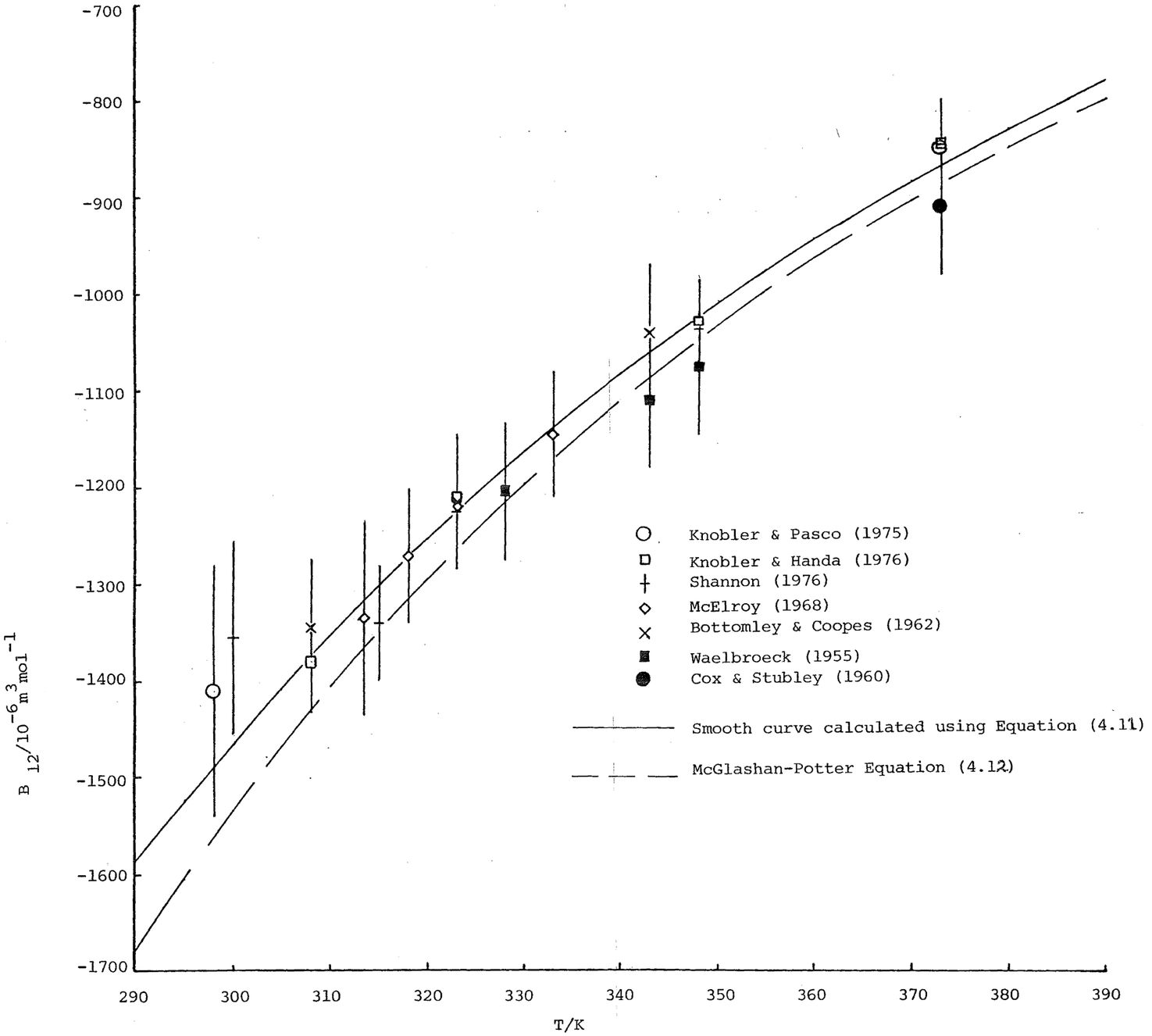

FIGURE 4-5 Interaction Second Virial Coefficient for Benzene and Cyclohexane with Temperature

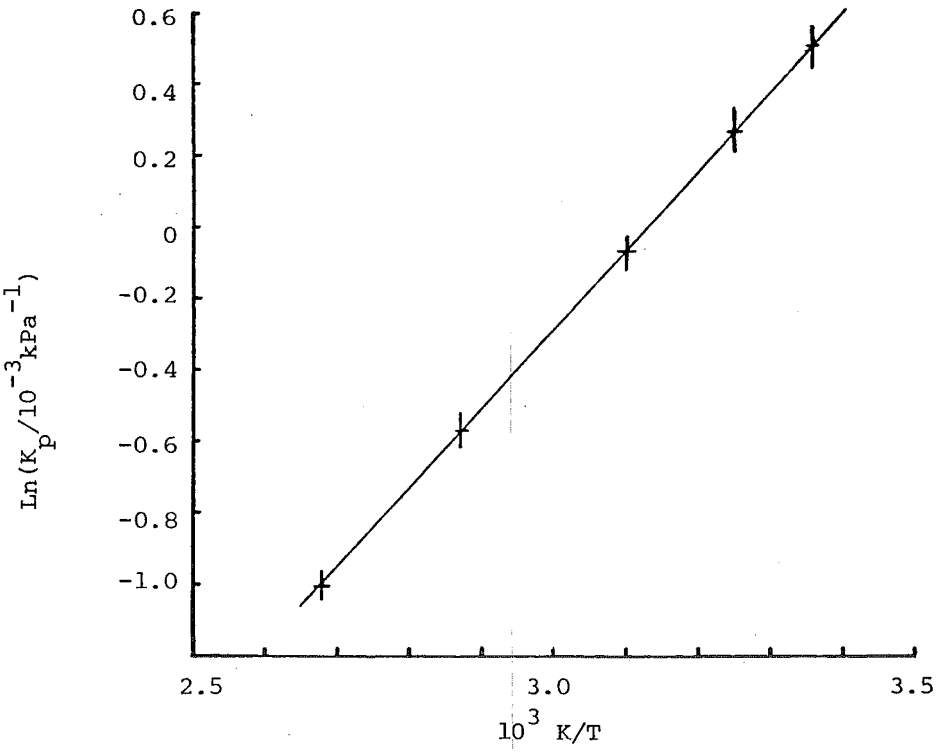

FIGURE 4-6 Plot of $\ln(K_p/10^3 kPa^{-1})$ Against 1/T for Acetone and Chloroform, Knobler and Pasco (1975)

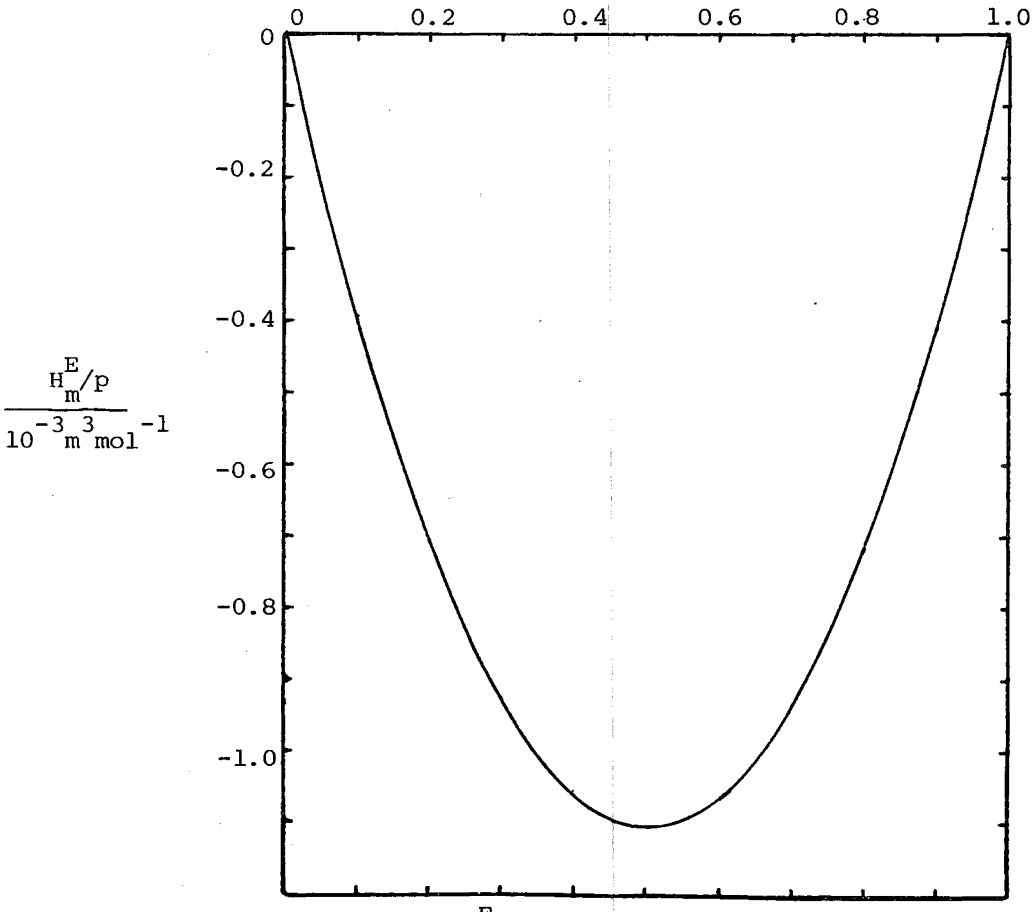

FIGURE 4-7 Plot of H_m^E/p Against Composition for Acetone and Chloroform at T = 343 K, Wormald (1969)

FIGURE 4-8 H_m^E Against Composition for the Liquid Systems,

(1) Acetone and Carbon Tetrachloride (Upper Curve)

(2) Acetone and Chloroform (Lower Curve)

at T = 298 K

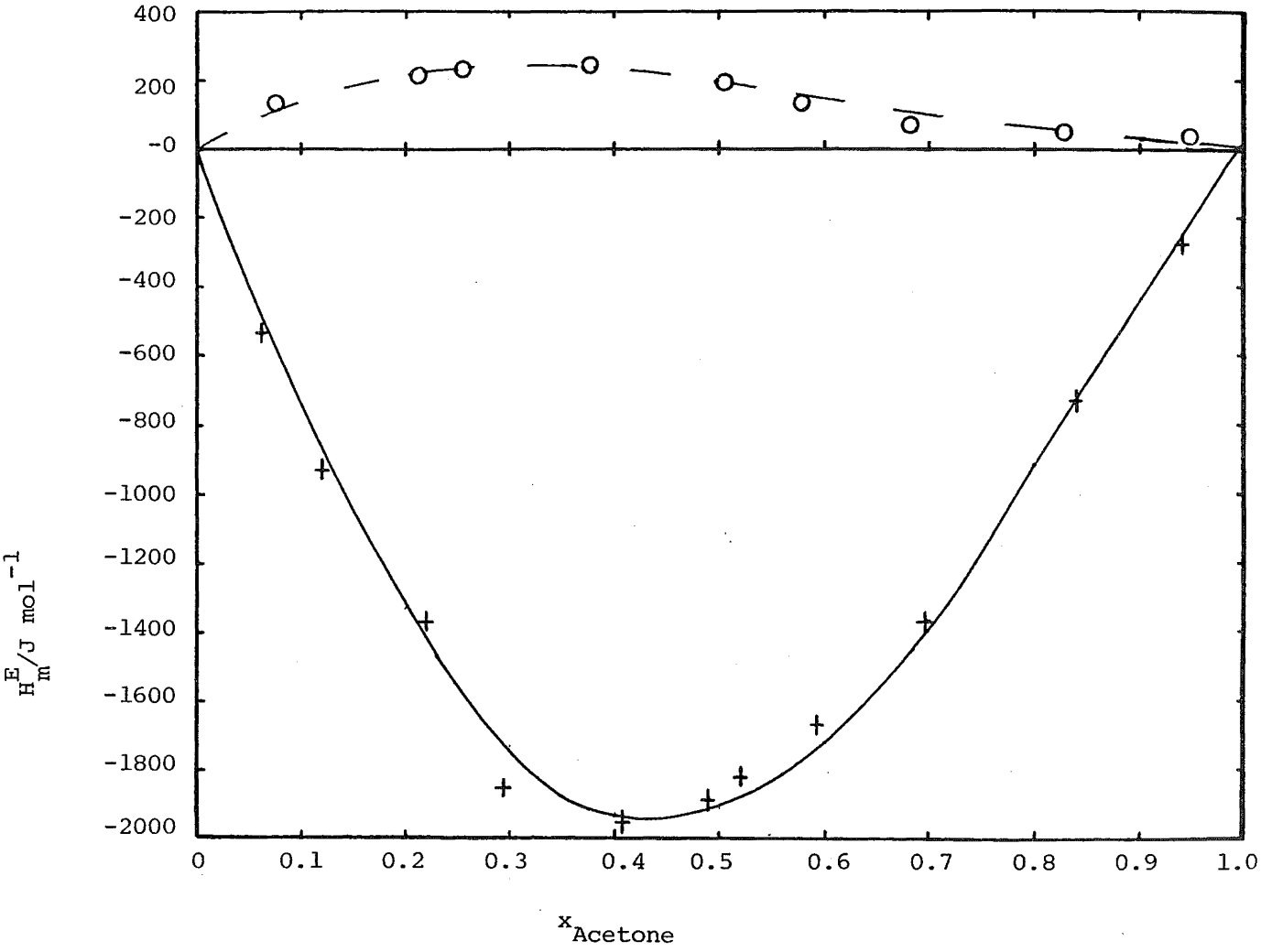

O Acetone & Carbon Tetrachloride, Campbell and Kartzmark (1960)

+ Acetone & Chloroform, Campbell and Kartzmark (1960)

— — — — Smooth curve through the results of Campbell and Kartzmark (1960)

———— Smooth Curve of Morcom and Travers (1965)

$H_m^E/J\ mol^{-1} = 7674\ x(1-x)+2161\ x(1-x)(1-2x)-1745\ x(1-x)(1-2x)^2$

where x is the molefraction of acetone.

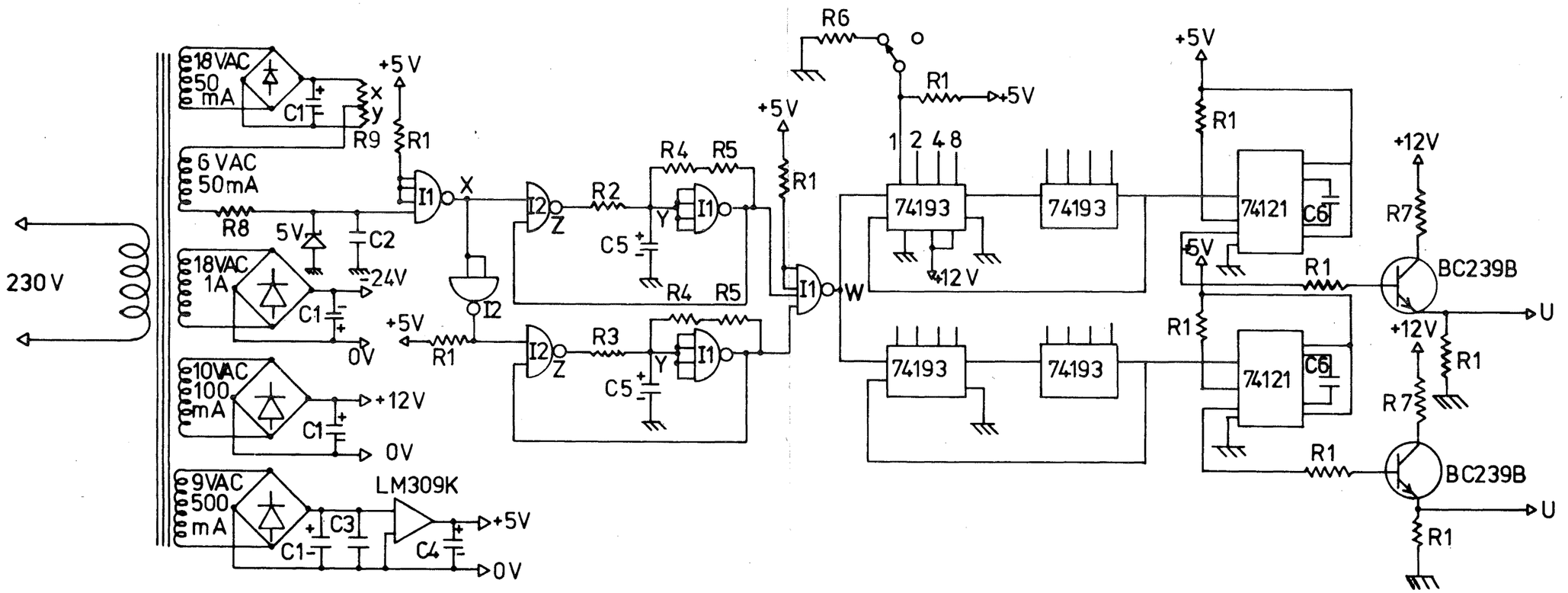

FIG.A-1 PULSE GENERATOR AND POWER SUPPLY FOR STEPPING MOTORS.

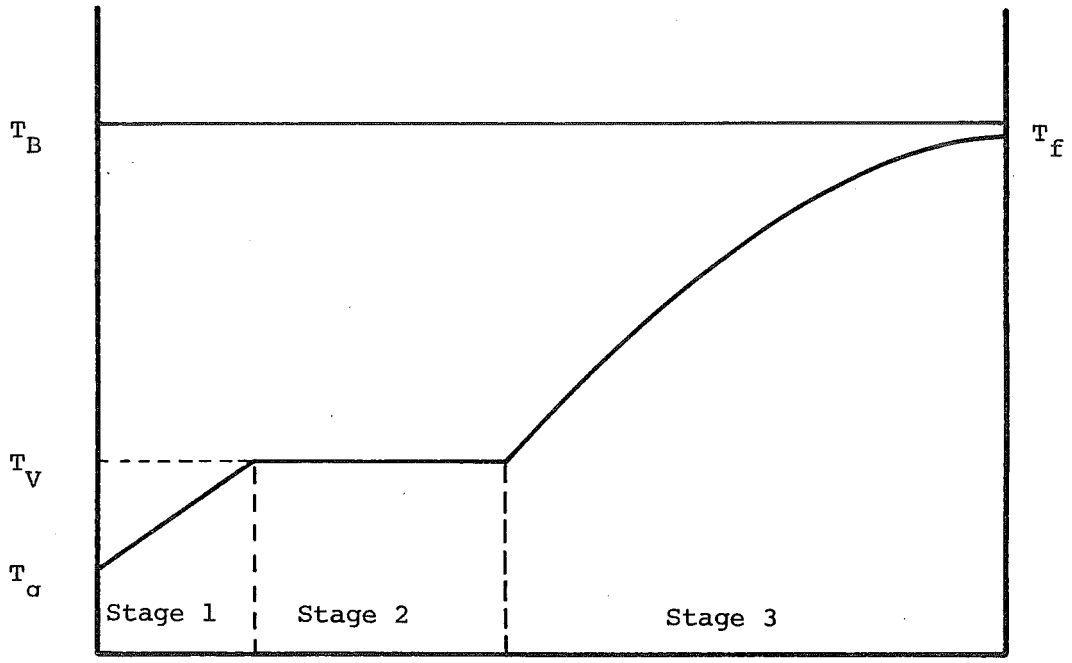

Feed Path Length Through Boiler.

FIGURE A-2 Boiler Effectiveness. A Plot of Feed Temperature as it Passes Through the Boiler and Equilibrator